Roles of the Srs2 helicase and the Ctf18 clamp loader in replication of structure-forming CAG repeats in *S. cerevisiae*

A dissertation submitted by

Jennifer HG Nguyen

In partial fulfillment of the requirements

for the degree of

Doctor of Philosophy in Biology

Tufts University

May 2016

Advisor: Catherine Freudenreich

ABSTRACT

Our genome is riddled with repetitive sequences. While the functions of these repetitive sequences largely remain elusive, expansions of a subset of structure-forming microsatellites have been found to be associated with the onset of several neurodegenerative diseases. These repeat sequences pose a natural threat to the cell during replication and repair, forming barriers that can interfere with these processes that need to occur with high fidelity to faithfully transmit and maintain genetic information. The structure-forming nature of these repetitive sequences can lead to genomic instability: expansions, contractions, chromosomal breakage and fork stalling, and therefore they need to be properly maintained to prevent damage. This work has characterized the roles of the Srs2 helicase and the Ctf18 clamp loader in maintaining repeat integrity. Srs2 and Ctf18 have previously been shown to have a general role in genome maintenance, but also a specialized role in repeat protection. We have found that the Rad51 displacement activity of Srs2 is needed to prevent repeat instability but is dispensable in preventing repeat fragility. Srs2 helicase activity and PCNA interaction are needed to prevent repeat fragility. RTEL1, a human anti-recombinase helicase, is capable of complementing some *srs2Δ* repeat-specific mutant phenotypes in *S. cerevisiae*, providing support that it is a potential human ortholog of Srs2. The alternative clamp loader Ctf18 is needed to prevent repeat fragility and in its absence, Srs2 recruitment through PCNA interaction is vital. We hypothesize that Ctf18 is preventing repeat fragility by unloading/loading PCNA when a hairpin structure is encountered. Alternatively, Srs2 hairpin unwinding can prevent repeat fragility. The absence of both of these pathways leads to a synergistic increase in fragility. This work has contributed to the

understanding of how cells cope with replication and repair through repetitive sequences, which our genome is mostly composed of.

Acknowledgements

First and foremost, I would like to thank my advisor and mentor Dr. Catherine Freudenreich for welcoming me into her lab to conduct this research. She has provided me with so much guidance and support throughout my time here. It is her unwavering enthusiasm for our work that has motivated me throughout the years.

I would like to thank my committee members for all their support and helpful advice both academically and professionally:

Dr. Juliet Fuhrman for her thoughtful comments on my research, words of encouragement and concern for my well-being

Dr. Mitch McVey for his scientific guidance and being mindful of my workload balance

Dr. Sergei Mirkin for his intellectual input and endless source of stories about the history and elegance of DNA

I would like to thank my outside committee member, Dr. Susan Lovett, for taking the time to participate in the defense process.

I would like to give a sincere thanks to all the members of the Tufts Biology department for their attention at seminars and their feedback.

I would finally like to thank my family and friends both here at Tufts and abroad for providing me with moral support all these years

Table of contents

Chapter 1

Introduction

Our genome is constantly exposed to both exogenous and endogenous sources of damage. Cells must replicate with high fidelity to prevent the passage of mutations to subsequent generations. Exogenous damage can be induced by chemical compounds like the platinum based compound cisplatin, which can intercalate DNA and create DNA crosslinks, or non-ionizing ultraviolet radiation, which can create bulky thymine dimers (Cheung-ong et al., 2013). Endogenous damage can result from errors in replication, repair, or metabolic processes that can generate free radicals (Helleday et al., 2014). If not properly repaired, damage occurring on DNA can be detrimental to the cell. In order to combat the onslaught of damage, cells have evolved several mechanisms to repair their DNA. Mechanisms of repair include: excision of damage, templated repair using homologous recombination, or damage bypass during replication for later repair (Freidburg et al., 2004). Although these mechanisms of repair can be redundant and intertwined, this thesis will focus on teasing apart the repair mechanisms needed when replication forks encounter a source of endogenous damage: a non-canonical structure-forming sequence.

Repetitive DNA and non-canonical structure formation

After the completion of the Human Genome project, it was discovered that over half of our genome is composed of repetitive sequences (Consortium, 2001). While initially it was thought that most of this was ‘junk’ DNA, these sequences are garnered more interest due to their connection to several neurodegenerative

diseases. Some of these repetitive sequences are a source of endogenous damage due to their unstable nature and it is the expansion of certain repeat sequences that have been linked to neurodegenerative diseases.

A key trait for repeat instability is the propensity for the repetitive sequence to form non-B form secondary structures (alternative DNA structures are depicted in Figure 1). Of all the identified structure-forming repeats, trinucleotide repeats are associated with the most diseases. One of the most common structures among trinucleotide repeats is a hairpin structure. CAG, CTG, CCG, and GGC are all sequences capable of folding back on themselves and base pairing within the same strand to form a hairpin structure (Darlow and Leach, 1998; Mitas, 1997; Pearson and Sinden, 1998; Rajeswari, 2012) (Figure 1). Guanine-rich sequences, such as the CCG and GGC repeats, can also form tetraplexes (G-quadruplex) (Fry and Loeb, 1994; Weisman-shomer et al., 2000). GAA/CTT repeats can form a triplex, or triple-stranded DNA, due to the homopurine-homopyrimidine stretches of nucleotides that can form Hoogsteen base pairing (Gacy and McMurray, 1998; Mariappan et al., 1999; Rajeswari, 2012). Slipped-stranded structures can form if a polymerase disassociates and reanneals to the template out of register creating loops (Pearson and Sinden, 1996, 1998). Other non-triplet repeat sequences are capable of forming alternative DNA structures as well, such AT or inverted repeats that can form cruciform structures, or the ATTCT repeat which is a DNA unwinding element (Cherng et al., 2011; Pearson et al., 1996; Zhang and Freudenreich, 2007).

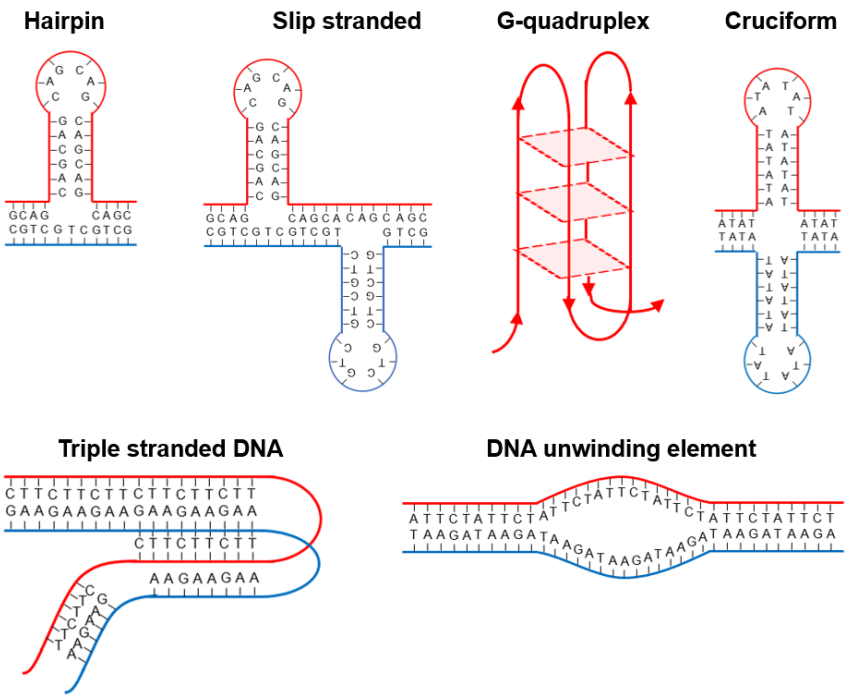

Figure 1. Alternative DNA Structures (Modified from (Usdin et al., 2015)).

While these structures are non-canonical, there is evidence that some of these structures have *in vivo* roles that aren't necessarily disease-linked. For example, small hairpins can extrude from bacteriophage N4 virion RNA polymerase promoters under specific superhelical densities to regulate transcription (Dai and Greizerstein, 1997). Hairpins can form at sites of replication within ssDNA viruses like ΦX174 (Bikard et al., 2010).Computational analysis of potential G-quadruplex forming sequences found they were non-randomly distributed throughout the genome and were concentrated in telomeric regions of chromosomes (Rhodes and Lipps, 2015). Further work with antibodies directed at G-quadruplex forming structures and deep sequencing revealed that these sequences were found throughout the genome in promoter regions as well as untranslated regions surrounding genes, suggesting these structures are

involved in gene expression (Yi et al., 2013). Cruciform formation could regulate replication by affecting the superhelical state near origins, relaxing the DNA (Pearson et al., 1996).

Repeat associated diseases

All individuals have repetitive sequences scattered throughout their genome in both coding and non-coding regions (Figure 2); however the disease phenotype is not manifested until a specific threshold of the repeat tract is surpassed (Budworth and Mcmurray, 2014). Some repeat associated diseases are listed in Table 1, including: CAG/CTG repeats that are associated with Huntington's disease and several spinocerebellar ataxias, CGG/CCG repeats that are associated with Fragile X syndrome, and G_4C_2 repeats that are associated with familial amyotrophic lateral sclerosis (ALS) and frontotemporal dementia (DeJesus-Hernandez et al., 2011; López Castel et al., 2010; Renton et al., 2011; Usdin et al., 2015). All of these diseases are associated with expansions of the repeat tract; the repeat number change can vary between affected individuals as well as within an individual as there are cell to cell variations of heterogeneous repeat lengths.

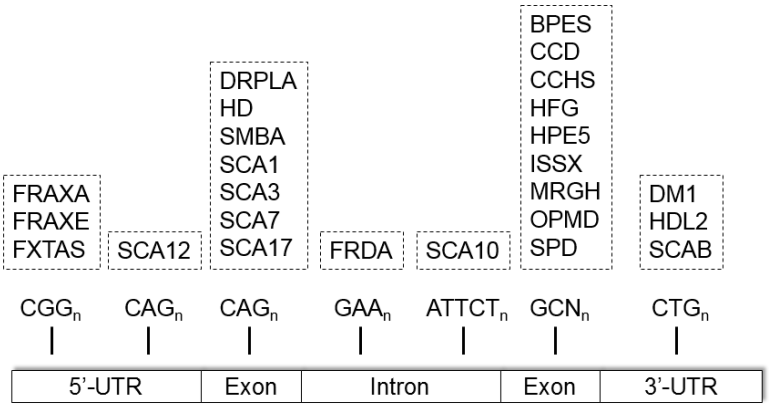

Figure 2. Repeat expansion associated diseases. Indicated repeat sequences are associated with genetic diseases listed above and are drawn at the relative location in the affected gene. (FRAXA: Fragile X syndrome. FRAXE: fragile X mental retardation. FXTAS: fragile X tremor and ataxia syndrome. SCA: spinocerebellar ataxia. DRPLA: dentatorubral–pallidoluysian atrophy. HD: Huntington's disease. SMBA: spinal and bulbar muscular dystrophy. FRDA: Freidreich's ataxias. BPES: blepharophimosis ptosis and epicanthus inversus. CCD: cleidocranial dysplasia. CCHS: congenital central hypoventilation syndrome. HFG: hand–foot–genital syndrome. HPE5: holoprosencephaly 5. ISSX: X-linked infantile spasm syndrome. MRGH: mental retardation with isolated growth hormone deficiency. OPMD: oculopharyngeal muscular dystrophy. SPD: synpolydactyly. DM1: myotonic dystrophy (Modified from (Mirkin, 2007))

Table 1. Subset of triplet and hexanucleotide repeat associated diseases (reviewed in (Usdin et al., 2015))

Disease	Gene	Repeat	Disease length
Huntington's (HD)	Huntingtin	CAG	40+
Myotonic Dystrophy (DM1)	DMPK	CTG	50+
Spinocerebellar ataxia 1 (SCA1)	ATXN1	CAG	40+
Fragile X (FRAXA)	FMR1	CGG	200+
ALS	C9ORF72	G_4C_2	250+

It was discovered over two decades ago that Huntington's disease is caused by the expansion of CAG repeats within the huntingtin gene (HTT) (MacDonald et al., 1993). Affected individuals have 36 or more repeats and a disease phenotype of cognitive decline and loss of motor function (Walker, 2007). Most studies believe that expanded CAG repeats create a stretch of polyglutamate within HTT that causes a toxic gain of function due to the conformation change of the protein (Shao and Diamond, 2007; Tobin and Signer, 2000), affecting protein aggregation and localization (Ross and Tabrizi, 2011). Fragile X is caused by an expansion of the CGG repeat within the 5' UTR of the FMR1 gene on the X chromosome (Oberlé et al., 1991; Verkerk et al., 1991). Affected individuals have more than 55 repeats and show cognitive dysfunction (Bagni et al., 2012). Expansion of these repeats change the methylation state of the surrounding area causing no transcription of the FMR1 gene (Sutcliffe et al., 1992). It was only recently discovered that G_4C_2 repeats cause familial ALS, which results in

muscle weakening and cognitive impairment (DeJesus-Hernandez et al., 2011). The repeats are found in a noncoding region within the C9ORF72 gene and expansion of this repeat affects splicing and transcript level of the gene, although the protein levels were unchanged (DeJesus-Hernandez et al., 2011). Due to the unstable nature of these repeat sequences that could lead to disease phenotype, it is important to study the molecular mechanisms involved in preventing repeat instability.

Some repetitive sequences have also been found to cause DNA double strand breaks (which we refer to as fragility) in a length-dependent manner. Using the model organism *Saccharomyces cerevisiae*, several researchers have found CTG/CAG, CGG/CCG, GAA/TCC, AT, and inverted repeats are capable of causing double strand breaks (Balakumaran et al., 2000; Freudenreich et al., 1997; Saini et al., 2013; Zhang and Freudenreich, 2007). Double strand breaks need to be expertly repaired to prevent loss of genetic information that could lead to cell death. Due to the repetitive nature of these sequences, repair could lead to non-allelic homologous recombination. GAA/TCC and inverted repeats have been shown to induce chromosomal rearrangement and DNA damage at distal chromosomal loci (Saini et al., 2013). Therefore, it is important to understand the mechanisms of repair cells utilize to prevent both repeat instability and fragility in order to get a full understanding of repeat maintenance within the cell. This thesis will focus specifically on the CAG/CTG repeats.

Replication model for repeat instability and fragility

The ability for the non-canonical hairpin structures to form is dependent on a single-stranded state of DNA. Not surprisingly, structure formation more readily occurs during cellular processes such as replication, repair, and recombination, all of which involve a period of single-strandedness. Generally these structures are transient intermediates and the stability of these structures is dependent on both the length of the repeat tract and the purity of the repeats. Repeats with longer tracts form structures more readily and are more stable than shorter tracts (Gacy and McMurray, 1998). Additionally, if there are interruptions within the repeat, the stability of hairpin formation dramatically decreases (Gacy et al., 1995; Sakamoto et al., 2001). If these structures form and persist, they can lead to the addition or deletion of repeat units (expansions, contractions; repeat instability) (Kim and Mirkin, 2013; Mirkin, 2007) or can block cellular processes that could lead to chromosomal breakage (fragility).

One model to describe how repeat instability is arising is during replication. Structure-forming sequences have been shown to stall DNA polymerases and this is dependent on the length of the repeat and the orientation relative to the replication origin (Gacy et al., 1998; Kang et al., 1995; Mirkin and Mirkin, 2007; Samadashwily et al., 1997; Usdin and KJ, 1995). When CTG_{70} was on the lagging strand template, it conferred a weak replication stall but when CAG_{70} was on the lagging strand template, it did not seem to affect replication progression (Samadashwily et al., 1997). Shorter CGG_{14-31} repeats resulted in a weak replication stall compared to CGG_{50}, indicating an increase in repeats leads to an increase in fork stalling. Since lagging strand synthesis intrinsically has portions of ssDNA, it is more likely hairpin formation can occur on the lagging strand,

although they can also form on the leading strand (Figure 3). Since the polymerases are linked, if one polymerase stalls once it encounters the repetitive sequence, the other will as well. If the hairpin is on the lagging strand, the polymerase could skip over the hairpin and resume synthesis on the next Okazaki fragment to prevent replication fork stalling, which could lead to deletion of sequence (Mirkin, 2006). If the forks stalls, repair and/or recombination can occur to restart replication and if this occurs within a repetitive sequence, the polymerase could misalign before start of synthesis and that could result in either a loss or addition of repeat units.

Metaphase spreads of chromosomes have more instances of gaps and breaks when exposed to various replication inhibitors (Freudenreich, 2007), providing evidence that perturbations at the replication fork, such as a hairpin causing stall, could also lead to chromosomal breakage. The rate of breakage has been shown to be tract length dependent, with longer tracts causing a higher rate of breakage (Freudenreich et al., 1998). Longer repeat tracts can persist and stall replication, consequently leading to more single stranded regions that are susceptible to nucleases or damage from mechanical force, which can result in double strand break formation (Mirkin and Mirkin, 2007).

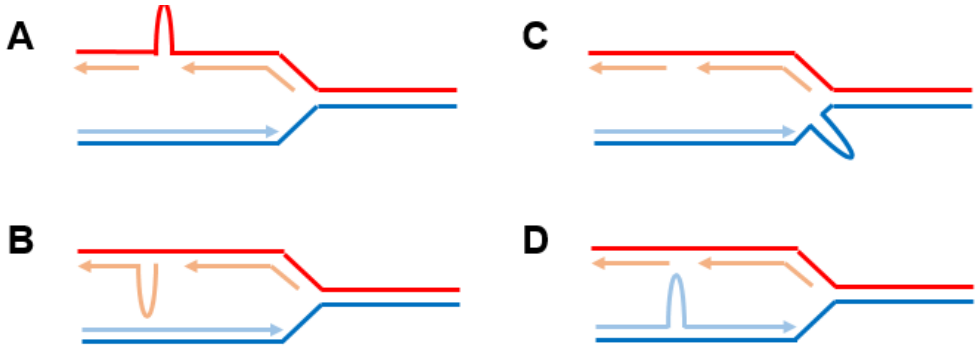

Figure 3. Possible hairpin formation during replication. A) Lagging template strand, B) Lagging nascent strand, C) Leading template strand, D) Leading nascent strand (Modeled after (Frizzell et al., 2014; Mirkin, 2007)

Overview of eukaryotic replication

Replication initiation is a highly coordinated process with many players involved. In eukaryotic cells, the initiation of replication involves the assembly of the pre-RC complex (composed of ORC, Cdc6, Cdt1, and MCM2-7) onto DNA at origins of replication (Aparicio et al., 1997). In *S. cerevisiae* the origins are well-defined (termed autonomous replication sequences, ARSs) but in other model eukaryotes and metazoans, the origins are less defined (Leman and Noguchi, 2013). Origin firing occurs when cyclin dependent kinases phosphorylate Cdc6, Cdt1, and MCM2-7, which will cause the MCM2-7 helicase to unwind DNA to allow assembly of the replisome and DNA synthesis (Leman and Noguchi, 2013). DNA synthesis is performed by three replicative polymerases: pol α synthesizes the RNA primer template for pol ε and pol δ to extend and synthesize on the leading and lagging strands, respectively (Leman and Noguchi, 2013). In order to improve DNA polymerase processivity, DNA clamps are utilized to stabilize the

interaction between the polymerase and DNA (Figure 4) (Burgers, 1991; Langston and O'Donnell, 2008; Mace and Alberts, 1984; Stukenberg et al., 1991). In bacteria, the γ clamp loader loads the β clamp onto DNA to interact with Pol III for replication. The polymerase of the *E. coli* replicase can only synthesize 10 bases per second without a clamp (Maki and Kornberg, 1985) but with a clamp, the polymerase can synthesize up to 1000 bases per second (McInerney et al., 2007; O'Donnell and Kornberg, 1985). In eukaryotes, the DNA clamp is a homotrimer named proliferating cell nuclear antigen (PCNA). PCNA interaction with the polymerases increases processivity during replication by 1000-fold (Bravo et al., 1987; Prelich et al., 1987).

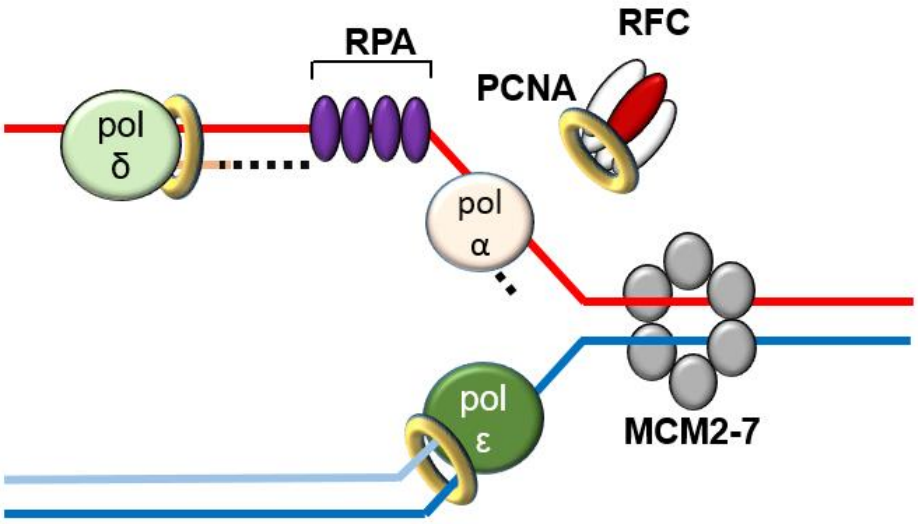

Figure 4. Simplified eukaryotic replication fork showing major proteins involved in DNA synthesis. As the MCM2-7 helicase unwinds the duplex (from left to right), pol α synthesizes an RNA primer for both pol ε and δ to synthesize from on the leading and lagging strands, respectively. Replication factor C (RFC) clamp loaders load PCNA clamps to increase polymerase processivity. Since lagging strand synthesis occurs discontinuously, multiple RNA primers need to be

synthesized and the intervening single stranded DNA is coated with RPA to protect against damage.

PCNA and clamp loaders

PCNA is part of a family of clamps that includes the aforementioned *E. coli* β clamp as well as the bacteriophage T4 gp45, and *P. furiosus Pfu*PCNA. These DNA clamps have structural and functional conservation through various species despite not having much sequence similarity (Krishna et al., 1994). DNA clamps form a ring encircling DNA in a sequence independent manner (Stukenberg et al., 1991) (Figure 5). PCNA is a homotrimer and each monomer contains two domains that are connected by a long linker called the interdomain connecting loop (Hedglin et al., 2013; Moldovan et al., 2007). Monomers are oriented in a head-to-tail orientation with an inner ring of positive alpha helices to associate with negatively charged DNA and an outer surface composed of β-sheets (Hedglin et al., 2013). This orientation creates two 'faces' of PCNA, one of which is the carboxyl terminal face where proteins such as the polymerases and replication factor C (RFC) interact with PCNA (Moldovan et al., 2007). PCNA is normally in a closed conformation (Schurtenberger et al., 1998; Zhuang et al., 2006), consequently there must be mechanism that can open/close the clamp to load/unload it onto DNA.

Clamp loaders, just like DNA clamps, are conserved through the three domains of life (Hedglin et al., 2013). In bacteria the γ clamp loader loads the β clamp and in eukaryotes and archaea the clamp loader RFC loads PCNA (Johnson and O'Donnell, 2005). The γ clamp loader is composed of five different subunits: γ, δ,

δ', χ, and ψ, (Kelman and O'Donnell, 1995) although clamp loading activity doesn't require χ or ψ (Onrust and O'Donnell, 1993). RFC is highly conserved from yeast to humans and is composed of five subunits: RFC1-5, which all share sequence similarity to each other and to the γ and δ' subunits of the bacterial clamp loader (Figure 6) (Cullmann et al., 1995; Hedglin et al., 2013). Each of the RFC subunits is part of the AAA+ family of ATPases that have ATP binding and hydrolyzing activity (Cullmann et al., 1995). RFC is normally in a closed state and undergoes a conformation change to an open state upon ATP binding (Zhuang et al., 2006). In eukaryotes, RFC binds ATP in a sequential manner: first it binds two ATP molecules leading to RFC opening, then it binds a third ATP upon PCNA binding to open the clamp, then a fourth ATP when at the primer/template junction which will trigger ATP hydrolysis and subsequent release of RFC, leaving closed PCNA on DNA (Gomes and Burgers, 2001) (Figure 5). RFC can bind primer-template junctions more strongly than single stranded DNA (Gomes and Burgers, 2001) and therefore has been predicted to readily load PCNA at these sites for replication and repair.

In addition to RFC, eukaryotes have three other alternative clamp loaders that have specialized functions within the cell. These alternative clamp loaders are also composed of the RFC2-5 subunits but rather than RFC1, they have other proteins that are specific to the cellular processes with which they are involved (Figure 6). The Rad24-RFC interacts with the 9-1-1 heterotrimer during the DNA damage checkpoint (Bermudez et al., 2003a). The 9-1-1 heterotrimer is composed of Rad17, Mec3, and Ddc1 in yeast (Rad9, Rad1, Hus1 in humans), has sequence similarity to PCNA and is structurally predicted to form a ring as well (Venclovas and Thelen, 2000). Rad24-RFC loads the 9-1-1 complex at

double-stranded/single stranded DNA junctions and gapped DNA (Majka and Burgers, 2004). Another alternative clamp loader is the Elg1-RFC. Elg1 was found to be important for DNA replication and genome stability (Bellaoui et al., 2003). Recent work has shown that Elg1-RFC is capable of unloading unmodified and SUMOylated PCNA from DNA during replication (Kubota et al., 2013a, 2015).The last alternative clamp loader, the one of interest in this thesis, is the Ctf18-RFC.

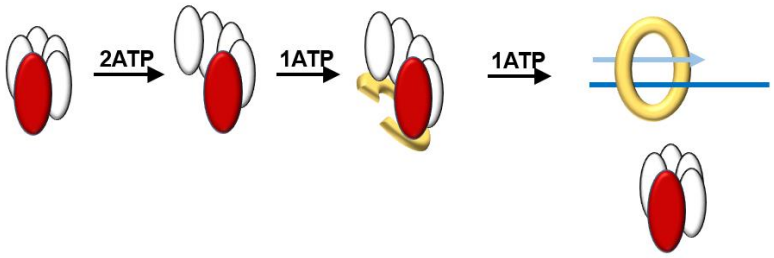

Figure 5. Mechanism of clamp loading in *S. cerevisiae* using RFC loading of PCNA at a primer-template junction as the example (Modeled after (Majka and Burgers, 2004))

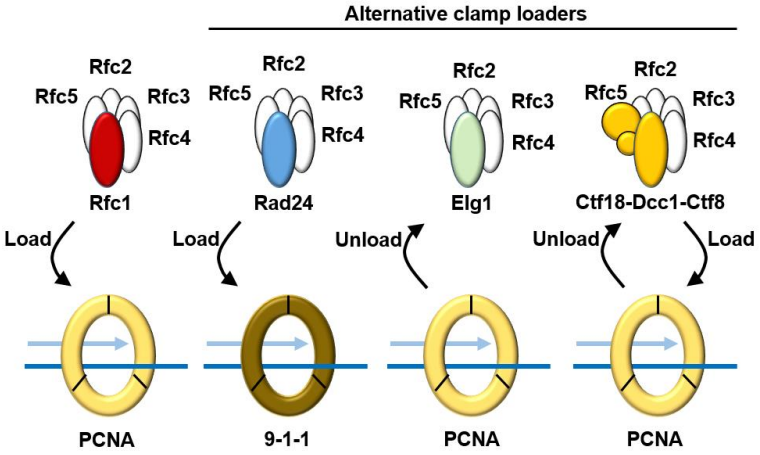

Figure 6. Clamp loaders and their associated activity with their specific clamp. Modified from (Kubota et al., 2013b)

Ctf18-RFC

Ctf18-RFC is unique amongst the clamp loaders because in addition to Ctf18 and RFC2-5, Ctf8 and Dcc1 make up the heptamer clamp loader. In the absence of Ctf18, cells are still viable but there are various problems with genome stability as discussed below. Ctf18 is important for establishing cohesion, where loss of Ctf18 leads to precocious sister chromatid separation and loss of chromosome condensation (Hanna et al., 2001; Mayer et al., 2001). Cohesion establishment is important during S phase to ensure newly synthesized sister chromatids aren't prematurely separated prior to cell division. Some proteins involved with cohesion establishment are also involved in replication (Branzei and Szakal, 2016).

Both yeast and human Ctf18 interact with pol ε through a trimeric Ctf18-Ctf8-Dcc1 complex (Murakami et al., 2010; Okimoto et al., 2016). This interaction requires the C-terminal end of Ctf18 and the N-terminal end of pol ε, the catalytic domain, suggesting Ctf18 could have an effect on DNA synthesis progression (Murakami et al., 2010). It was shown that Ctf18 localizes to the replication fork when cells are treated with HU, a replication inhibitor (Lengronne et al., 2006) and that fork progression was slowed in its absence (Crabbé et al., 2010). Additionally, the absence of the Ctf18-RFC leads to slowed cell cycle progression with a G2/M delay and this is dependent on the spindle checkpoint (Gellon et al., 2011; Hanna et al., 2001; Mayer et al., 2001). Loss of Ctf18 also leads to an increase in asymmetrical fork formation, supporting a role for Ctf18 in fork stabilization to promote replication fork progression and prevent fork collapse when forks stall (Crabbé et al., 2010). When the pol ε interacting domain of Ctf18 is removed, Rad53 activation is perturbed in HU treated cells, indicating that

activation of the S phase checkpoint in the presence of DNA damage becomes defective (García-Rodríguez et al., 2015). The c*f18Δ* proteomic profile of HU treated cells (discussed below) was similar to HU treated *mrc1Δ* cells, mirroring similar de-repression of late origin activation profiles, putting them in the same DNA replication checkpoint pathway (Crabbé et al., 2010; Kubota et al., 2011).

In vitro work has shown that Ctf18 is able to both unload and load PCNA at primer-template junctions (Bermudez et al., 2003b; Bylund and Burgers, 2005), although the *in vivo* function of Ctf18 is still controversial. The absence of Ctf18 in HU treated cells resulted in a decrease in PCNA signal at an early firing origin (Lengronne et al., 2006), suggesting Ctf18 is needed to load PCNA to facilitate replication progression or fork restart. Conversely, another study performed a proteomic analysis of HU treated *ctf18Δ* cells and observed an increase in replication machinery on chromatin including PCNA, RPA, GINS and Mec1 (Kubota et al., 2011), providing support for Ctf18 as a PCNA unloader. Yet another study showed Ctf18 had no effect on PCNA levels on chromatin but instead Elg1 was the major PCNA clamp unloader (Kubota et al., 2013a). However, this study did not expose cells to HU so perhaps Ctf18 has a role when replication is perturbed. Taken together, these phenotypes provide support for Ctf18 having an important role in replication and genome stability.

Post translational modification of PCNA: Post replication repair

Although PCNA is essential for replication, serving as a processivity factor for the replicative polymerases as well as recruiting DNA ligase I and FEN1, which are involved in Okazaki fragment maturation, it also serves as a platform for binding

of many other proteins involved in recombination and repair (Majka and Burgers, 2004). DNA damage occurring during S phase causes post-translational modification of PCNA to coordinate the DNA damage tolerance (DDT) pathway (Figure 7). In response to blocked replication forks, PCNA is ubiquitinated at the conserved Lysine 164 (K164) residue by the Rad6/Rad18 complex (Hoege et al., 2002). Blocked replication forks can lead to an accumulation of ssDNA due to an uncoupling of the MCM helicase and/or out of sync leading and lagging strand synthesis when the replisome stalls (Berti and Vindigni, 2016; Byun et al., 2005; Sogo et al., 2002). Additionally, RPA is required for ubiquitination of PCNA because RPA coating of ssDNA at stalled forks is needed to recruit Rad18 to ubiquitinate PCNA (Davies et al., 2008).

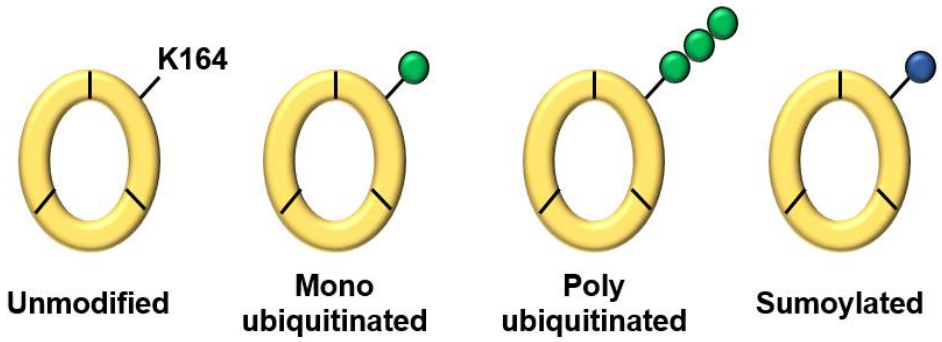

Figure 7. The eukaryotic DNA clamp, PCNA. PCNA can be modified on K164 to signal the DNA damage tolerance pathway. Modifications include mono ubiquitination, poly ubiquitination, and SUMOylation and will be discussed in text.

Rad18 is a multidomain E3 ligase that can bind Rad6, DNA, PCNA, and RPA (Davies et al., 2008). The Rad18 DNA binding domain has a high preference for forked and ssDNA (Tsuji et al., 2008), therefore it is thought that the DNA and RPA binding domains of Rad18 work together to localize it to RPA coated

regions near stalled replication forks. The absence of Rad18 leads to increased sensitivity to UV, ionizing radiation, and other DNA damaging agents (Andersen et al., 2008; Bailly et al., 1994). Rad18 has also been shown to have a role in double strand break repair in human and DT40 cells (Huang et al., 2009; Szüts et al., 2006). Rad6 is an E2 conjugating enzyme that has no affinity to DNA and needs to interact with Rad18 to be recruited to stalled forks for PCNA ubiquitination (Bailly et al., 1994). Similar to *rad18Δ*, *rad6Δ* mutants show increased sensitivity to UV and other DNA damaging agents (Andersen et al., 2008; Bailly et al., 1994). Rad6 also has a role in protein degradation when it complexes with another E3 ligase, Ubr1 (Bailly et al., 1997). Additionally *rad6Δ* mutants have a slow growth phenotype and diploids have sporulation defects (Andersen et al., 2008). While both Rad6 and Rad18 are both predominantly known for their role in DDT, it is necessary to keep in mind their other cellular functions.

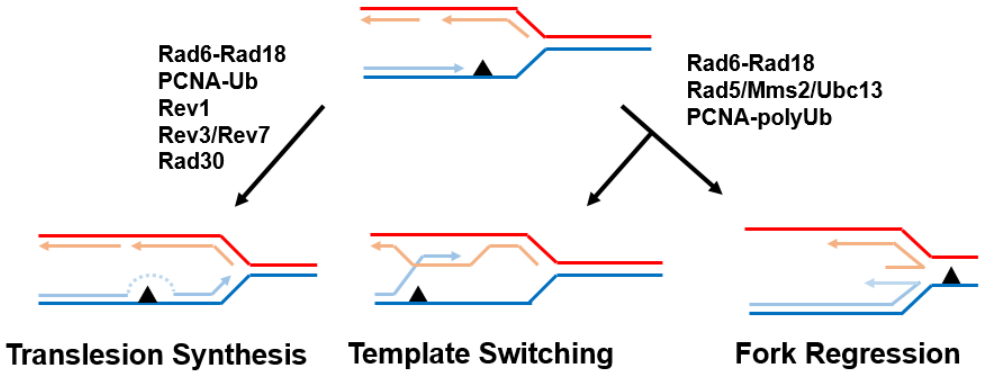

Figure 8. DNA damage tolerance pathways. This is coordinated by PCNA post-translational modification by Rad6-Rad18 and also subsequently by Rad5/Mms2/Ubc13 (Modified from (Andersen et al., 2008)).

DDT is composed of two parallel pathways, an error-prone and an error-free pathway (Figure 8). The error-prone pathway requires monoubiquitination of PCNA at K164 to recruit translesion polymerases. All translesion polymerases are part of the Y family of polymerases, except pol ζ which is part of the B family of polymerases alongside replicative polymerases δ, ε, and α (Waters et al., 2009). Unlike the replicative polymerases, all translesion polymerases lack 3' to 5' exonuclease activity and have less constrained active sites leading to lower fidelity during synthesis (Yang and Woodgate, 2007). This allows for these polymerases to be able to incorporate bases across damaged DNA templates. Yeast have three translesion polymerases: Rev1, Rad30 (pol η), and Rev3/7 (pol ζ) and each of these polymerases have different incorporation profiles. Rev1 can only incorporate dCMP at abasic sites, Rad30 is efficient at bypassing thymine dimers, and Rev3/Rev7 can extend off of misincorporated bases leading to increased mutagenesis (Waters et al., 2009; Yang and Woodgate, 2007). Translesion polymerases can interact with PCNA through a conserved PIP box motif and can more strongly bind to ubiquitinated PCNA through ubiquitin binding motifs (Bienko, 2005; Guo et al., 2006).

The error-free pathway of DDT is coordinated by further addition of ubiquitin moieties to monoubiquitinated PCNA. This is performed by the E2 conjugating heterodimer Mms2-Ubc13 and the E3 ligase Rad5, which creates a non-canonical Lysine 63 linked ubiquitin chain at K164 on PCNA (Hoege et al., 2002; Hofmann and Pickart, 1999; Torres-Ramos et al., 2002). Polyubiquitination via Mms2/Ubc13/Rad5 occurs sequentially and requires initial Rad6/Rad18 monoubiquitination prior to the addition of the chain (Parker and Ulrich, 2009). Mutations arising in *mms2Δ* mutants are dependent on Rev3 and *mms2Δrev3Δ*

are synergistic to UV and MMS sensitivity, supporting two branches of DDT that work in parallel to each other (Broomfield et al., 1998).

Error-free bypass utilizes the sister chromatid as a template strand for synthesis past a lesion. There are two working models of error-free bypass: replication fork regression and template switch. Replication fork regression can occur when a replication block is encountered, leading to the unwinding of the newly synthesized strands that can anneal to one another and the rebinding of the parental strands as the fork backtracks, forming a four way junction (Figure 8, right pathway) (Neelsen and Lopes, 2015). Until recently, fork regression was viewed as a consequence of fork collapse since it was only seen in checkpoint defective cells (Lopes et al., 2001). Recent work has shown that fork regression occurs as a response to replication stress such as DNA lesions, topological strain, or secondary structures (Kerrest et al., 2009; Ray Chaudhuri et al., 2012; Zellweger et al., 2015). Fork regression can facilitate synthesis past a lesion by using the nascent sister strand to template and reanneal downstream of the lesion or regressing the nascent strands can provide more time for repair/removal of the lesion. The template switch model of bypass utilizes recombination proteins to promote strand invasion of the blocked nascent strand to synthesize off the non-damaged sister chromatid (Figure 8, middle pathway) (Xu et al., 2015). Once past the lesion, the strand can reanneal to its original template and proceed with replication. It is important to note that these two error-free pathways aren't mutually exclusive and could act sequentially to bypass a lesion.

In the absence of DNA damage during S phase, PCNA can be post-translationally modified with SUMO (small ubiquitin-like modifier) (Figure 5).

PCNA SUMOylation occurs at primarily at K164 and to a lesser extent at Lysine 127 (K127) (Hoege et al., 2002; Stelter and Ulrich, 2003). SUMOylation on both K164 and K127 is mainly performed by the E2 conjugating enzyme, Ubc9, and the E3 ligase Siz1, while K127 has been shown to be SUMOylated either by Ubc9 alone (Papouli et al., 2005; Stelter and Ulrich, 2003) or Ubc9 and another E3 ligase, Siz2 (Parker et al., 2008). SUMOylation of PCNA serves to recruit the Srs2 helicase to the replication fork (Papouli et al., 2005; Pfander et al., 2005).

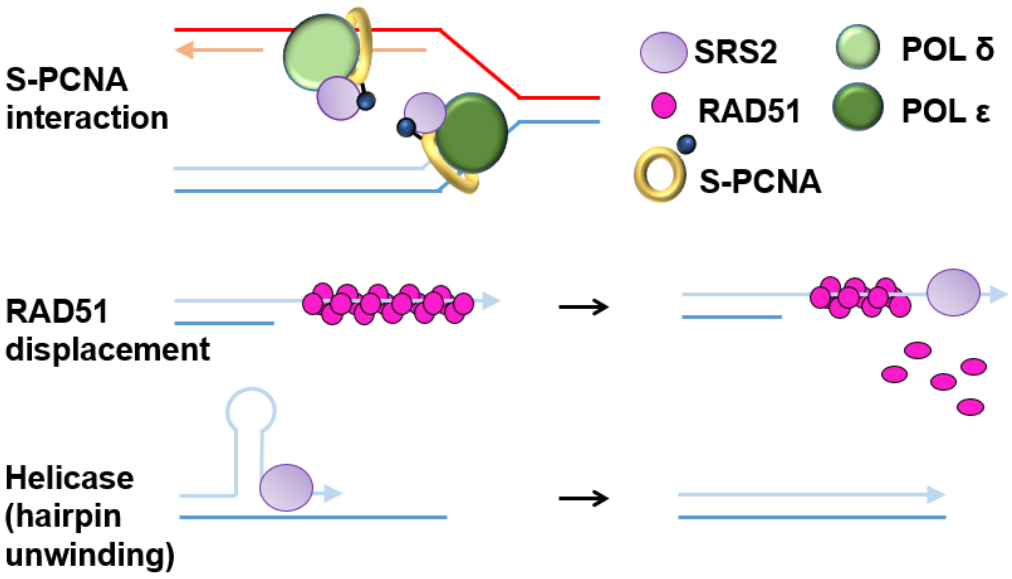

Figure 9. Srs2 functions. Srs2 interacts with SUMOylated PCNA for replication fork recruitment. Srs2 inhibits recombination by displacing Rad51 off the presynatiptic filament. Srs2 helicase activity is efficient at unwinding triplet repeat hairpin structures.

Srs2 Helicase

Srs2 was first discovered as a suppressor of DNA damage sensitivity in *rad6Δ* and *rad18Δ* mutants (Aboussekhra et al., 1989) and this suppression requires functional homologous recombination (Aguilera and Klein, 1988; Gangloff et al., 2000; Schiestl et al., 1990). Srs2 is a member of the superfamily I helicases with 3' to 5' polarity and shares homology with the *E. coli* RepA and UvrD helicases (Aboussekhra et al., 1989; Hall and Matson, 1999; Rong and Klein, 1993), except Srs2 has a long C-terminal tail that facilitates protein-protein interaction with Rad51 and PCNA (Figure 9) (Krejci et al., 2004; Papouli et al., 2005; Veaute et al., 2003). Srs2 can inhibit recombination by disassembling the Rad51 coated presynaptic filament (Krejci et al., 2004; Veaute et al., 2003). Absence of Srs2 leads to a hyperrecombination phenotype (Aboussekhra et al., 1992; Rong and Klein, 1993) and when knocked out in combination with Sgs1, a DEAH-box helicase needed to dissolve double Holliday junctions to prevent crossovers (Hickson, 2014; Ira et al., 2003), it will result in synthetic lethality due to unrestricted recombination (Gangloff et al., 2000). Srs2 prevents recombination through its ATPase activity, which allows it to translocate on the presynaptic filament and trigger ATP hydrolysis within Rad51 to cause Rad51 disassociation from DNA (Antony et al., 2009; Krejci et al., 2004). Srs2 ATPase and helicase activity requires an intact Walker A motif for functionality (Krejci et al., 2004). Srs2 preferentially unwinds 3' overhangs but is also capable of unwinding dsDNA, 5' overhangs, and D loops bound with Rad51 (Dupaigne et al., 2008; Van Komen et al., 2003). Srs2 is directly implicated in DNA checkpoint activation and recovery. Loss of Srs2 leads to lack of Rad53 phosphorylation, which is needed to slow replication in response to DNA damage (Liberi et al., 2000a).

Moreover, Srs2 is needed for checkpoint recovery after repair has completed and without Srs2 cells with DNA damage arrest in G2/M and adaption to resume mitosis is greatly reduced (Liberi et al., 2000b; Vaze et al., 2002). Altogether, Srs2 plays an important role in genome stability.

Srs2 human orthologs

Despite the various functions Srs2 has in maintaining genome integrity, there hasn't been a human homolog identified based on sequence homology. A combination of multiple helicases could be needed in higher eukaryotes to perform the equivalent functions. Several studies have identified a few key helicases that could be Srs2 human orthologs, playing the same functional role as Srs2. RTEL1 is a 5' to 3' helicase and belongs to the DEAH subgroup of the superfamily 2 helicases (Uringa et al., 2011). Spar1 (RTEL1) was identified in *C. elegans* to have similar functions as Srs2: it had synthetic lethality with the Sgs1 homolog (Him-6) due to uncontrolled recombination and loss of the Spar1 helicase led to an increase in meiotic recombination (Barber et al., 2008). RTEL1 is an essential conserved helicase that has been found to be important for telomere length maintenance and DNA repair in mice (Uringa et al., 2011). RTEL1 can antagonize homologous recombination by disrupting D loops and promoting synthesis dependent strand annealing (Barber et al., 2008; Youds et al., 2010). RTEL1 also has the conserved amino acid PIP box sequence present at its C-terminal end, which would aid in PCNA interaction (Uringa et al., 2011). Another potential Srs2 human ortholog is Fbh1, which has been found to have several overlapping functions with Srs2. Fbh1 is a 3' to 5' F-box helicase found in fission yeast with orthologs found in humans, mice, and chicken (Kim et al.,

2002). Fbh1 can substitute for Srs2 in post replication repair in *S. cerevisiae* and can also prevent hyperrecombination seen in ***srs2Δ*** (Chiolo et al., 2005). Recent work has shown that Fbh1 antagonizes homologous recombination by ubiquitinating Rad51 and this requires an F-box domain (Chu et al., 2015), which is not present in Srs2. Additionally, Fbh1 is needed to catalyze replication fork regression in HU treated cells (Fugger et al., 2015). Yet another potential Srs2 human ortholog is the helicase PARI, which has UvrD related helicase domain, similar to Srs2. Unlike these other helicases, PARI does not have a Walker A or B motif and only very weak ATP hydrolysis activity, indicating it isn't an active helicase (Moldovan et al., 2012). PARI prevents recombination by competing with pol δ to regulate D loop extension and this is dependent on its PCNA interaction and not on the UvrD helicase domain (Burkovics et al., 2016).

Thesis Focus

This thesis will focus on two proteins mentioned above that are known to be important for replication, repair, and genome integrity: Srs2 and Ctf18. Importantly, previous work has shown that both of these proteins are specifically needed to protect CAG/CTG repeat integrity.

The Srs2 helicase has been shown to have many roles in protecting repeat integrity. Srs2 is needed to prevent repeat expansion of both short and longer CAG/CTG repeat tracts (ranging from 13-70 repeats) (Bhattacharyya and Lahue, 2004; Kerrest et al., 2009). This mutator phenotype is specific to structure-forming triplet repeats since the absence of Srs2 did not affect the mutation rate at non-structure-forming $(CTA)_{25}$ repeats, dinucleotide repeats, or unique

sequences (Bhattacharyya and Lahue, 2004). Compared to Sgs1, a related helicase, Srs2 can more efficiently unwind hairpin structures of short $(CTG)_{5\text{-}15}$ and $(CGG)_{11}$ repeats *in vitro,* highlighting its specificity for structure-forming triplet repeats (Anand et al., 2012; Bhattacharyya and Lahue, 2005). Repeat instability of the longer repeat tracts in the absence of both Srs2 and Sgs1 was dependent on recombination (although to a greater extent with Srs2), indicating instability was caused by unrestricted recombination (Kerrest et al., 2009). Chromosome fragility, at $(CAG)_{70}$ repeats was also increased in the absence of both of these helicases and fragility was dependent on recombination proteins Rad51 and Rad52 in *srs2Δ* (Kerrest et al., 2009). Furthermore, Srs2 is needed for the formation of joint molecules (potentially regressed forks or recombination intermediates) that occur at CTG_{55} repeats (Kerrest et al., 2009). While both Sgs1 and Srs2 have been shown to have a role in repeat maintenance, Srs2 seems to have a more prominent role.

Knowing that Srs2 has both helicase and anti-recombinase function, this thesis work focused on determining how each of these functions contributed to repeat maintenance with respect to instability, fragility, and fork reversal. Srs2 also interacts with SUMOylated PCNA for recruitment to the replication fork; therefore another question to be addressed is whether repeat protection requires Srs2 localization to the progressing fork. Previous evidence has shown Srs2 functions can be separated; Srs2 does not require PCNA interaction to prevent the formation of recombination intermediates (Le Breton et al., 2008), recruitment of Srs2 to replication foci and recombination foci occur independently from one another (Burgess et al., 2009), and Srs2 requires helicase activity and PCNA interaction but not Rad51 displacement to prevent fork stalling at $(CGG)_{40}$

repeats (Anand et al., 2012). Based on this, we hypothesized a separation of function of the Srs2 activities in protecting CAG repeat integrity. We addressed this by utilizing previously characterized Srs2 mutants (Le Breton et al., 2008; Colavito et al., 2009; Krejci et al., 2003, 2004; Pfander et al., 2005) that attenuated one or two of its functions to determine if helicase activity, Rad51 displacement activity, and/or PCNA interaction was needed to prevent repeat instability, fragility, and formation of regressed forks.

We were also interested in investigating how two other helicases, Mph1 and Rad5, contribute to repeat maintenance since both helicases have similar functions to Srs2. Mph1 (FANCM in humans) is a 3' to 5' helicase that has sequence homology to the superfamily 2 DEAH helicases (Prakash et al., 2005). Mph1 prevents crossover events by inhibiting recombination by disassociating D loops and it does this in a pathway separate from Srs2 and Sgs1 (Prakash et al., 2009). Mph1 has been shown to biochemically act on a variety of structures including 5' and 3' flaps, promoting branch migration of Holliday junctions, and unwinding three way and four way junctions as well as replication fork structures (Kang et al., 2012; Zheng et al., 2011). This latter function suggests Mph1 could facilitate fork regression. Rad5 is a helicase and E3 ligase that is prominently known to be involved in error-free bypass in post replication repair. Rad5 helicase activity is needed to unwind replication fork structures *in vitro* although its fork reversal functions *in vivo* are less defined (Blastyák et al., 2007; Johnson et al., 1994). HLTF, the Rad5 human homolog, also has demonstrated fork reversal activity *in vitro* (Blastyák et al., 2010). Unlike Srs2, Rad5 has been shown to promote expansions of various repeats (CAG, ATTCT, GAA) (Cherng et al., 2011; House et al., 2014; Shishkin et al., 2009). We were interested in

determining how Mph1 and Rad5 might function to protect repeat fragility, instability and whether either could promote fork regression *in vivo.*

Several potential functional Srs2 human orthologs have been identified that either have similar mutant phenotypes as Srs2 (hyperrecombination, synthetic lethality with Sgs1) or can substitute for Srs2 to rescue mutant phenotypes as described above. We were interested in extending this work to determine if these helicases had specificity in preventing repeat fragility and instability like Srs2. We focused on two potential candidates: RTEL1 and Fbh1, both of which have helicase and anti-recombinase function. We expressed the open reading frames of these genes in *S. cerevisiae* in the absence of Srs2 to determine if either could complement Srs2 phenotypes and rescue the increased CAG repeat fragility and instability. We also tested if either of these genes could substitute for Srs2 in post replication repair in *rad5Δ* mutants. *rad5Δ* mutants are sensitive to MMS mostly due to Srs2 restricting homologous recombination (Pfander et al., 2005). It was previously shown that expression of hFbh1 in *rad5Δ* mutants could suppress DDT repair defects (Chiolo et al., 2007) and we were interested in testing hFbh1 and hRTEL1 in our system.

A second goal of my research was investigation of the function of alternative clamp loader, Ctf18 at CAG repeats. Ctf18 is important for overall genome stability having a prominent role in promoting proper sister chromatid cohesion and replication. Previous work has shown Ctf18 was specifically important in preventing $(CAG)_{70}$ and $(CAG)_{155}$ repeat fragility and instability while the other alternative clamp loaders, Egl1 and Rad24, did not have as great of an effect on either (Gellon et al., 2011). The mechanism of repeat protection is occurring independently from Ctf18's role in cohesion (Gellon et al., 2011), leading us to

question how Ctf18 might function to prevent repeat fragility. Some key pieces of evidence led us to further investigate the relationship between Ctf18 and DDT. In the absence of Ctf18, there is an increase in Rad52 foci during S phase, indicative of damage occurring during replication (Gellon et al., 2011; Lisby et al., 2001). DDT is coordinated by modification of PCNA when replication forks encounter DNA damage during S phase. Since Ctf18 has been shown to interact with PCNA and has been biochemically shown to be capable of unloading/loading PCNA onto DNA substrates, could Ctf18 and DDT be working together to prevent repeat fragility? If so, are both the error-prone and error-free pathways needed? Could Srs2, which is recruited to SUMOylated PCNA, also protect against fragility through the same pathway as Ctf18 or are the pathways complimentary?

My research focuses on how cells utilize various repair mechanisms to protect genome integrity. Using CAG repeats as a source of endogenous DNA damage, we've been able to highlight the need for hairpin structure removal, controlled recombination, and proper hairpin bypass to allow cells to properly replicate. Failure to do so leads to an increase in genome instability.

Chapter 2

Differential requirement of Srs2 helicase and Rad51 displacement activities in replication of hairpin-forming CAG/CTG repeats

Authors:

Jennifer Nguyen^, David Viterbo#, Ranjith Anand^, Lauren Verra^, Laura Sloan^, Guy-Franck Richard# and Catherine H. Freudenreich^

^Department of Biology, Tufts University, Medford MA 02155, USA

Institut Pasteur, Génétique Moléculaire des Levures, Department Genomes & Genetics, CNRS, UMR3525, Université Pierre et Marie Curie, UFR927, 25 rue du Dr Roux, F-75015 Paris, France

Currently in submission at Nature Structure and Molecular Biology

Author contributions:

Jennifer Nguyen: performed Srs2 domain no tract and CTG_{70} fragility assays, contributed to Srs2 domain CAG_{70} fragility and instability assays, Mph1 fragility and instability assays, data analysis, and contributed to the first draft of introduction and results

David Viterbo: performed the CTG_{98} 2D analyses and data analysis

Ranjith Anand: contributed to Srs2 domain CAG_{70} fragility and instability assays, data analysis, and contributed to the first draft of introduction and results

Lauren Verra: performed the rad5Δ no tract and CAG_{70} fragility and instability assays

Laura Sloan: contributed to the srs2-(1-998) CAG_{70} fragility assays

Guy-Franck Richard: supervised 2D gel experiments and analysis; participated in manuscript writing and editing

Catherine Freudenreich: planned and supervised experimental design and data analysis, authored the discussion and remaining drafts

ABSTRACT

Endogenous replication-blocking DNA secondary structures are a source of genome instability. Trinucleotide repeats cause replication fork stalling, chromosome fragility, and impaired repair, all of which can lead to repeat expansions and contractions. Specialized helicases play an important role in unwinding DNA structures to maintain genome stability. The Srs2 helicase unwinds DNA hairpins, facilitates replication, and prevents repeat instability and fragility. However, since Srs2 is a multifunctional protein with both helicase activity and the ability to displace the Rad51 recombinase, it was unclear which functions were required for its various protective roles. In the current study, we take advantage of characterized Srs2 separation-of-function alleles to clarify its vital activities. Our data suggests that the Srs2 protein locates to the stalled fork via its interaction with PCNA and utilizes its helicase activity to unwind a fork-blocking CAG/CTG hairpin structure. In the absence of recruitment of Srs2 to SUMOylated PCNA or in helicase-deficient mutants, the lack of hairpin unwinding leads to an accumulation of reversed forks and fork breakage. Independent of PCNA binding, Srs2 also displaces Rad51 from nascent strands to prevent recombination-dependent repeat expansions and contractions. These results clarify the role of Srs2 in facilitating fork restart at replication-blocking hairpin lesions.

INTRODUCTION

Aside from the various known exogenous factors such as ultraviolet light, base modifying chemicals and ionizing radiation that can negatively impact genome

instability (Jackson and Bartek, 2009; Lindahl, 2000), it is increasingly recognized that genome instability and disease can often result from endogenous replication-blocking sources such as DNA secondary structures (Aguilera and García-Muse, 2013; Usdin et al., 2015; Wang and Vasquez, 2014). Recent evidence supports a role for specialized helicases to copy through replication-blocking structures faithfully and maintain genome stability; known examples include Rrm3 helicase for programmed protein blocks (Ivessa et al., 2003), Pif1 for G-quadruplex sequences (Bochman et al., 2012; Paeschke et al., 2011; Ribeyre et al., 2009) and Srs2 for hairpin sequences (Anand et al., 2012; Bhattacharyya and Lahue, 2004, 2005; Daee et al., 2007; Kerrest et al., 2009).

Triplet repeat expansions are known replication-blocking lesions and have been implicated in many hereditary neurodegenerative diseases (McMurray, 2010; Mirkin, 2007; Pearson et al., 2005). A common property shared among disease-causing repeat sequences is their ability to form non-B DNA conformations in single stranded DNA. CAG/CTG repeats, which have been implicated in Huntington's disease, myotonic dystrophy, and multiple spinocerebellar ataxias, are capable of forming hairpin structures (Liu et al., 2010; Miret et al., 1998; Pearson and Sinden, 1996). These structure-forming sequences can interfere with cellular processes such as replication, transcription, and repair, causing stalled forks, nicks, gaps or double-strand breaks in the DNA. (Mirkin, 2007; Richard et al., 2008; Usdin et al., 2015). Paradoxically, the processes of replication fork restart or DNA repair must then occur within the repeat DNA, providing opportunity for expansions or contractions during DNA synthesis or end processing.

In *Saccharomyces cerevisiae*, it has been shown that the Srs2 helicase is a key protein involved in unwinding CAG/CTG hairpin structures (Anand et al., 2012; Bhattacharyya and Lahue, 2004, 2005). The Srs2 helicase is a member of superfamily 1 helicases with 3' to 5' polarity and homology to the helicase domains of *E. coli* RepA and UvrD (Aboussekhra et al., 1989; Hall and Matson, 1999; Rong and Klein, 1993). Unlike RepA and UvrD, Srs2 has an extended C-terminal region that contains domains that facilitate protein-protein interactions, including with the Rad51 recombinase (Krejci et al., 2003; Veaute et al., 2003) and the DNA replication clamp PCNA (Papouli et al., 2005; Watts, 2006). Srs2 is required to prevent expansions of short $(CAG/CTG)_{13-25}$ repeats (Bhattacharyya and Lahue, 2004) and longer $(CAG/CTG)_{55-70}$ repeats (Kerrest et al., 2009). The role of Srs2 in preventing repeat expansions is specific for hairpin-forming triplet repeats, because *srs2* mutants did not exhibit increased instability of poly (GT) dinucleotide repeats, non-structure forming CTA repeats, or unique sequences with similar GC content (Bhattacharyya and Lahue, 2004). Furthermore, Srs2 was able to facilitate replication through a fork stall caused by a $(CGG/CCG)_{40}$ repeat *in vivo*, whereas Sgs1, Pif1 and Rrm3 helicases did not (Anand et al., 2012). Srs2 did not act on other types of replication barriers such as a G-quartet-forming sequence or a protein-mediated stall (Anand et al., 2012). The ability of Srs2 to facilitate replication through the hairpin stall was dependent on both its ATP-dependent helicase activity and its interaction with PCNA, but not on ability to interact with and displace Rad51 (Anand et al., 2012). Thus, due to its interaction with SUMOylated PCNA, Srs2 seems to be uniquely positioned to unwind hairpin structures at an advancing fork and thereby facilitate replication through triplet repeats. Recently, it was shown that the RTEL1 helicase in human cells can perform some of the same functions as Srs2 in both human and yeast

cells, including CAG and CTG hairpin unwinding and prevention of CAG expansions and repeat fragility (Frizzell et al., 2014).

Another important Srs2 function is the ability to dismantle Rad51-mediated filament formation by stimulating Rad51's ATP hydrolysis activity to promote disassociation off of DNA (Antony et al., 2009; Krejci et al., 2003; Veaute et al., 2003). Previous work has shown that recombinational repair can be a source of triplet repeat expansions (Gellon et al., 2011; Richard and Pâques, 2000; Richard et al., 2003; Sundararajan and Freudenreich, 2011). For longer $(CAG/CTG)_{55\text{-}70}$ repeats, expansions and contractions in cells deleted for *SRS2* were suppressed by deletion of *RAD51* (Kerrest et al., 2009). Thus we proposed that the repeat instability occurring in the *srs2Δ* background was due to excess sister chromatid recombination.

In addition to a role for Srs2 in preventing CAG repeat instability, we identified two other roles for Srs2 at expanded CAG/CTG repeat tracts in our previous study (Kerrest et al., 2009). First, we showed that Srs2 prevented fragility (breakage) of a $(CAG)_{70}$ or $(CTG)_{70}$ tract integrated on a yeast chromosome (e.g. in both orientations with respect to replication; the sequence on the lagging strand template is named). The absence of Srs2 led to a 2 to 6 fold increase in fragility over wild-type. Secondly, by analysis of replication intermediates, we identified structured DNA molecules, which we termed joint molecules (JMs), that appeared when a $(CTG)_{55}$ tract was replicated in wild-type cells. JMs were dependent on the repeat tract and also on Srs2, since they were severely reduced in a *srs2Δ* background, but were not significantly reduced in the absence of Rad51. We previously proposed that these JMs represented reversed forks (Kerrest et al., 2009). This was based on the appearance of the JMs as a

cone structure emanating from the location of the repeat tract on the Y arc of replication intermediates as well as dependence on replication and independence from Rad51 (Kerrest et al., 2009).

Additionally, CTG repeats are predisposed to undergo fork reversal in a plasmid assay (Fouché et al., 2006). If this was the case, expanded CTG repeats represent a natural site of *in vivo* fork reversal, and their formation in wild-type cells suggested that fork reversal may be a way to replicate through a repeat structure without fork breakage, recombination, or changes in the number of repeat units. JMs could also represent a mixture of reversed forks and other kinds of structured recombination intermediates that would show aberrant migration and are distinct from migrations of classic X-shaped structures such as Holiday junctions or replication-coupled sister-chromatid junctions due to hairpin structures formed by CAG/CTG trinucleotide repeats (Kerrest et al., 2009). The reduction of the joint molecules/reversed forks in ***srs2Δ*** cells suggested a role for Srs2 in formation or stabilization of reversed fork structures *in vivo*.

Because Srs2 is such a multifunctional protein, it wasn't clear which activity was involved in each of its roles in maintaining CAG repeats (instability, fragility, JM formation). To understand the role of Srs2 at CAG repeats and in genome maintenance in general, here we take advantage of multiple well characterized Srs2 domain mutants missing one or more of the protein's functions (Le Breton et al., 2008; Colavito et al., 2009; Krejci et al., 2003, 2004; Pfander et al., 2005). Using this approach, we were able to find that there is a differential requirement of Srs2 helicase activity, PCNA binding, and Rad51 displacement functions in CAG/CTG repeat instability, fragility, and fork reversal. The Srs2-PCNA interaction is required to prevent repeat fragility but dispensable for preventing

repeat instability, whereas Rad51 displacement is vital for prevention of instability, but not fragility. JMs appear to be a mixture of reversed forks that occur independently of Srs2 and are processed by Exo1, and recombination intermediates that are prevented by Srs2 Rad51 displacement activity; this further expands on our previously proposed hypothesis (Kerrest et al., 2009). Our data support a role for Srs2 helicase unwinding of structures encountered during replication in facilitating fork restart and prevention of fork breakdown. We also investigated the role of Mph1 and Rad5 in maintaining CAG repeats and found that unlike Srs2, they play a more modest role in preventing $(CAG)_{70}$ repeat instability, do not affect repeat fragility, and deletion mutants exhibit increased JMs, not reduced as predicted if Rad5 or Mph1 played an active role in fork regression. Together these results show that multiple functions contribute to triplet repeat maintenance, and reveal important roles for the Srs2 protein in preventing fork breakdown and recombination at structure-forming barriers in the genome.

MATERIALS AND METHODS

Strains

All strains used for instability and fragility experiments were the isogenic BY4705, BY4742 or S288C backgrounds (Appendix 2.1) and contained a yeast artificial chromosome containing no repeat, a $(CAG)_{70}$ or a $(CTG)_{70}$ tract as previously described (Callahan et al., 2003; Sundararajan and Freudenreich, 2011). Gene knockouts were generated by directed gene replacement and confirmed by PCR for absence of the target gene and presence of the marker gene at the target

locus. Key mutants were also checked via Southern using DIG-high prime labeling and detection (Roche) using probes hybridizing to marker genes to confirm proper integration location. Srs2 domain mutants were created by PCR-mediated gene replacement using yeast genomic DNA or plasmids as templates: *srs2-(1-860)*, *srs2-(875-902Δ)*, and *srs2-(1-998)* were obtained from Patrick Sung (Colavito et al., 2009), and *srs2-K41R* was obtained from Hannah Klein (Colavito et al., 2009; Krejci et al., 2004). All inserted mutations were confirmed by PCR and sequencing; primer sequences available upon request. The presence of the YAC and the length of the CAG or CTG tract was confirmed by PCR amplification followed by size analysis of the product on a high resolution 2% Metaphor gel.

Analysis of CAG/CTG repeat stability and fragility

Fragility and instability assays were done as previously described (Kerrest et al., 2009). Briefly, single colonies were grown on yeast complete (YC) media lacking uracil and leucine to maintain YAC selection. Tract lengths were confirmed by PCR amplification from cells from these starting colonies using primers flanking the repeat. Cells were resuspended in YC-Leu liquid media, grown at 30^{o}C for 6-8 divisions, and plated on 5-FOA selective media. The rate of 5-FOA^{R} was calculated by the method of the maximum likelihood using FALCOR software. YAC end loss was confirmed in a subset of FOA^{R} colonies to be 94-100% for (CAG/CTG)70 YACs in both wild-type and *srs2* strain backgrounds (30-50 independent clones checked for each). The stability of the repeat tract was analyzed via PCR amplification of cells from daughter colonies that grew on YC-Leu total cell count plates using primers 2076/2077, which flanked the repeat. Amplicons were visualized using high resolution 2% Metaphor gels (Lonza),

which can accurately resolve +/- 9 bp (3 repeats) in the relevant size range; repeat size estimates were made by subtracting the unique sequence length of 159 bp and dividing by three.

Analysis of replication intermediates by 2D gels

Cells were grown overnight at 23°C, in 200 ml YPD cultures. In the morning, they were centrifuged, washed and resuspended in 800 ml fresh YPD medium at a concentration of 0.8-0.9x10^7 cells per ml and grown for another hour at 23°C. Subsequently, 10 mg alpha factor were added to the culture for two and a half hours at 23°C. G1 arrest was checked by microscope observation. When 90% of the cells were arrested, the culture was washed and resuspended in 200 ml fresh YPD medium preheated at 23°C. Progression of S phase was followed by microscope observation and confirmed by FACS analysis on a MACSQuant Analyser (not shown). Cells were harvested after 30 min, 40 min, 60 min and 90 min for the wild-type strain, or 40 min, 50 min, 60 min and 90 min for mutant strains, and killed by addition of sodium azide (0.1% final concentration). Total genomic DNA was extracted by the CTAB procedure (Liberi et al., 2006) with the following modifications: Cells were frozen one night at -80°C, thawed on ice, resuspended in 2 ml water and 2.5 ml solution I (2% CTAB, 1.4 M NaCl, 100 mM Tris HCl pH 7.6, 25 mM EDTA pH 8.0) was added. Then, 167 µl Zymolyase 100T (Seikagaku, 30 mg/ml) and 5 µl DTT (2M) were added and tubes were left 1 hour at 30°C. After that step, the CTAB extraction and the gel set up were performed as described in (Liberi et al., 2006). DNA was transferred overnight in 10X SSC on a charged nylon membrane (Sigma) and UV cross-linked on a Stratagene Stratalinker. Hybridization was performed with a 750 bp randomly primed probe,

corresponding to the 5' end of the *ARG2* gene. Detection of radioactive signals were performed on a Fujifilm FLA-9000, after 4-7 days exposure. Quantifications were made using the ImageQuant software. Individual shapes were drawn around each structure (Y arc, cone, pause, linear DNA). Shapes with identical areas were used in a uniformly unlabeled part of the gel for background calculation. After signal correction by background subtraction, intensity of JMs was determined by: (Cone signal/Y arc signal)/(Cone area/Y arc area). In the wild-type strain, this ratio is 0.5 on the average, meaning that the cone contains half as much signal per square millimeter as compared to the Y arc. Only gels with a good Y arc signal to background ratio (>1.2) were used in quantifications. Statistical analysis was performed with the R package (G. Millot, 2011, Comprendre et réaliser les tests statistiques à l'aide de R. Manuel de biostatistique. de boek ed. 2° edition). Statistical tests were performed on pooled data collected at all time points, for each strain.

RESULTS

Srs2 ATPase and Rad51 displacement activities are required for preventing CAG/CTG repeat instability

Srs2 is a multifunctional protein with three major domains defined: a helicase domain, a Rad51 interacting domain, and a $PCNA^{SUMO}$ interacting domain. Previously characterized domain mutants that have at least one of the functions of Srs2 attenuated (Le Breton et al., 2008; Colavito et al., 2009; Krejci et al., 2003; Pfander et al., 2005) (Figure 1A) were used to investigate whether there was a differential requirement for these domains in preventing repeat instability.

The endogenous *SRS2* gene was replaced with each of these domain mutants at the *SRS2* chromosomal locus. Yeast strains contained a yeast artificial chromosome (YAC) with a CAG/CTG tract of 70 repeats. PCR amplification of the repeat tract was used to determine expansion and contraction frequencies in daughter colonies of wild-type and mutant backgrounds (Figure 1B). Sequence nomenclature refers to the repeat that serves as the lagging strand template.

First, we tested to see if one of the catalytic activities of Srs2 was required to prevent $(CAG)_{70}$ repeat instability by using the *srs2-K41R* mutant, which is ATPase defective and therefore lacking both helicase and Rad51 displacement activities. The CAG orientation exhibits both elevated expansions and contractions in *srs2*Δ strains (Kerrest et al., 2009). Indeed, a significant increase in both expansion and contraction frequencies was observed in *srs2-K41R* strains (4.5 and 3.7 fold over wild-type, respectively), similar to the frequencies in *srs2*Δ strains (Table 1, Appendix 2.2). To distinguish between the helicase and Rad51 displacement activities, we tested the *srs2-(875-902Δ)* mutant, which retains the helicase domain but lacks most of the Rad51 binding domain and is defective for Rad51 displacement *in vitro* (Colavito et al., 2009) (Figure 1A). The *srs2-(875-902Δ)* mutant also had a significant increase in both repeat expansions and contractions, 3.6 and 3.8 over wild-type respectively, similar to *srs2-K41R* (Table 1). These results suggest that inability to bind and displace Rad51 is the likely cause of the increased level of CAG instability in *srs2*Δ strains. This conclusion is also supported by the *srs2-(1-860)* mutant, which retains the helicase domain but lacks the entire C terminus of the protein, including both the Rad51 and PCNA interaction domains. The *srs2-(1-860)* mutant also exhibited a significant increase in both expansions and contractions; interestingly the

contraction frequency was even higher than in the *srs2*Δ strain (12.5% compared to 6.5%), suggesting this mutant may have a dominant-negative effect. We previously showed that CAG instability was Rad51 dependent in an *srs2* null background (Kerrest et al., 2009). To confirm that this suppression also occurred in a background defective in Rad51 displacement, repeat instability was tested in the *srs2-K41R rad51*Δ double mutant. As predicted, CAG expansions and contractions were both suppressed to wild-type levels (Table 1). Together, these data support the conclusion that repeat instability arises through HR and that Srs2 prevents this instability by antagonizing HR via its Rad51 displacement activity.

In contrast to the Rad51 displacement deficient mutants, *srs2-(1-998)*, which retains both helicase and Rad51 displacement activity, had instability at wild-type levels, 1.5 and 1.3 fold over wild-type for expansions and contractions, respectively (Table 1). The *srs2-(1-998)* mutant is missing the PCNA interaction domain; therefore PCNA interaction is apparently not required to prevent repeat instability. Since Srs2 interacts with SUMOylated PCNA engaged in replication, this result suggests that expansions and contractions are not occurring during replication fork progression. Instead, instability appears to be occurring during a process where Srs2 is acting independently from its interaction with SUMOylated PCNA.

Table 1. $(CAG)_{70}$ Instability on YAC in Srs2 Domain Mutants

Strain Name	No. colonies analyzed	% Expansions	Fold Over WT	% Contractions	Fold over WT
wild-type	269	1.1	1.0	2.6	1.0
srs2Δ	231	5.6*	5.1*	6.5*	2.5*
srs2-(1-860)	152	5.3*	4.8*	12.5*	4.8*
srs2-(875-902Δ)	162	4.3*	3.6*	9.9*	3.8*
srs2-K41R	201	5.0*	4.5*	9.5*	3.7*
srs2-(1-998)	122	1.6	1.5	3.3	1.3
srs2-K41R rad51Δ	174	1.2	1.1	1.7	0.7

*p<0.05 compared to wild-type using Fisher's Exact Test

Srs2 helicase activity and PCNA interaction are required to prevent CAG/CTG repeat fragility

It was previously shown that in the absence of Srs2, there is a significant increase in CAG repeat fragility (Kerrest et al., 2009). We therefore wanted to investigate whether there was a differential requirement of the Srs2 functions in preventing repeat fragility. To determine if there were differences depending on which repeat sequence was on the lagging strand template, we tested the rate of FOA-resistance (FOA^R) in both CAG and CTG orientations utilizing a previously described breakage assay that measures YAC end loss (Kerrest et al., 2009) (Figure 1B).

We hypothesized that the *srs2-K41R* strain would exhibit an increase in repeat fragility because the mutant protein lacks both helicase and Rad51 displacement activity. Indeed, a significant 2.3 fold increase in $(CAG)_{70}$ and 2.1 fold increase in

$(CTG)_{70}$ fragility compared to wild-type were observed, statistically equivalent to the rates for the *srs2*Δ strain (Figure 1C, Table S3). As we observed previously (Kerrest et al., 2009), deleting *SRS2* had a greater effect on fragility of tracts in the CAG orientation. To distinguish which activity was important, we tested the *srs2-(875-902Δ)* mutant lacking Rad51 binding. We saw no increase in fragility in either orientation, indicating that, in contrast to the result observed for instability, the Rad51 displacement activity is dispensable for preventing fragility. Further, this result implicates the ATPase activity of Srs2 in preventing both CAG and CTG fragility.

To determine the contribution of PCNA interaction, we tested the s*rs2-(1-998)* mutant. A significant 2.8-fold increase in $(CAG)_{70}$ and 1.5-fold increase in $(CTG)_{70}$ fragility compared to wild-type was observed, rates similar to a complete deletion of *SRS2* (Figure 1C). Therefore, Srs2 interaction with PCNA is crucial to prevent repeat fragility. This result contrasts with the effect of the *srs2-(1-998)* mutant on instability, where lack of PCNA binding had no effect. The increase in fragility in *srs2-(1-998)* is not due to loss of the Srs2 SUMOylation sites in the C-terminus, as mutation of those sites to non-modifiable residues did not have the same effect (data not shown). Furthermore, the *srs2-(1-860)* mutant, which retains helicase activity but lacks the PCNA interaction domain, also exhibited a significant increase $(CAG)_{70}$ fragility compared to wild-type. In conclusion, Srs2 PCNA interaction and helicase activity are both needed to prevent fragility of expanded CAG/CTG repeats. Thus prevention of repeat fragility and instability are mediated by different functions of the Srs2 protein. In addition, the absolute requirement for PCNA interaction suggests that Srs2 is preventing fragility via its helicase activity while located at the replication fork.

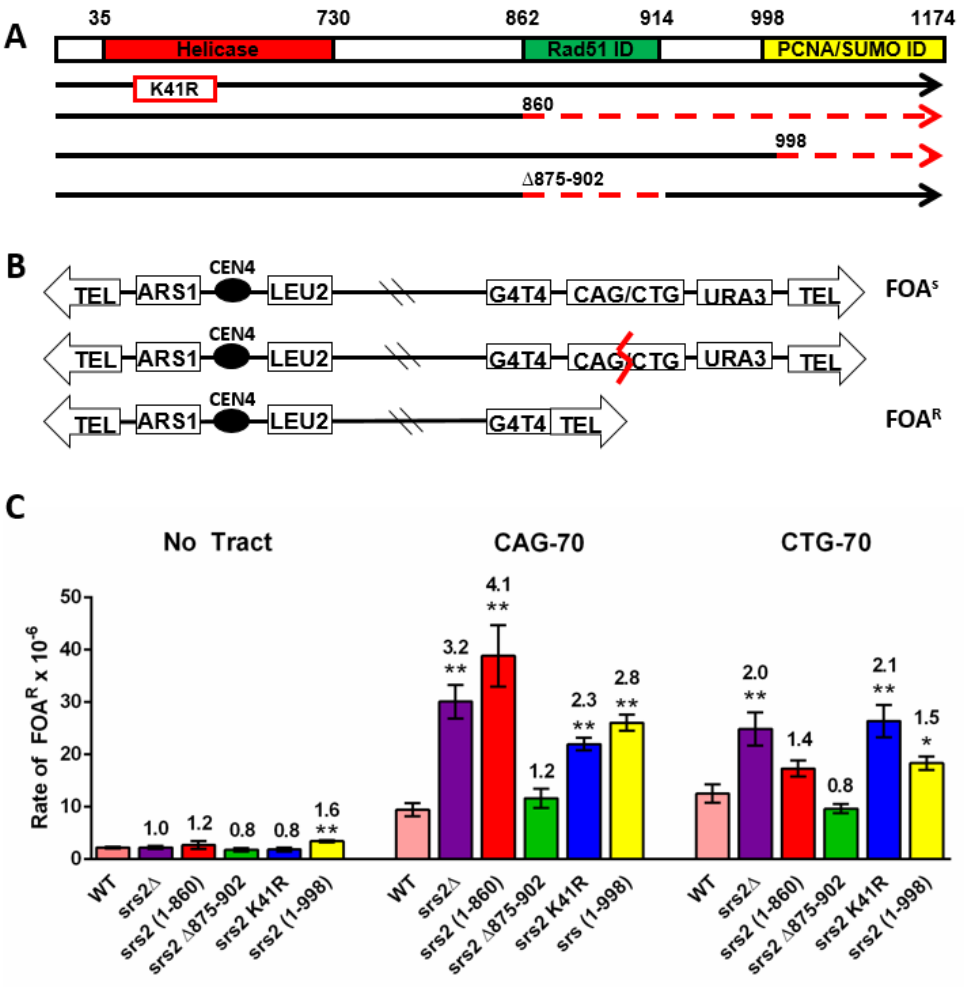

Figure 1. (**A**) Schematic of Srs2 domain mutants used in this study. The red box represents the helicase domain, the green box indicates the Rad51 interacting domain, and the yellow box indicates the PCNA interacting domain. Dotted red lines represent deletions, numbered according to base-pair position of the *SRS2* ORF. *Srs2-K41R* renders Srs2p ATPase dead, no helicase or translocase activity. *Srs2-(1-860)* retains helicase function but cannot interact with Rad51 or PCNA. *Srs2-(1-998)* lacks PCNA interaction but has intact helicase and translocase activities. *Srs2-(875-902Δ)* retains helicase activity and PCNA interaction but has impaired Rad51 interaction. (**B**) Schematic of the YAC system. A breakage event occurring within or near the repeat can result in the

loss of the URA3 marker gene and healing at the G_4T_4 telomere seed, leading to strains becoming resistant to 5-fluoroorotic acid (5-FOA). (**C**) Rate of FOA^R x 10^{-6} is shown. Data represents the average of at least three experiments (numbers in Appendix 2.3). Error bars represent SEM. Numbers of bars represent fold over wild-type. No tract: no repeat tract on YAC, CAG-70: $(CAG)_{70}$ repeats on the lagging strand template, CTG-70: $(CTG)_{70}$ repeats on the lagging strand template. (Unpaired student t-test comparing averages to wildtype *p<0.05; **p<0.01; *srs2-(1-860)* $(CTG)_{70}$ p value is 0.06).

Mph1 and Rad5 play a lesser role in preventing $(CAG)_{70}$ instability and fragility

In addition to Srs2, several other proteins could be involved in regulation of recombination or fork restart including Rad5, Mph1 and Sgs1. The Sgs1 helicase was shown to have a role in preventing $(CAG/CTG)_{70}$ repeat instability and fragility (Kerrest et al., 2009), however the effect of Mph1 and Rad5 on long CAG repeats had not been fully determined.

Mph1 is a 3' to 5' helicase and FANCM homolog that regulates recombination by unwinding Rad51 formed D-loops (Prakash et al., 2009) and processes Holliday junction intermediates through branch migration (Zheng et al., 2011). Cells deleted for Mph1 exhibited a 2-2.5-fold increase in both repeat contractions and expansions, respectively, though neither effect is statistically different from wild-type (Table 2). Deletion of Mph1 resulted in a rate of $(CAG)_{70}$ breakage that is also slightly elevated compared to wild-type (1.5 fold, p=0.024, Figure 2). Altogether, Mph1 appears to have a minor role in preventing chromosomal

instability and fragility at CAG repeats.

Rad5 is a DNA-dependent ATPase and E3 ubiquitin ligase involved in the error-free branch of DNA damage bypass. The Rad5/Mms2/Ubc13 complex catalyzes PCNA polyubiquitination to facilitate a template switch of the nascent strand to copy information from an alternative template (usually the other nascent strand) (Branzei, 2011). Previous studies have shown that in the absence of Rad5, there is a reduction in instability of several types of non-hairpin forming repeats including poly$(GT)_{29}$ (Johnson et al., 1992), $(ATTCT)_{60}$ (Cherng et al., 2011), and $(GAA)_{100}$ (Shishkin et al., 2009), when compared to wild-type. In contrast, deletion of Rad5 led to a 4-6 fold increase in expansion rate in short $(CAG/CTG)_{13\text{-}25}$ repeat tracts (Daee et al., 2007) and a 3-fold increase in longer $(CAG)_{85}$ tracts (House et al., 2014). To have a direct comparison with the Srs2 domain mutants, *RAD5* was deleted in strains with $(CAG)_{70}$ repeats, and both instability and fragility were measured. Deletion of *RAD5* led to a slight increase in repeat expansions and contractions (1.9 and 1.8 fold increase compared to wild-type, respectively) (Table 2). Deletion of *RAD5* led to no significant change in CAG repeat fragility when compared to wild-type (Figure 2). We conclude that Rad5 does not have a major role in maintenance of $(CAG)_{70}$ repeats, at least in a wild-type background.

Table 2. $(CAG)_{70}$ Instability on YAC in *srs2*Δ, *mph1*Δ, *rad5*Δ Mutants.

Strain Name	No. colonies analyzed	% Expansions	Fold Over WT	% Contractions	Fold over WT
wild-type	269	1.1	1.0	2.6	1.0
srs2Δ	231	5.6*	5.1*	6.5*	2.5*
*mph1*Δ	290	2.8	2.5	5.2	2.0
*rad5*Δ	190	2.1	1.9	4.7	1.8

*p<0.05 compared to wild-type using Fisher's Exact Test

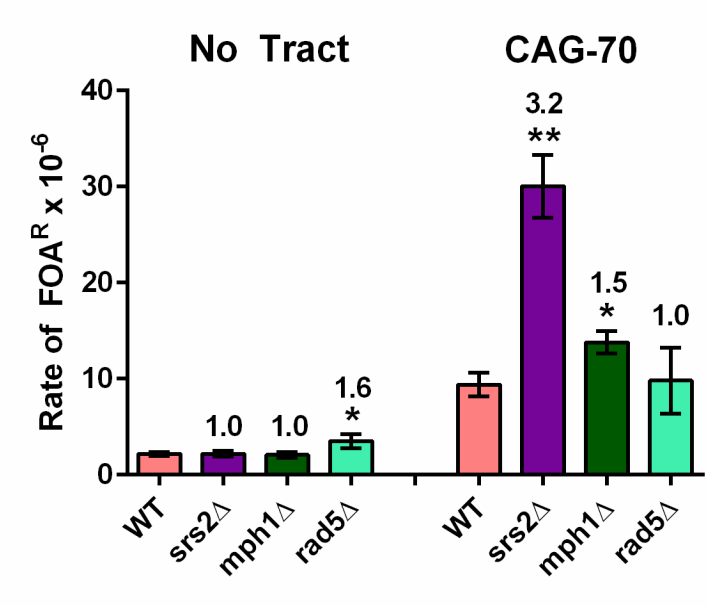

Figure 2. Deletion of MPH1 or RAD5 does not impact $(CAG)_{70}$ repeat fragility. Rate of FOA^R x 10^{-6} is shown. Data represents the average of at least three experiments (Appendix 2.3). Error bars represent SEM. Numbers over bars represent fold over wild-type. No tract: no repeat tract, CAG-70: $(CAG)_{70}$ repeats on YAC. (Unpaired t-test comparing averages to wildtype *p<0.05; **p<0.01)

Analysis of replication and recombination intermediates by 2D gel electrophoresis in Srs2 domain mutants

In our previous study, we identified joint molecules (JMs) that occurred during replication of a $(CTG)_{55}$ trinucleotide repeat tract that were dependent on the presence of Srs2, suggesting a role for Srs2 in formation or stabilization of reversed fork structures *in vivo* (Kerrest et al., 2009). In order to better characterize this function of Srs2, replication of a $(CTG)_{98}$ repeat tract integrated at the same *ARG2* locus on yeast chromosome X was analyzed by 2D gel electrophoresis in the *srs2* domain mutants. This locus is replicated by an efficient origin (ARS1010) located 7 kb telomere-proximal to the repeats in the CTG orientation, in which the CTG strand, which can form a stable hairpin structure, is the lagging-strand template.

DNA extracted 30-60 minutes after release into S phase from a G1 arrest was analyzed for replication intermediates by 2D gel electrophoresis. In wild-type cells, a signal corresponding to replication fork stalling is detected on the descending Y arc, at the exact place where the triplet repeats are integrated (Figure 3, wild-type, arrow). Such a pausing signal was not clearly detected with shorter repeats (Kerrest et al., 2009). We conclude that $(CTG)_{98}$ repeats stall forks more efficiently than $(CTG)_{55}$ repeats, likely because this longer repeat tract has a higher probability of hairpin structure formation. Interestingly, the JMs are somewhat less prominent for the CTG_{98} tract compared to $(CTG)_{55}$, suggesting there could be an inverse relationship between a stable fork stall and JMs. None of the *srs2* mutants showed any evidence for a stalling signal, showing that the

presence of a full-length functional Srs2p is essential to stably stall forks at long chromosome-borne CTG repeats.

In order to identify which part of the Srs2 protein was responsible for JM formation, the JM signal intensity was quantified in comparison to the Y arc in the wild-type strain and the different *srs2* mutants. In *srs2-(1-998)* and *(1-860)* mutants, the amount of JMs is not different from wild-type (Figure 3). We conclude that the C-terminal part of the protein, interacting with PCNA, is not required for JM formation or maintenance.

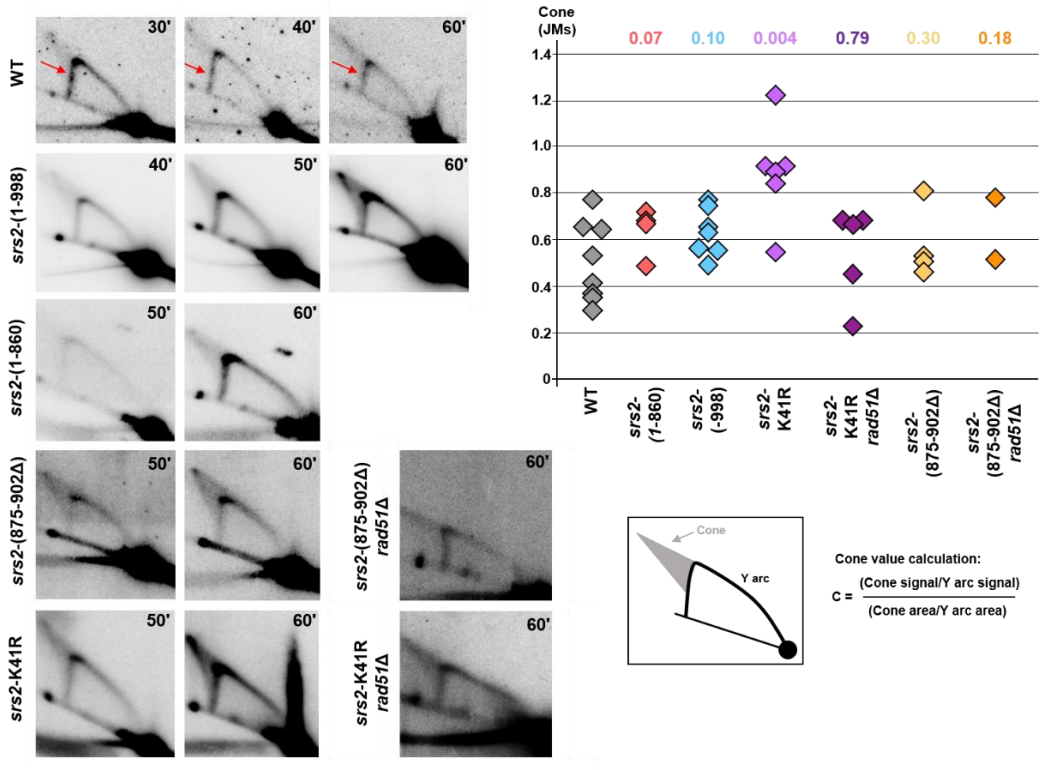

Figure 3. Representative 2D gels for wild-type and *srs2* mutant strains. Times at which cells were collected after alpha-factor release are indicated in the top right corner of each gel. Quantifications of the ratio of cone (JMs) over Y arc signals

obtained for each individual gel in a particular background are shown on the accompanying graph. P values compared to wild-type (Mann-Whitney Wilcoxon rank test) are listed above the quantifications. Arrows point to the site where replication pauses are clearly visible. Mean quantified pause signals and cone values for individual gels are given in Appendix 2.4.

It was shown that in the absence of helicase catalytic activity, Srs2p cannot unwind CAG/CTG hairpins (Anand et al., 2012). If the decrease in JMs in the *srs2Δ* strain was due to the helicase activity of Srs2 actively reversing hairpin-stalled forks, they should also decrease in a *srs2* helicase deficient strain. Surprisingly however, JMs were significantly increased in the *srs2-K41R* mutant, as compared to wild-type (Figure 3). Since the ATPase is needed for both the helicase and the Rad51 displacement activity, the increase in JMs in the *srs2-K41R* mutant could be due to increased Rad51 binding and a resultant increase in recombination structures. To test this idea, replication intermediates were visualized in a *srs2-K41R rad51Δ* double mutant. Notably, the JMs decreased to the wild-type level in the double mutant (Figure 3). Thus, in the *srs2-K41R* mutant, there is an accumulation of recombination intermediates that run in the same area as the reversed forks, though we note that the signal is especially high at the tip of the cone in this background, where X-shaped recombination intermediates are known to migrate. This data is consistent with the result that recombination-dependent repeat instability is occurring in the *srs2-K41R* background (Table 1). In contrast, the JMs that remain in the *srs2-K41R rad51Δ* double mutant are presumably not recombination intermediates (or perhaps Rad-51 independent template switch intermediates); similar to the situation in wild-

type cells where the cone structure was not measurably reduced in the *rad51Δ* background (Kerrest, 2009). We conclude that the JMs that represent reversed forks are not likely to be created by active Srs2 helicase activity.

Replication intermediates were also visualized in the *srs2-(875-902Δ)* mutant, lacking efficient Rad51 displacement activity but retaining helicase activity. The *srs2-(875-902Δ)* mutant showed no difference in the level of JM structures compared to wild-type, despite the expectation that recombination intermediates may increase in this background (Figure 3). We conclude that the presence of the helicase activity combined with PCNA binding is sufficient to unwind hairpin structures encountered at the fork to prevent undue accumulation of recombination intermediates (though apparently not to prevent all excess recombination as repeat instability was increased in this background).

Altogether, analysis of replication intermediates indicates that structured intermediates formed during replication of a hairpin-forming CAG/CTG repeat do not require Srs2 for their formation, but are influenced by Srs2p activity. In particular, Srs2 anti-recombinase function is important for preventing accumulation of fork-associated recombination structures that lead to increased repeat expansions. Fork-coupled helicase activity appears to be most important for preventing fork breakdown and chromosome fragility, rather than causing fork reversal.

Effect of Rad5 and Mph1 on CAG repeat replication

In vitro studies have shown that both Mph1p and Rad5p can convert model fork substrates to a 4 stranded reversed-fork like structure (Blastyák et al., 2007; Gari

et al., 2008; Kang et al., 2012; Sun et al., 2008; Zheng et al., 2011). Thus, it has been speculated that these proteins may catalyze fork reversal *in vivo*. To test the effect of these proteins on replication through CAG repeats, replication intermediates were analyzed in *mph1*Δ and *rad5Δ* strains.

Interestingly, JMs are significantly increased in both *mph1*Δ and *rad5Δ* strains (Figure 4). This result shows that neither protein is required to generate JMs, suggesting that either they are not involved in fork reversal *in vivo*, or that the JMs present in these backgrounds do not represent reversed forks. Since Mph1 is expected to reduce recombination intermediates by unwinding Rad51 formed D-loops, the observed increase in JMs in the *mph1Δ* background could be due to recombination intermediates at the CAG tract that are running in the area of the cone, perhaps in addition to reversed forks. However the increase of JMs in the *rad5Δ* strain which should decrease template switches, is somewhat counter-intuitive. The increase is mostly due to the spot at the tip of the spike, where Holiday Junctions are expected to run, suggesting a shift to recombination structures could be occurring.

To further investigate the nature of the JMs, replication intermediates were visualized in an *exo1Δ* mutant. In an *in vivo* fork reversal model in bacteriophage T4, it was shown that unprocessed reversed forks run as a spike off the Y arc in exonuclease deficient strains, which is converted to a cone structure in wild-type strains with exo-dependent fork processing (Long and Kreuzer, 2008). Exo1 has also been shown to process forks stalled by nucleotide depletion or a protein barrier (Cotta-Ramusino et al., 2005; Tsang et al., 2014). At the $(CTG)_{98}$ repeat, deletion of *EXO1* resulted in a reduction of the cone structure and an increase in JMs in a spike emanating from the top of the Y arc (Figure 4). This data supports

the idea that in wild-type cells, when recombination is controlled, the cone mostly represents resected reversed fork structures.

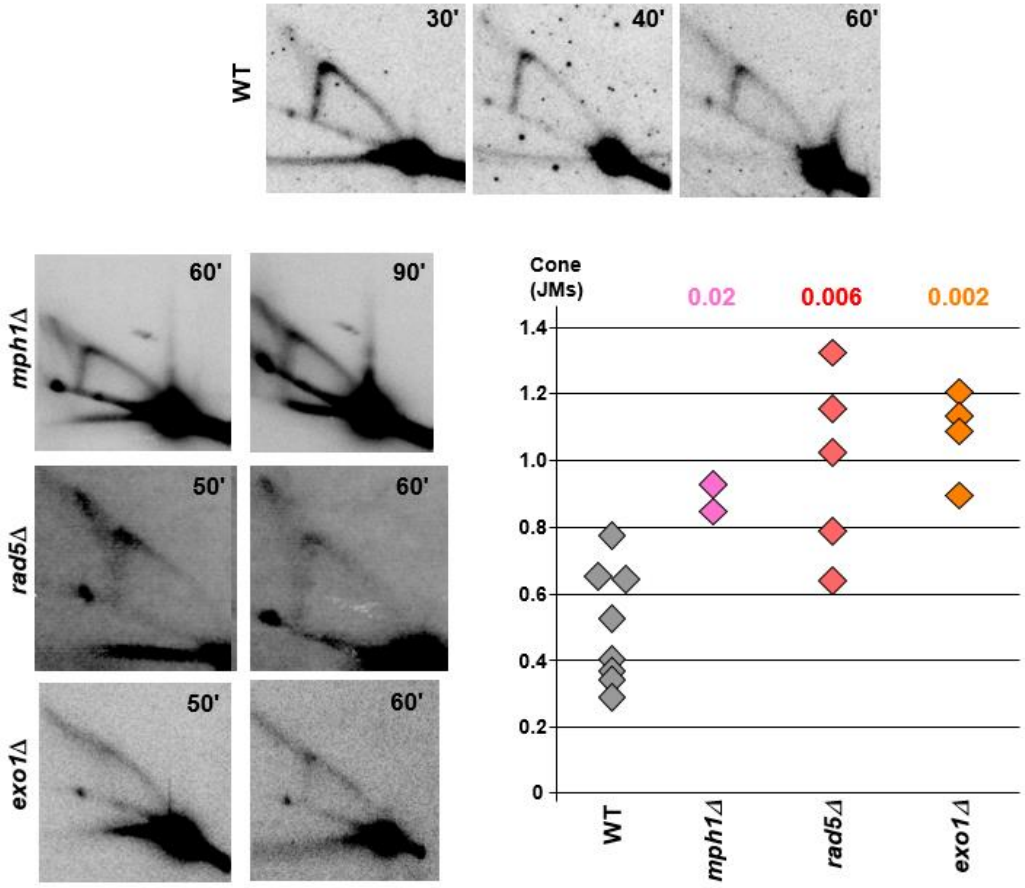

Figure 4. Representative 2D gels for *mph1Δ, rad5Δ,* and *exo1Δ* strains. Times at which cells were collected after alpha-factor release are indicated in the top right corner of each gel. Quantifications of the ratio of cone (JMs) over Y arc signals are shown on the accompanying graph; p values compared to wild-type (Mann-Whitney Wilcoxon rank test) are listed above the respective mutant. Mean quantified pause signals and cone values for individual gels are given in Appendix 2.4.

DISCUSSION

Srs2 prevents $(CAG/CTG)_{70}$ instability and fragility via different activities

Srs2 plays an important cellular role in genome maintenance at structure-forming repeats, but because of the multi-functional nature of this protein, it was unclear which activities protect against instability and fragility, and promote replication at CAG/CTG repeats. By using previously described Srs2 domain mutants, we investigated how the different Srs2 functions contribute to the maintenance of triplet repeats. We show that the CAG/CTG_{70} expansion and contraction phenotypes can be genetically uncoupled from the breakage phenotype. From our experiments, Rad51 displacement activity appears to be critical and PCNA interaction dispensable for preventing repeat expansions and contractions, whereas PCNA interaction and helicase activity are critical for preventing CAG/CTG_{70} breakage.

Since no significant increase in expansions or contractions were observed in the mutant where Srs2 retained its Rad51 displacement activity (*srs2-(1-998)*), it is likely that repeat instability is primarily arising from aberrant recombination as a result of unrestricted binding of Rad51. This conclusion is re-inforced by the observation of increased expansions and contractions in all the mutants with defective Rad51 displacement, as well as a reduction of instability levels in the *srs2-K41R rad51Δ* double mutant. This data re-inforces our previous conclusion (Kerrest et al., 2009) that recombination is a major source of triplet repeat instability if not properly controlled.

A consideration for this hypothesis is if Rad51-dependent recombination is a source of repeat instability, then *rad51* mutants should have no changes in

repeat tract length. Rather than seeing reduction in instability due to the loss of Rad51-dependent recombination, we either see no change in expansions or an increase in expansions and contractions in *rad51* mutants (Su et al., 2015; Sundararajan et al., 2010). One explanation is recombination isn't completely abolished in *rad51* mutants and recombination could be occurring through a Rad52/Rad59-dependent process, single strand annealing (SSA). During SSA repair, ssDNA with homology on either side of a double strand break can be annealed and ligated (Krejci et al., 2012). Repair of double strand breaks occurring within CAG/CTG repeats has been shown to most likely generate contractions (Richard et al., 2014). Studies have shown that Rad51 inhibits SSA, promoting repair with higher fidelity utilizing longer sequences of homology (Bai and Symington, 1996; Wu et al., 2008). Therefore in the absence of Rad51, SSA could be utilized for repair which could result in repeat instability, especially contractions which we do observe (Su et al., 2015).

Rad52 is a key player in recombination and in its absence recombination is greatly reduced but not eliminated (Rattray and Symington, 1994). Aside from Rad52, Rad54 can also function as a mediator for Rad51 filament formation although to a lesser extent (Wolner et al., 2003), suggesting that recombination could still occur even in the absence of Rad52. To fully confirm recombination as source of repeat instability, we should test *rad51Δrad52Δ* strains with the expectation of no tract changes if recombination is indeed a source of instability. However previous research has shown Rad52 is epistatic to Rad51 (Rattray and Symington, 1994), so perhaps instability could be arising in a mechanism that is not fully dependent on recombination or the other proteins involved in recombination can somehow facilitate recombination, albeit inefficiently.

Another consideration is perhaps recombination doesn't normally lead to repeat instability in wild-type cells but only when recombination regulation is perturbed. Only when cells have an increase in repeat instability due to unregulated recombination can a reduction be observed when recombination is removed.

The *srs2-(1-998)* allele that suppressed instability cannot interact with PCNA (Le Breton et al., 2008; Colavito et al., 2009; Pfander et al., 2005), suggesting that Srs2 prevents recombination-dependent repeat instability in a manner independent from the replication fork. Evidence supports that recruitment of Srs2 to replication and repair centers occurs independently of one another, as Srs2 can localize to Rad54 foci in the absence of PCNA interaction (Burgess et al., 2009). Perhaps the interaction between Srs2 and Rad51 can recruit Srs2 to presynaptic filaments, as other work has also shown Srs2 can prevent recombination independently from its PCNA interaction (Le Breton et al., 2008).

We hypothesize that in wild-type cells, the preferred pathway is to recruit Srs2 to SUMOylated PCNA to unwind template or nascent strand hairpins, perhaps in conjunction with transient fork reversal, and prevent recombination (Figure 5, top and middle pathways). However if Rad51 nucleation is not prevented, recombination can occur behind the replication fork. Instability can result when the nascent strand invades or anneals out of register, or due to hairpin-facilitated slippage during D-loop extension (Figure 5, left pathway). We note that Srs2 unwinding of hairpins on the nascent lagging strand has also been proposed as a pathway to prevent repeat expansions (see (Usdin et al., 2015; Viterbo et al., 2016), for review), and our data do not rule out this mechanism. Indeed, CAG expansions are slightly higher in the *srs2*Δ compared to *srs2-(875-902Δ)*, which can be accounted for by this second pathway.

Based on our genetic data testing triplet repeat fragility, it appears that Srs2 helicase activity is utilized primarily in the context of PCNA recruitment to the replication fork to prevent breakage. Although we cannot attenuate only the helicase activity since both helicase and Rad51 displacement are ATPase dependent, comparison of *srs2-(875-902Δ)* to the *srs2-K41R* mutant suggests that it is the helicase activity that is required to prevent chromosomal breakage. The helicase domain could be used to unwind hairpin structures to prevent replication stalling and fork collapse (Figure 5, right pathway). In agreement with this conclusion, both the Srs2 helicase activity and PCNA interaction are required for replication through CGG/CCG repeats, which form strong replication blocking hairpins (Anand et al., 2012).

Although previous research from our lab and others have shown breaks within the repeat can result in repeat expansion and contraction (Kerrest et al., 2009; Richard et al., 2014; Sundararajan et al., 2010), our *srs2-(1-998)* data highlights an aspect of the relationship between repeat instability and fragility: chromosomal breakage does not necessarily lead to repeat expansions and contractions. While the efficiency of repair in *srs2-(1-998)* is decreased or inefficient hairpin unwinding could result in higher levels of fragility, the fidelity of repair remains unchanged (wild-type levels of instability). This could be due to breakage events precluding the instability event therefore recovery of tract changes are rarely recovered.

Chromosome breakage possibly serves as an alternative method to rescue forks stalled at hairpins when unwinding fails. We note that in the CAG orientation, CTG template hairpins would be more likely to form on the leading strand template (not shown in Figure 5), which appears to be particularly deleterious in

the absence of Srs2 unwinding, leading to higher levels of fragility. The human RTEL1 helicase, which can unwind CAG and CTG hairpins, can complement Srs2 in yeast to prevent CAG repeat fragility (Frizzell et al., 2014). Since it also associates with SUMOylated PCNA at the replisome to prevent replication fork stalling and telomere fragility (Vannier et al., 2013), RTEL1 may be acting equivalently in human cells.

Formation of reversed forks and other joint molecules after fork stalling, and the role of Srs2.

Our previous study using a shorter $(CTG)_{55}$ repeat showed the appearance of a cone structure emanating from the location of the repeat tract on the Y arc of replication intermediates that was dependent on both the repeat tract and replication, but independent of Rad51 (Kerrest et al., 2009). Paused forks were not clearly visible. In the current study using a longer $(CTG)_{98}$ repeat, we were able to see a distinct pause signal in wild-type cells, showing that expanded CAG/CTG repeats on a eukaryotic chromosome pause replication, consistent with other recent results (Viterbo et al., 2016). Interestingly, this pause was not visible in any of the Srs2 mutants, suggesting that Srs2 is important for maintaining a stable paused fork, or preventing its conversion to alternate structures that would run off the Y arc, such as reversed forks or recombination intermediates.

In addition to paused replication, we observed a cone structure that appeared in replication intermediates from both wild-type and mutant strains, confirming that it is an inherent characteristic of CAG repeat replication. The precise molecular

nature of these structured molecules that run off the Y arc (JMs) is unclear, but their migration pattern is strongly reminiscent of structures detected in other systems that were concluded to be reversed replication forks (Courcelle et al., 2003; Long and Kreuzer, 2008, 2009; Lopes et al., 2001). Other authors have suggested that the cone-signal could be a mixture of replication molecules in which initiation occurs randomly outside the locus being analyzed (Schvartzman et al., 2012), leading to double Y structures with various points of fork convergence. In the present case, we find this hypothesis unlikely, since the replication origin normally used to replicate this locus is clearly identified (Raghuraman et al., 2001; Yabuki et al., 2002). In addition, to create the double Ys in this scenario, the JMs should be dependent on the level of fork stalling, increasing with more stalling, which is not the case; if anything there may be an inverse correlation. Our new data showing that the cone shifts to a spike in *exo1*Δ cells further supports the interpretation of reversed forks, as stalled and reversed forks are known to be processed by exonucleases in multiple systems, resulting in a reduced level of diversity and a tighter migration pattern of structured molecules (Cotta-Ramusino et al., 2005; Long and Kreuzer, 2008; Tsang et al., 2014).

Since the cone disappeared in cells lacking the Srs2 protein, it was possible that the Srs2 helicase function actively caused fork reversal. Surprisingly, we found that additional, not fewer, JMs were formed in the *srs2-K41R* ATPase mutant that is lacking both helicase and translocase activity. Further analysis indicated that the additional JMs that occur in the *srs2-K41R* mutant are Rad51-dependent, and thus may be distinct from those formed in wild-type cells. Therefore the cone likely contains a mixture of structures, which are mostly reversed forks in wild-

type cells but can also include recombination intermediates, especially in mutants with disregulated recombination. The diverse nature of the JM structures indicates that these intermediates may be at various stages of D-loop extension and could also include hairpin structures that affect mobility in the second dimension of gel electrophoresis.

It is striking that the *srs2-K41R* mutant, lacking in both Srs2 catalytic functions, showed an increase in JM formation, whereas the complete deletion of *SRS2* leads to a near-complete disappearance of JMs (Kerrest et al., 2009). These results suggest that there may be a dominant negative effect of having a catalytically inactive Srs2 protein that can nonetheless bind to PCNA and DNA, explaining the difference from the *srs2*Δ situation. Interestingly, the complete deletion of Srs2 also led to a reduction in structured molecules formed by template switch at a protein-mediated stall (Lambert et al., 2010). At a CGG repeat that causes a stable fork stall, the *srs2-K41R* mutation caused a significant increase in fork stalling (Anand et al., 2012), supporting the idea that fork restart is inhibited in this background. In addition, *srs2-(1-998)*, *srs2-(875-902Δ)* and *srs2-(1-860)* mutants, that retain helicase activity but are defective in either PCNA binding or Rad51p-interaction or both, did not exhibit a decrease or increase in JMs compared to wild-type, even though each of these mutants variously affected repeat fragility and instability. These results further suggest that DNA binding in the absence of catalytic activity blocks fork restart and traps the DNA in a reversed fork or recombination structure. This interpretation fits with a recent role identified for Srs2 in inhibiting polymerase delta access to PCNA (Burkovics et al., 2013). The *Srs2-K41R* protein that can still bind PCNA could block Pol delta access but also be unable to unwind hairpins, resulting in a

persistent reversed fork, increase in recombination intermediates, and the continued presence of the cone on 2D gels.

Altogether, our data support the model that wild-type Srs2 facilitates fork restart by hairpin unwinding to minimize formation of joint molecules, rather than causing fork reversal or stabilizing reversed forks.

Role of Mph1 and Rad5 at long CAG/CTG repeats

Several helicases have been shown to regress model branched substrates *in vitro* (see (Atkinson and McGlynn, 2009) for review). From analysis of replication intermediates at the CTG repeat in *mph1* and *rad5* cells, it appears that neither Mph1 nor Rad5 are needed to form JMs, suggesting that either fork reversal *in vivo* happens spontaneously when the fork encounters a hairpin barrier, or that we have not yet identified the helicase that is involved in fork reversal *in vivo*. CAG/CTG and telomere repeats both undergo extensive reversal in a plasmid assay system (Fouché et al., 2006), and may be inherently “slippery” because of the extensive region of homology available in multiple possible alignments. Non-helicase mediated fork regression can also occur, as RecA can promote fork regression on branched DNA molecules in the absence of the replisome (Gupta et al., 2014; Robu et al., 2001), and Rad51 is required for fork regression at forks stalled by low dose replication inhibitors in eukaryotic cells (Zellweger et al., 2015).

In contrast, deletion of either Mph1 or Rad5 *increased* the level of JMs, suggesting that reversed forks were stabilized and/or converted to recombination intermediates more often than in wild-type cells. It has been suggested Mph1

prevents the formation of recombination intermediates by disassembling D loops to prevent crossovers, leading to an increase in JMs in its absence (Mazón and Symington, 2013). Deletion of either protein also mildly increased CAG expansions and contractions, consistent with more recombination-dependent repeat instability in these backgrounds. Mph1 could prevent instability from occurring at a stalled fork by dismantling D-loops and preventing formation of recombination intermediates. Similarly, Rad5-dependent post-replication repair has been shown to prevent expansion of short CAG repeats in a manner epistatic to Srs2 (Daee et al., 2007), though unregulated Rad5-dependent template switches can also cause repeat expansions (House et al., 2014). Similar to the result for the *srs2-(875-902Δ)* mutant, repeat fragility was not increased in either *rad5* or *mph1* cells.

A Model for Replication through Structure-Forming CAG/CTG Repeats

Our current results clarify the dynamic nature of events that can occur in response to replication fork stalling at a structure-forming DNA sequence. In wild-type cells, an expanded CTG repeat on the template strand causes transient fork stalling, which was evident as an accumulation of Y-shaped structures. In addition, Rad51-independent JMs are detected and shift to a spike of X-shaped molecules in an *exo1Δ* mutant, supporting the conclusion that they are mostly reversed forks (Figure 5, top). Our data suggest that the Srs2 protein locates to the stalled fork via its interaction with PCNA and utilizes its helicase activity to unwind the fork-blocking hairpin structure and facilitate fork restart (Figure 5, top row).

In the absence of Srs2-PCNA association or in an ATPase-deficient mutant, fork breakage results. Both helicase and Rad51 displacement are ATPase dependent, but comparison of *srs2-(875-902Δ)* and *srs2-K41R* mutants suggests that it is the helicase activity that is required to prevent chromosomal breakage, probably by unwinding hairpin structures (Figure 5, middle fork and right pathway). In agreement with this conclusion, both the Srs2 helicase activity and PCNA interaction are required for replication through $(CGG/CCG)_{40}$ repeats, which form strong replication blocking hairpins (Kerrest et al., 2009). We note that in the CAG orientation, CTG template hairpins would be more likely to form on the leading strand template, which appears to be particularly deleterious in the absence of Srs2 unwinding, leading to higher levels of fragility. The human RTEL1 helicase, which can unwind CAG and CTG hairpins, can complement Srs2 in yeast to prevent CAG repeat fragility (Frizzell et al., 2014). Since it also associates with SUMOylated PCNA at the replisome to prevent replication fork stalling and telomere fragility (Vannier et al., 2013). RTEL1 may be acting equivalently in human cells.

Independently of PCNA binding, Srs2 also displaces Rad51 from nascent strands to prevent recombination. In the absence of Rad51 displacement, such as in the *srs2* mutants lacking ATPase activity or the Rad51 interaction domain, increased recombination occurs, providing an increased probability of repeat expansions and contractions. Instability can result when the nascent strand invades or anneals out of register, or due to hairpin-facilitated slippage during D-loop extension (Figure 5, left pathway). The *srs2-K41R* mutant led to a visible increase in recombination intermediates by 2D gels. This was not observed in the *srs2-(875-902Δ)* mutant, most likely because the presence of helicase activity is

still allowing hairpin unwinding to limit the amount of recombination intermediates, which is supported by the lack of repeat-induced fragility observed in this mutant.

In summary, our results show that the Srs2 protein plays an important role in facilitating fork restart at replication-blocking hairpin lesions, both by unwinding structures to prevent fork stalling and breakage, and by blocking sister-chromatid recombination to prevent undue microsatellite instability.

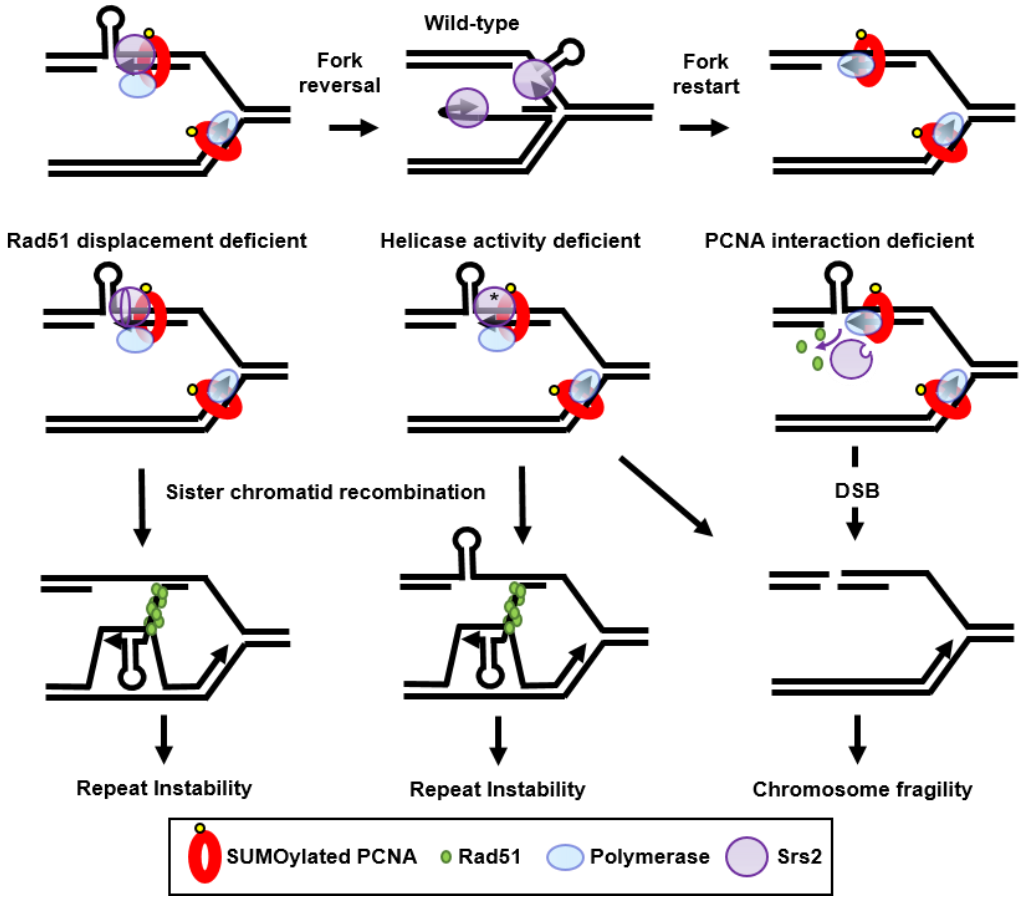

Figure 5. A model to explain how the different domains of the Srs2 protein are involved in repeat instability, chromosomal fragility and JM formation. Top row: in the wild-type situation Srs2 is brought to the fork by PCNA interaction and

unwinds hairpins formed by triplet repeats. For simplicity, only a lagging strand template hairpin is shown, though we note that leading strand template or nascent strand hairpins are also possible. Transient fork reversal may facilitate unwinding, or reversal may occur when unwinding fails, forming some JMs in wild-type cells (reversed fork JMs, Rad51 independent). Homologous recombination is discouraged by Srs2-dependent Rad51 displacement, but may occasionally happen. Right: in the absence of interaction with PCNA, Srs2 is not recruited to the fork to unwind template hairpin structures, leading to fork breakage. Srs2 may still displace Rad51, preventing recombination-dependent instability. Center: when Srs2 ATPase activity is absent hairpins will not be unwound, leading to more fork breakdown, and Rad51 is not displaced, leading to increased recombination intermediates. In this case, JMs are increased, consisting of both reversed forks and recombination intermediates. Left: Srs2 is brought to the fork by PCNA and can unwind secondary structures to prevent fork breakdown, but cannot displace Rad51p. Increased homologous recombination occurs, leading to repeat instability.

Acknowledgements

We thank Patrick Sung and Hannah Klein for providing Srs2 domain mutant genes, which were key reagents without which this project would not have been possible.

Appendix 2.1

Strain table

Strain	Background	Genotype	Reference
CFY765	BY4705	*MATα, ade2Δ::hisG, his3Δ200, leu2Δ0, lys2Δ0, met15Δ0, trp1Δ63, ura3Δ0, can^R* YAC: *LEU2* No Tract *URA3*	Kerrest et al. 2009
CFY766	BY4705	*MATα, ade2Δ::hisG, his3Δ200, leu2Δ0, lys2Δ0, met15Δ0, trp1Δ63, ura3Δ0, can^R* YAC: *LEU2* CAG-70 *URA3*	Kerrest et al. 2009
CFY1626	BY4705	*MATa, ade2Δ::hisG, his3Δ200, leu2Δ0, lys2Δ0, met15Δ0, trp1Δ63, ura3Δ0, can^R* YAC: *LEU2* No Tract *URA3*	This study
CFY1628	BY4705	*MATa, ade2Δ::hisG, his3Δ200, leu2Δ0, lys2Δ0, met15Δ0, trp1Δ63, ura3Δ0, can^R* YAC: *LEU2* CAG-70 *URA3*	This study
CFY925 **CFY926**	BY4742	*MATα, his3Δ1, leu2Δ0, lys2Δ0, ura3Δ0, can^R, srs2::KANMX6* YAC: *LEU2* No Tract *URA3*	Kerrest et al. 2009
CFY927 **CFY928**	BY4742	*MATα, his3Δ1, leu2Δ0, lys2Δ0, ura3Δ0, can^R, srs2::KANMX6* YAC: *LEU2* CAG-70 *URA3*	Kerrest et al. 2009
CFY2623	BY4705	*MATα, ade2Δ::hisG, his3Δ200, leu2Δ0, lys2Δ0, met15Δ0, trp1Δ63, ura3Δ0, can^R, srs2::TRP* YAC: LEU2 CAG-70 URA3	This study
CFY1701	BY4705	*MATα, his3Δ1, leu2Δ0, lys2Δ0, ura3Δ0, can^R* YAC: *LEU2* CTG-70 *URA3*	Kerrest et al. 2009
CFY1712	BY4705	*MATα, his3Δ1, leu2Δ0, lys2Δ0, ura3Δ0, can^R, srs2::KANMX6* YAC*: LEU2* CTG-70 *URA3*	Kerrest et al. 2009
CFY2497 **CFY2498**	BY4705	*MATα, ade2Δ::hisG, his3Δ200, leu2Δ0, lys2Δ0, met15Δ0, trp1Δ63, ura3Δ0, can^R, srs2::srs2-(1-860)*-HYG YAC: *LEU2* No Tract *URA3*	This study
CFY2087 **CFY2088**	BY4705	*MATα, ade2Δ::hisG, his3Δ200, leu2Δ0, lys2Δ0, met15Δ0, trp1Δ63, ura3Δ0, can^R,srs2::srs2-(1-860)*-HYG YAC: *LEU2* CAG-70 *URA3*	This study
CFY2499 **CFY2500**	BY4705	*MATα, his3Δ1, leu2Δ0, lys2Δ0, ura3Δ0, srs2::srs2-(1-860)*-HYG YAC: *LEU2* CTG-70 *URA3*	This study

CFY2501	BY4705	*MATα, ade2Δ::hisG, his3Δ200, leu2Δ0, lys2Δ0, met15Δ0, trp1Δ63, ura3Δ0, can^R, srs2::srs2-(875-902Δ)*-HYG YAC: *LEU2* No Tract *URA3*	This study
CFY2135 **CFY2136**	BY4705	*MATα, his3Δ1, leu2Δ0, lys2Δ0, ura3Δ0, can^R, srs2::srs2-(875-902Δ)*-HYG YAC: *LEU2* CAG-70 *URA3*	This study
CFY2503 **CFY2504**	BY4705	*MATα, his3Δ1, leu2Δ0, lys2Δ0, ura3Δ0, can^R, srs2::srs2-(875-902Δ)*-HYG YAC: *LEU2* CTG-70 *URA3*	This study
CFY2505 **CFY2506**	BY4705	*MATα, ade2Δ::hisG, his3Δ200, leu2Δ0, lys2Δ0, met15Δ0, trp1Δ63, ura3Δ0, can^R, srs2::srs2-K41R*-HIS3MX6 YAC: *LEU2* No Tract *URA3*	This study
CFY2305 **CFY2306** **CFY2307**	BY4705	*MATα, ade2Δ::hisG, his3Δ200, leu2Δ0, lys2Δ0, met15Δ0, trp1Δ63, ura3Δ0, can^R, srs2::srs2-K41R*-HIS3MX6 YAC: *LEU2* CAG-70 *URA3*	This study
CFY2507 **CFY2508**	BY4705	*MATα, his3Δ1, leu2Δ0, lys2Δ0, ura3Δ0, can^R, srs2::srs2-K41R*-HIS3MX6 YAC: *LEU2* CTG-70 *URA3*	This study
CFY2509 **CFY2510**	BY4705	*MATα, ade2Δ::hisG, his3Δ200, leu2Δ0, lys2Δ0, met15Δ0, trp1Δ63, ura3Δ0, can^R, srs2::srs2-(1-998)*-HIS3MX6 YAC: *LEU2* No Tract *URA3*	This study
CFY2299 **CFY2300**	BY4705	*MATα, ade2Δ::hisG, his3Δ200, leu2Δ0, lys2Δ0, met15Δ0, trp1Δ63, ura3Δ0, can^R, srs2::srs2-(1-998)*-HIS3MX6 YAC: *LEU2* CAG-70 *URA3*	This study
CFY2511 **CFY2512**	BY4705	*MATα, his3Δ1, leu2Δ0, lys2Δ0, ura3Δ0, can^R, srs2::srs2-(1-998)*-HIS3MX6 YAC: *LEU2* CTG-70 *URA3*	This study
CFY2600 **CFY2601**	BY4705	*MATα, ade2Δ::hisG, his3Δ200, leu2Δ0, lys2Δ0, met15Δ0, trp1Δ63, ura3Δ0, can^R, mph1::KANMX6* YAC: *LEU2* No Tract *URA3*	This study
CFY2602 **CFY2603**	BY4705	*MATα, ade2Δ::hisG, his3Δ200, leu2Δ0, lys2Δ0, met15Δ0, trp1Δ63, ura3Δ0, can^R, mph1::KANMX6* YAC: *LEU2* CAG-70 *URA3*	This study

CFY1664 **CFY1665**	BY4705	*MATα, ade2Δ::hisG, his3Δ200, leu2Δ0, lys2Δ0, met15Δ0, trp1Δ63, ura3Δ0, can^R,rad5::KANMX6* YAC: *LEU2* No Tract *URA3*	This study
CFY1666	BY4705	*MATα, ade2Δ::hisG, his3Δ200, leu2Δ0, lys2Δ0, met15Δ0, trp1Δ63, ura3Δ0, can^R, rad5::KANMX6* YAC: *LEU2* CAG-70 *URA3*	This study
GFY117	S288C	*MAT*a *ura3*Δ851 *leu2*Δ1 *his3*Δ200 *trp1*Δ63 *ade2*-opal *SUP4* *arg2*Δ::CTG98-*TRP1*	Kerrest et al. 2009
GFY195	S288C	*MAT*a *ura3*Δ851 *leu2*Δ1 *his3*Δ200 *trp1*Δ63 *ade2*-opal *SUP4* *arg2*Δ::CTG98-*TRP1 rad5*Δ::KAN^R	This study
CFY3078	S288C	*MAT*a *ura3*Δ851 *leu2*Δ1 *his3*Δ200 *trp1*Δ63 *ade2*-opal *SUP4* *arg2*Δ::CTG98-*TRP1 exo1*Δ::KAN^R	This study
GFY196	S288C	*MAT*a *ura3*Δ851 *leu2*Δ1 *his3*Δ200 *trp1*Δ63 *ade2*-opal *SUP4* *arg2*Δ::CTG98-*TRP1 mph1*Δ::KAN^R	This study

Appendix 2.2

Raw instability data for CAG_{70} YAC CF1

Contractions

Strain	No. of colonies	#	%	Fold over WT	p-value (compared to WT)	p-value (compared to *srs2Δ*)
Wild-type	269	7	2.60			
***srs2*Δ**	231	15	6.49	2.50	0.0474	
srs2-(1-860)	152	19	12.5	4.80	0.0001	0.0649
srs2-872-902Δ	162	16	9.88	3.80	0.0016	0.2555
srs2-K41R	201	19	9.45	3.63	0.0018	0.2852
srs2-(1-998)	122	4	3.28	1.36	0.7454	0.3206
srs2-K41R rad51Δ	174	3	1.72	0.66	0.7466	0.0474
srs2-(875-902Δ) rad51Δ	232	22	9.48	3.64	0.0017	0.3038
mph1Δ	290	15	5.17	0.80	0.1322	0.5726
rad5Δ	190	9	4.74	0.92	0.3015	0.5287
srs2Δrad5Δ	108	14	13.0	4.98	0.0002	0.0361

Expansions

Strain	No. of colonies	#	%	Fold over WT	p-value (compared to WT)	p-value (compared to *srs2Δ*)
Wild-type	269	3	1.12			
***srs2*Δ**	231	13	5.63	5.03	0.0047	
srs2-(1-860)	152	8	5.26	4.70	0.0207	1
srs2-872-902Δ	162	7	4.32	3.86	0.0456	0.6458
srs2-K41R	201	10	4.98	4.45	0.0194	0.8321
srs2-(1-998)	122	2	1.64	1.46	0.6493	0.0977
srs2-K41R rad51Δ	174	2	1.15	1.03	1	0.0178
srs2-(875-902Δ) rad51Δ	232	8	3.45	3.09	0.1232	0.2745
mph1Δ	290	8	2.76	0.49	0.2256	0.1179
rad5Δ	190	4	2.11	0.76	0.4453	0.0829
srs2Δrad5Δ	108	3	2.78	2.48	0.3595	0.4093

Appendix 2.3

Raw fragility data for YAC CF1

No Tract						
	WT	***srs2Δ***	***srs2-(1-860)***	***srs2-(875-902Δ)***	***srs2-K41R***	***srs2-(1-998)***
	1.73	1.33	1.37	1.12	0.91	3.77
	2.62	1.41	1.40	2.89	1.57	2.99
	2.10	2.27	2.86	1.58	2.26	3.41
	2.07	1.41	2.20	1.23	2.47	
	2.59	1.95	1.73	2.03		
	2.78	3.34				
	1.32	1.47				
		3.89				
		2.65				
Average Rate of FOA^R x $\mathbf{10}^{-6}$	2.17	2.19	1.91	1.77	1.80	3.39
SEM	0.20	0.31	0.28	0.32	0.35	0.23
p-value compared to wild-type		0.9639	0.4528	0.2877	0.3467	0.0076
p-value compared to *srs2*Δ			0.5639	0.4013	0.4765	0.0611

CAG_{70}						
	WT	***srs2Δ***	***srs2-(1-860)***	***srs2-(875-902Δ)***	***srs2-K41R***	***srs2-(1-998)***
	13.37	18.98	22.61	16.91	19.56	29.11
	14.04	17.84	38.56	14.80	22.93	24.11
	12.19	29.70	44.14	10.62	23.34	24.89
	12.58	22.03	49.98	8.31		
	4.24	25.36		7.35		
	5.15	17.98				
	8.49	26.55				
	7.40	19.75				
	7.03	26.94				
		63.35				
		37.16				
		32.05				

		34.61				
		22.00				
		30.81				
		55.56				

Average Rate of FOA^R x 10^{-6}	9.39	30.04	38.82	11.60	21.94	26.04
SEM	1.24	3.25	5.89	1.85	1.20	1.55
p-value compared to wild-type		0.0001	< 0.0001	0.3248	0.0003	< 0.0001
p-value compared to *srs2*Δ			0.2355	0.0062	0.3071	0.6097

	CTG_{70}					
	WT	***srs2Δ***	***srs2-(1-860)***	***srs2-(875-902Δ)***	***srs2-K41R***	***srs2-(1-998)***
	11.01	39.55	29.19	8.25	37.38	23.95
	12.17	15.73	15.58	11.62	21.73	18.41
	8.45	18.40	16.09	10.59	25.93	16.45
	6.38	17.82	12.58	12.19	15.32	14.50
	12.42	14.08	20.29	7.35	36.58	18.83
	18.06	27.07	16.94	7.65	14.10	17.64
	18.88	26.96	12.97		42.32	
		39.10	13.05		27.06	
		25.05	19.21		24.16	
			16.75		18.78	

Average Rate of FOA^R x 10^{-6}	12.48	24.86	17.27	9.61	26.34	18.30
SEM	1.75	3.16	1.56	0.87	3.05	1.30
p-value compared to wild-type		0.007	0.0614	0.1899	0.0032	0.0249
p-value compared to *srs2*Δ			0.0397	0.0021	0.7418	0.1293

	No tract		CAG_{70}	
	mph1Δ	***rad5Δ***	***mph1Δ***	***rad5Δ***
	1.36	4.07	10.40	16.59
	2.39	4.42	13.95	5.49
	2.66	2.04	10.38	7.35
	1.86		12.01	
			17.60	
			17.74	
			14.39	
Average Rate of FOA^R x $\mathbf{10}^{-6}$	2.07	3.51	13.78	9.81
SEM	0.29	0.74	1.16	3.43
p-value compared to wild-type	0.7604	0.0396	0.0244	0.8848
p-value compared to *srs2*Δ	0.8126	0.0794	0.0040	0.0187

Appendix 2.4

$(CTG)_{98}$ 2D mean quantifications for pause and cone signal

Strain Number	Strain Name	Mean Pause	Mean Cone
GFY117	**Wild-type**	**1.2**	**0.51**
CFY2201	***srs2-(1-860)*-HYG**	**0.94**	**0.64**
CFY2301	***srs2-(1-998)*-HIS**	**0.88**	**0.63**
GFY177	***srs2-(875-902Δ)*-HYG**	**0.82**	**0.55**
GFY198	***srs2-(875-902Δ)*-HYG *rad51Δ***	**1.2**	**0.66**
CFY2303	***srs2-K41R*-HIS**	**0.96**	**0.89**
GFY197	***srs2-K41R*-HIS *rad51Δ***	**0.91**	**0.54**
GFY195	***rad5Δ***	**1.0**	**0.99**
CFY3078	***exo1Δ***	**0.60**	**1.1**
GFY196	***mph1Δ***	**1.0**	**0.89**

Appendix 2.5

CAG_{70} YAC CF1 status check (Southern method)

		YAC status					
Strain Name	**CAG tract**	**Healing at G_4T_4**	**Healing at CAG**	**Healing at λ**	**Unbroken YAC**	**# colonies tested**	**Ref**
WT BY4705	0	8	0	0	1	9	(1)
	70	8	1	0	2	11	
***srs2Δ* BY4742**	0	3	0	0	4	7	(2)
	70	5	0	0	1	7*	

Strain Name	CAG tract	% YACs healed at G_4T_4	**% YAC end loss**	Ref
WT (BY4705)	0	89	89	(1)
	70	73	82	
***srs2Δ* (BY4742)**	0	43	43	(2)
	70	71	71	

Southern performed on a subset of FOA^R colonies to confirm breakage and subsequent healing. Breakage can result in healing at the backup telomere (healing at G_4T_4), the CAG tract (healing at CAG), or behind the backup telomere sequence (healing at λ). FOA^R can also result in mutation to URA3 expression without breakage (unbroken YAC). %YACs healed at G_4T_4= (# healing at G_4T_4/# total colonies). %YAC end loss= (# healing at G_4T_4+ healing at CAG + healing at λ)/# total colonies). *1 colony not shown in table had a chromosome rearrangement

(1) Sundararajan (unpublished)
(2) Anand (unpublished)

YAC CF1 status check in FOA^R colonies (PCR method)

Strain	# FOA^R colonies	YAC end loss (%)
Wild-type CAG_{70} (JN+XS)*	32	100
Wild-type CTG_{70} (JN)	12	100
***srs2Δ* CAG_{70}**	30	100

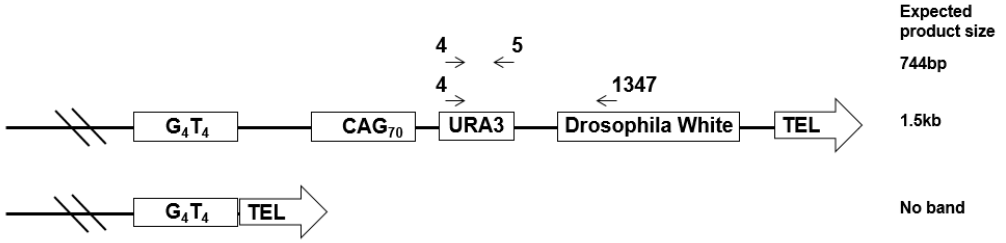

Schematic of PCR performed on a subset of FOA^R colonies to confirm FOA^R was due to YAC end loss and not due to point mutation in URA3. PCRs performed with primers 4/1347. *12 PCR reactions with primers 4/1347, 20 PCR reactions with primers 4/5

YAC CF1 status check in FOA^R colonies (Total)

Strain Name	CAG tract	Total no. colonies	% YAC end loss
WT (BY4705)	0	9	89
	70	43	95
	CTG-70	12	100
***srs2Δ* (BY4742)**	0	7	43
	70	37	95

Combined Southern and PCR checks of YAC status

Appendix 2.6

Primer table

#	Primer Name	Purpose	Sequence
2076	newCAGfor	To amplify across the repeat	cctcagcctggccgaaagaaagaaa
2077	newCAGrev	To amplify across the repeat	cagtcacgacgttgtaaaacgacgg
795	srs2_25bpdownFAfor	Generate His3 marker downstream of *SRS2*	aaatcatagtcatcgattagtagcactttcatgcctgactcggatccccgggttaattaa
796	srs2_75bpdownpFArev	Generate His3 marker downstream of *SRS2*	attaactcctatgtgctttaaataaaaattataaaccgccgaattcgagctcgtttaaac
499	200bp upstream Srs2 ORF	To amplify across *SRS2* ORF	ctccagctatcctgatacta
500	200bp downstream Srs2 ORF	To amplify across *SRS2* ORF	catactgctcattcatagct
678	Srs2_225upstream	To amplify across *SRS2* ORF; check integration of alleles at 5' junction	agaataggagcgagttagagttac
687	Srs2_300downstream	To amplify across *SRS2* ORF; check integration of alleles at 3' end	tctctactggtttagtcaatatgtc
853	Srs2_1943-1963R	5' junction check of *SRS2* alleles	gacctttggcaccgtgaattg
852	Srs2_1950-1970F	3' junction check of *SRS2* alleles	ggtgccaaaggtcttgagtg
858	Srs2_2694-2713R	Internal check of *srs2-(875-902Δ)*	cgtattgaggtgcatacacc
1866	Srs2_1577-1596for	To sequence *SRS2* alleles	gattcgaatcatgacgccgc
1867	Srs2_2018-2038for	To sequence *SRS2* alleles	ctccgtgcccaatttgacctg
1742	Srs2_2506-2525F	To sequence *SRS2* alleles	gatttcacgtcagctgcgga
1868	Srs2_3900-3921for	To sequence *SRS2* alleles	cgaggaaggacaaagttactcg
683	mph1200bpfor	To amplify across MPH1 locus	cacggagctaagatattgtgattcaaga
684	mph1200bprev	To amplify across MPH1 locus	ttgttgcttcaaaaacagtgccgtatc
685	mph1300bpfor	To check integration of KO marker at MPH1 locus	caaaattcaaactccaaaggggataat

1760	Mph1_407-426F	To check MPH1 ORF absence	ctgctccaacaagaccttt g
1674	Mph1int_3984-3005rev	To check MPH1 ORF absence	caatgtctcgtgacattccg g
495	Rad5upstreamfor	To amplify across RAD5 locus	cttactgctaagcgcattgc tc
496	Rad5dwnstreamrev	To amplify across RAD5 locus	gaagttgcatgaagtagct g
1115	Rad5-ForChk	To check integration of KO marker at RAD5 locus	cattctggacctttctgcac
1935	Rad5internalfor_161bpfromstart	To check RAD5 ORF absence	caacagaaggagaggg agac
2015	Rad5_1690-1708R	To check RAD5 ORF absence	ctgagactgctgtgttctc
490	Rad51upstreamfor	To amplify across RAD51 locus	tttctgtcctggtttgtttacag ta
491	Rad51dwnstreamrev	To amplify across RAD51 locus	gcagtagggttgcgaggt atatgac
1688	Rad51-For3'Int243bp	To check RAD51 ORF absence	gtcgtcgttactaaccaagt
1689	Rad52-For3'Int397bp	To check RAD52 ORF absence	atacccaggcacaatcca tta
604	Rad52_300bpdwn_rev	To check RAD52 ORF absence	tccgagttgccatatttgtat agttt
476	Rad52upstrmfor	To check integration of KO marker at RAD52 locus	tgctcttcccgttagtgatt
477	Rad52 down	To check integration of KO marker at RAD52 locus	aatgaacctaaggattccg c
1259	Exo1 upstream	To amplify across EXO1 locus	caggtccttgctccttcag
1260	Exo1 downstream	To amplify across EXO1 locus	gtgaattgcacatgcccag
1263	Exo1_275bpupstream	To check integration of KO marker	cttacgcgtctttagcaaag gc
1783	Exo1_300bpfor	To check EXO1 ORF absence	gccatagctgaaagactgt gg
1784	Exo1_1500bprev	To check EXO1 ORF absence	CTC AGG TTG TCG TCA TCC TC
375	His3rvsk	To check integration of KO marker	ttagataaatcgactacgg cac
140	Trp verif	To check integration of KO marker	gctgcactgagtagtatgtt gc
15	KanB	To check integration of KO marker	ctgcagcgaggagccgta at
16	KanC	To check integration of KO marker	tgattttgatgacgagcgta at

4	ura3rev	To check loss of right arm of YAC	TCCCAGCCTGCTTTTCTGTA
5	ura3for2	To check loss of right arm of the YAC	TGCTGCTACTCATCCTAG
1347	DrosophW5'rev	To check loss of right arm of YAC	gcacaattggtgacgttacg

Chapter 3

RTEL1 Inhibits Trinucleotide Repeat Expansions and Fragility

Authors:

Aisling Frizzell[1], Jennifer Nguyen[3], Mark I. R. Petalcorin[4], Katherine D. Turner[1,2], Simon J. Boulton[4], Catherine H. Freudenreich[3] and Robert S. Lahue[1,2]

[1]Centre for Chromosome Biology, School of Natural Sciences and [2]NCBES Galway Neuroscience Centre, National University of Ireland Galway, Newcastle Road, Galway, Ireland

[3]Department of Biology, Tufts University, Medford, MA 02155, USA

[4]DNA Damage Response laboratory, London Research Institute, Cancer Research UK, Clare Hall, South Mimms, EN6 3LD, United Kingdom

Published in Cell Reports February 2014

****This chapter is modified from this publication to represent the work I contributed and other key findings; includes correction of the published data to remove data gather using imperfect gene replacement strains and replaced with data gathered using correct strains****

Author contributions (subset):

Mark I.R. Petalcorin in Simon Boulton's lab: performed RTEL helicase unwinding assays

Jennifer Nguyen: performed yeast assays and analyzed data

Robert Lahue and Catherine Freudenreich planned and supervised experimental design, analyzed data, and wrote the manuscript

ABSTRACT

Human RTEL1 is an essential, multifunctional helicase that maintains telomeres, regulates homologous recombination and helps prevent bone marrow failure. Here, we show that RTEL1 also blocks trinucleotide repeat expansions, the causal mutation for 17 neurological diseases. Increased expansion frequencies occurred in human cells following knockdown of RTEL1. This is reminiscent of budding yeast Srs2, which inhibits expansions, unwinds hairpins and prevents triplet repeat-induced chromosome fragility. Accordingly, we found expansions and fragility were suppressed in yeast *srs2* mutants expressing RTEL1 but not Fbh1. We propose that RTEL1 serves as a human analog of Srs2 to inhibit trinucleotide repeat expansions and fragility, likely by unwinding problematic hairpins.

INTRODUCTION

Expansions of trinucleotide repeats (TNRs) are the causative mutations in 17 human neurological disorders, including Huntington's disease, myotonic dystrophy type 1 and fragile X syndrome (López Castel et al., 2010; McMurray, 2010; Mirkin, 2007). Expansions often recur in affected families, driving the repeat length longer and thereby affecting subsequent generations either earlier in life or more severely than their parents. In contrast, unaffected individuals have shorter, genetically stable TNRs with very low risk of expansion. Although complex molecular mechanisms drive expansions (López Castel et al., 2010; McMurray, 2010; Mirkin, 2007), it is clear that two categories of protein factors are crucial in determining whether an expansion occurs. Pro-mutagenic factors

favor the expansion process, relentlessly driving TNRs towards longer allele lengths. Anti-mutagenic proteins inhibit the expansion process and are important in helping prevent the initiating expansions that trigger instability. Both categories of proteins likely act on aberrant DNA secondary structures, such as hairpins, that are widely thought to be intermediates in the expansion process (Liu et al., 2010; López Castel et al., 2010; McMurray, 2010; Mirkin, 2007). Proteins that favor expansion accelerate the formation of aberrant secondary structure or its subsequent processing to an expansion, while inhibitory proteins do the opposite. One of the most pressing issues is to identify human factors in both categories and determine how they regulate the enigmatic expansion process. In this study, we sought human proteins that inhibit expansions, by examining model organisms for inhibitory factors that have human counterparts.

Several studies in budding yeast identified the helicase Srs2 as a key protein for inhibiting TNR expansions. The likelihood of an expansion is increased up to 40-fold in *srs2* mutants (Bhattacharyya and Lahue, 2004; Daee et al., 2007; Kerrest et al., 2009). The expansion signature of *srs2* mutants is specific, as neither dinucleotide repeat mutations nor overall mutation rates was altered (Bhattacharyya and Lahue, 2004; Daee et al., 2007). Furthermore, mutation of a related helicase gene, *SGS1*, did not recapitulate the expansion defects of *srs2* mutants (Bhattacharyya and Lahue, 2004; Kerrest et al., 2009). In one study, Srs2 was shown to function with components of the error-free branch of post-replication repair (PRR; also referred to as DNA damage tolerance (DDT)) (Daee et al., 2007). Mutants in PRR genes such as *RAD5* or *RAD18* also showed higher rates of expansion, and double mutant analysis was consistent with an epistatic relationship between *SRS2* and PRR genes with regard to expansions.

In vitro, purified Srs2 enzyme was particularly effective at unwinding a number of TNR hairpin structures, which are thought to be key intermediates in the expansion process (Anand et al., 2012; Bhattacharyya and Lahue, 2005; Dhar and Lahue, 2008). *In vivo*, ATPase-defective alleles of *srs2* were also deficient at blocking expansions (Bhattacharyya and Lahue, 2004) and in facilitating replication through CGG repeats (Anand et al., 2012). Thus, Srs2 most likely inhibits expansions by unwinding TNR hairpins, precluding their further processing into the full expansion mutation. This anti-expansion activity of Srs2 is in addition to its better-known role as a negative regulator of homologous recombination (HR) (Karpenshif and Bernstein, 2012; Marini and Krejci, 2010). During HR, Srs2 disassembles Rad51-single-stranded DNA filaments to prevent toxic recombination (Krejci et al., 2003; Veaute et al., 2003). Mutants of *SRS2* are synthetically lethal when combined with *SGS1* defects (Lee et al., 1999), due to uncontrolled levels of recombination (Gangloff et al., 2000). The anti-recombinase activity of Srs2 also plays a role in preventing TNR instability for long disease-length alleles, which are prone to breakage. Srs2 achieves this role by controlling sister-chromatid recombination initiated by repeat-associated fork blockage or breaks (Anand et al., 2012; Kerrest et al., 2009). Thus Srs2 makes a major contribution to genomic stability by inhibiting TNR expansions both via hairpin unwinding and by blocking excessive HR.

Despite the absence of sequence homologs of yeast Srs2 protein in metazoan organisms, several helicases have functions analogous to Srs2 (Karpenshif and Bernstein, 2012; Uringa et al., 2011). The essential helicase RTEL1 is a key factor in regulating telomere length in mice (Ding et al., 2004), where it dismantles T loops and counteracts G4-DNA (Vannier et al., 2012). Other

functions of RTEL1 parallel those of Srs2 (Uringa et al., 2011). RTEL1 negatively regulates HR (Barber et al., 2008; Uringa et al., 2011), and RTEL1 is a helicase capable of unwinding unusual DNA structures *in vitro* (Vannier et al., 2012). Furthermore, *rtel1* mutants in *C. elegans* are synthetically lethal when combined with mutation of *HIM-6,* the invertebrate homolog of yeast *SGS1* (Barber et al., 2008). Inherited mutations in *RTEL1* cause Hoyeraal-Hreidarsson syndrome, a severe form of dyskeratosis congenita that leads to early bone marrow failure (Ballew et al., 2013; LeGuen et al., 2013; Walne et al., 2013). A second protein with functions analogous to Srs2 is Fbh1, a human helicase/F-box protein (Kim et al., 2002). Fission yeast Fbh1 regulates recombination (Morishita et al., 2005; Osman et al., 2005). Human Fbh1 expressed in budding yeast suppressed recombination defects of *srs2* mutants, and rescued the MMS sensitivity of *rad18* or *rad5* mutants in the presence of *srs2* (Chiolo et al., 2007). A third analog, PARI, was recently found to inhibit recombination and to stabilize the genome in a manner requiring PCNA interaction (Moldovan et al., 2012). Unlike Srs2, PARI does not appear to be an active helicase and little is known about its *in vivo* function.

The goal of this study was to determine whether RTEL1 or Fbh1 inhibits TNR expansions and fragility. Our evidence supports RTEL1, not Fbh1, as a novel inhibitor of expansions and repeat-mediated chromosome fragility in budding yeast. Furthermore, the data suggest RTEL1 acts as a helicase to unwind TNR hairpins and thereby preclude the expansion process.

MATERIALS AND METHODS

Yeast strains

Strains used in genetic assays for chromosome fragility and repeat instability were isogenic BY4705 background containing a yeast artificial chromosome (YAC) with either no or 70 or 85 CAG/CTG repeats, with the CAG strand on the lagging strand template, as previously described (Callahan et al., 2003; Sundararajan et al., 2010). Mutants were created through PCR-mediated gene replacement. *srs2::hFBH1-HIS3MX6,* a gift from G. Liberi (Chiolo et al., 2007), was amplified with primer pairs 200bp upstream and downstream of the *SRS2* ORF and transformed into CFY1626, CFY1628, CFY810, and CFY1666. Transformants were checked by PCR to determine absence of SRS2 ORF and to confirm proper knock-in. Correct knock-ins were sequenced to confirm no point mutations were introduced during integration. hRTEL1 cDNA was amplified from pDONR221 (received from S. Boulton) with a primer containing a 5' tail homologous to sequence flanking the *SRS2* locus. HIS3MX6 was amplified with a primer including a 3' tail homologous to sequence flanking the *SRS2* locus. Both fragments had homologous regions to each other and were co-transformed into CFY1626, CFY1628, CFY810, and CFY1666. Transformants were checked by PCR to determine absence of SRS2 ORF and to confirm proper knock-in of hRTEL1 at Srs2 locus. Correct knock-ins were sequenced to confirm no point mutations were introduced during integration.

CAG tract length was tested in transformants and starting strains for experiments by PCR amplification using Taq polymerase (IDPol™ from ID Labs or Taq Pol from SibEnzyme US) and primers flanking 42 bp and 117 bp down from the

repeat tract, and analyzed for expansions on high resolution 2% Metaphor gels, which can accurately resolve +/- 9 bp (3 repeats) in the 0-200bp size range.

Fragility and instability assays

Fragility and instability assays were performed as previously described (Kerrest et al., 2009). In short, starting single colonies were grown on yeast complete media (YC) –Leu-Ura to select for the YAC and tract lengths were checked via PCR amplification as described above. Cells were resuspended in YC-Leu liquid media to a starting OD 0.01-0.04, grown for 6-8 divisions; for fragility assays, cells were plated on both selective (FOA-Leu) and non-selective media (YC-Leu) and only non-selective media for instability assays. Repeat fragility was determined by calculating rate of 5-FOA^{R} for 100µL by the method of the maximum likelihood using FALCOR software. Repeat instability was analyzed in 150+ daughter colonies via PCR amplification and size analysis as described above.

MMS sensitivity spot assay

Spot assays were performed and cell growth was observed on YC –Leu-Ura media with or without indicated concentrations of methyl methanesulfonate (MMS, 0.02). Strains grown in liquid culture were standardized to 1.0 OD, sequentially diluted 1:5, and spotted on plates. Growth was assessed after incubation at 30˚C for 2-3 days. Experiments were repeated twice independently to test reproducibility.

RT PCR

Cells were grown to OD_{600} ~0.8 and then treated with 100T Zymolyase and lysed. RNA was isolated using Illustra™ RNAspin Mini RNA Isolation Kit. cDNA was generated with oligo(dT) primers and the SuperScript ™ First-Strand Synthesis System for RT-PCR using 0.5μg of RNA, as determined by nanodrop reading. PCR amplification of cDNA using primers within gene of interest was used to determine expression

RESULTS

RTEL1 unwinds TNR hairpins

Both yeast Srs2 and human RTEL1 are DNA helicases. Several lines of evidence suggest that the helicase function of Srs2 is critical for inhibiting expansions. An ATPase mutant of Srs2, K41A, is defective in blocking expansions in yeast (Bhattacharyya and Lahue, 2004) and a similar mutant, K41R, is defective in facilitating replication through a CGG hairpin (Anand et al., 2012). Purified Srs2 efficiently unwinds TNR hairpins of different sizes and sequences (Bhattacharyya and Lahue, 2005; Dhar and Lahue, 2008). Similarly, the K48R ATPase mutant of RTEL1 fails to disassemble T-loops in cell-free extracts (Vannier et al., 2012). We extended this analysis by performing helicase assays on a TNR hairpin substrate with wild-type or K48R RTEL1. A duplex molecule containing a $(CTG)_{11}$ hairpin was chosen to mimic a presumptive intermediate in the expansion process, and because +11 repeat expansions lie in the mid-range of RTEL1 activity based on the size spectra described above. *In vitro*, the wild-type enzyme but not the mutant protein efficiently unwound the $(CTG)_{11}$ hairpin in a

concentration-dependent manner (Figures 1C). RTEL1 was also effective on a substrate with extrahelical CAG repeats. A $(CAG)_{11}$ substrate was efficiently unwound by wild-type RTEL1 but not the K48R variant (Figure 1D). In summary, the helicase assays are consistent with the notion that RTEL1 inhibits expansions by unwinding TNR hairpins.

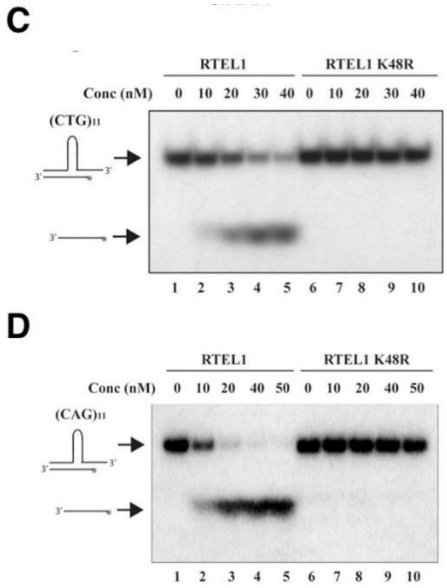

Figure 1. Modified from (Frizzell et al., 2014). RTEL helicase unwinding activity (C) Unwinding of $(CTG)_{11}$ hairpin by purified wild-type RTEL1 or K48R mutant RTEL1. (D) Unwinding of $(CAG)_{11}$ hairpin by purified wild-type RTEL1 or RTEL1 K48R.

RTEL1 and Fbh1 cannot restore MMS resistance in *srs2* strains

If RTEL1 or Fbh1 is an analog of Srs2, then expressing these human helicases in budding yeast might reverse *srs2* phenotypes. The human *RTEL1* and *FBH1*

genes were integrated into the *SRS2* locus, thereby inactivating the yeast gene and permitting expression of the human genes from the endogenous *SRS2* promoter (Appendix 3.1). Cells lacking Srs2 are moderately sensitive to the cytotoxic effects of the DNA alkylating agent methyl methanesulfonate (MMS) and it was previously shown FBH1 could suppress *srs2Δ* sensitivity (Chiolo et al., 2007). We wanted to test this in our strain background with both RTEL1 and FBH1.

We previously published the expression of hRTEL1, but not hFBH1, under the control of the Srs2 promoter could rescue *srs2Δ* MMS sensitivity ((Frizzell et al., 2014); Figure 2), suggesting hRTEL1 is the better substitute for Srs2.

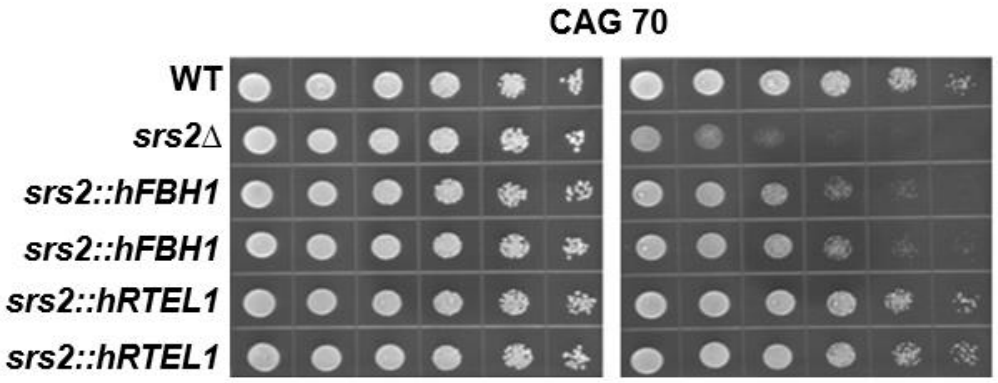

Figure 2. Expression of RTEL1 in yeast suppresses *srs2* phenotypes. Human RTEL1 (hRTEL1) can complement Srs2 and rescue *srs2Δ* sensitivity to MMS more efficiently than hFbh1. WT: CFY1628, *srs2Δ*: CFY2623, *srs2::hFBH1*: CFY2775, CFY2776, *srs2::hRTEL1*: CFY2806, CFY 2807. (Frizzell et al., 2014)

The genetic interaction of the helicases with Rad5 was also examined because Rad5 is needed for the error-free branch of PRR (Smirnova and Klein, 2003; Zhang and Lawrence, 2005). *rad5Δ* mutants are exquisitely sensitive to MMS, in part because Srs2 restrains recombination. This hypersensitivity can be partly overcome in an *srs2Δ rad5Δ* double mutant, because deletion of Srs2 is thought to promote HR and therefore bypass the requirement for Rad5 (Schiestl et al., 1990; Ulrich, 2001). This leads to the prediction that MMS hypersensitivity should be restored in a *srs2Δ rad5Δ* double mutant upon expression of a human analog of Srs2.

We previously published that expression of hRTEL1 in a *rad5Δ* background, but not hFBH1, resulted in MMS sensitivity in the double mutant ((Frizzell et al., 2014); Figure 3). We concluded RTEL1, but not hFbh1, could substitute for the role of Srs2 in the Rad5 branch of the PRR pathway in yeast.

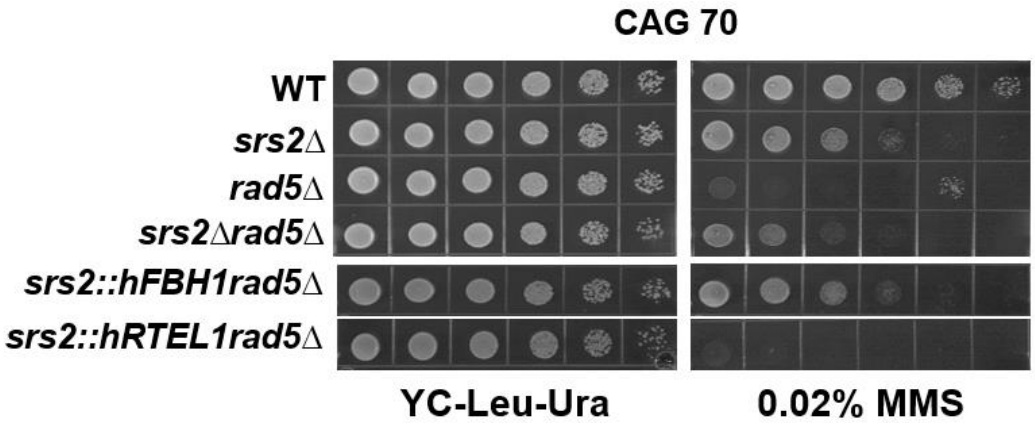

Figure 3. Expression of RTEL1 in yeast suppresses *srs2* phenotypes. hRTEL1, but not Fbh1, expression in *rad5Δ* mutants restores hypersensitivity to MMS. WT: CFY1628, *srs2Δ*: CFY2623, *rad5Δ*: CFY1666, *srs2Δrad5Δ*: CFY2984, *srs2::hFBH1rad5Δ*: CFY2988, *srs2::hRTEL1rad5Δ*: CFY2949. (Frizzell et al., 2014)

After publication, we discovered *srs2::hRTEL1* $(CAG)_{70}$ (CFY2806, CFY2807) and *srs2::hRTEL1rad5Δ* (CFY2949, CFY2950) strains still retained the Srs2 ORF at the Srs2 locus. Human RTEL1 was also detected in some strains suggesting perhaps it integrated somewhere else in the genome, or was maintained extra-chromosomally. New *srs2::hRTEL1* (CFY3604) and *srs2::hRTEL1rad5Δ* (CFY3654) strains were constructed and confirmed through junction PCRs as well as sequencing. (Further details on strain issues and checks can be found in Appendix 3.4).

Strains were re-tested for MMS sensitivity. *srs2::hRTEL1* (CFY3604) was as sensitive to MMS as *srs2Δ* (Figure 4). Unlike what we previously published, this suggests that hRTEL1 cannot substitute for Srs2 in protecting against MMS induced damage. Additionally, when we tested a new *srs2::hRTEL1rad5Δ* (CFY3594) strain, we found that expression of hRTEL1 did not result in hypersensitivity with *rad5Δ*, suggesting that it could not substitute for Srs2 in PRR (Figure 4).

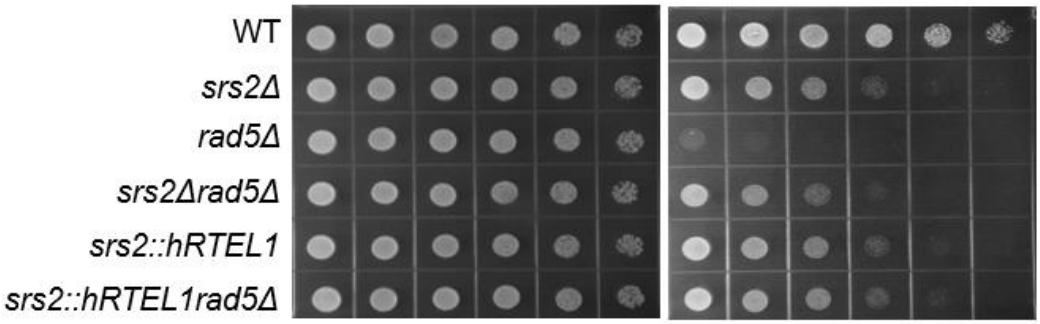

Figure 4. Expression of RTEL1 does not rescue *srs2Δ* MMS sensitivity. hRTEL1 expression in *rad5Δ* mutants does not restore hypersensitivity to MMS. WT: CFY1628, *srs2Δ*: CFY2623, *rad5Δ*: CFY1666, *srs2Δrad5Δ*: CFY2984, *srs2::hRTEL1*: CFY3597, *srs2::hRTEL1rad5Δ*: CFY3654.

RTEL1 suppresses triplet repeat-mediated chromosome fragility and expansions of yeast *srs2* mutants

The yeast strains expressing RTEL1 or Fbh1 were tested for triplet repeat-mediated chromosomal fragility and instability. Long TNR tracts, such as $(CAG)_{70}$, undergo chromosome fragility in yeast (Anand et al., 2012; Callahan et al., 2003; Freudenreich et al., 1998; Kerrest et al., 2009). DNA breaks are prevented by Srs2, based on the finding that *srs2* mutants show increased levels of chromosome fragility (Anand et al., 2012; Kerrest et al., 2009). The protective activity of Srs2 against chromosome fragility was attributed to its function as a helicase that unwinds hairpins encountered during replication (Kerrest et al., 2009) and/or to a role in promoting fork reversal (Kerrest et al., 2009). We previously published that chromosome fragility in the control strain lacking a repeat tract was unchanged in the *srs2Δ* mutant, and expression of Fbh1 or RTEL1 caused modest increases in breakage rates (Figure 5 and Appendix 3.2).

The presence of the $(CAG)_{70}$ tract resulted in higher levels of breakage in the wildtype strain, an effect that is exacerbated by the *srs2Δ* mutation, in agreement with previous studies (Anand et al., 2012; Kerrest et al., 2009). Expression of Fbh1 did not detectably alter fragility rates compared to the *srs2Δ* strain, whereas expression of RTEL1 resulted in a significant decrease compared to *srs2Δ*, although not to wildtype levels (Figure 5 and Appendix 3.2). The fragility data suggest that RTEL1 can substitute for Srs2 in facilitating replication through TNRs.

After publication, we discovered the *srs2::hRTEL1* no tract (CFY2804, CFY2805) as well as the *srs2::hRTEL1* $(CAG)_{70}$ (CFY2806, CFY2807) strains still retained Srs2 ORF at the SRS2 locus. Human RTEL1 was also detected in some strains suggesting perhaps it integrated somewhere else in the genome, or maintained extra-chromosomally. A new *srs2::hRTEL1* no tract (CFY3593) strain was constructed and confirmed through junction PCRs as well as sequencing. We also used *srs2::hRTEL1* $(CAG)_{70}$ (CFY3597) from MMS studies for re-testing (Further details on strain issues and checks can be found in Appendix 3.4).

We re-tested fragility on both *srs2::hRTEL1* strains. Unlike what we previously published, *srs2::hRTEL1* no tract did not result in an increase in fragility compared to wild-type (Figure 5). Similarly to what we previously published, we found *srs2::hRTEL1* $(CAG)_{70}$ suppressed the increased fragility of *srs2Δ* although not to the wild-type level (Figure 5). This data supports RTEL1 substituting for

Srs2 in facilitating replication through TNRs and preventing fragility.

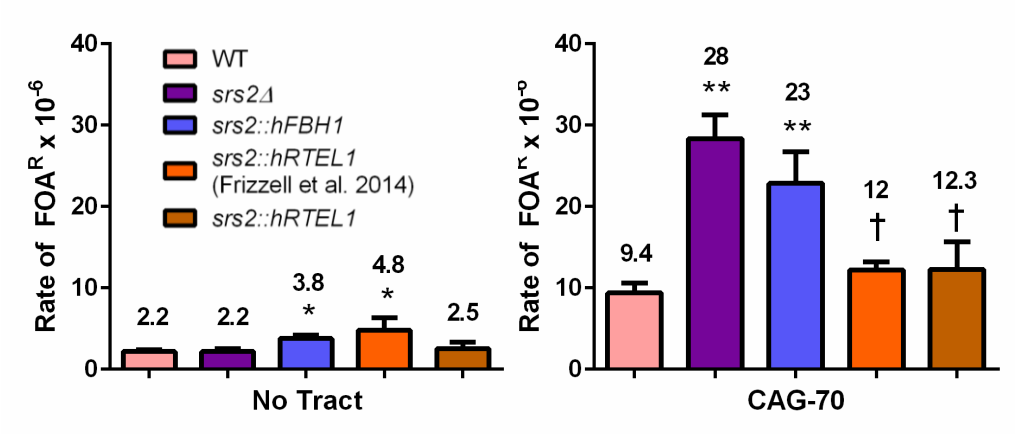

Figure 5. Expression of RTEL1, but not Fbh1, in yeast suppresses increased fragility seen in s*rs2Δ*. Chromosome fragility on a YAC CF1 carrying a $(CAG)_{70}$ tract (Kerrest et al., 2009). Rate values indicated above the bars; error bars represent SEM. Significance was determined compared to wild-type (*p≤0.05, **p≤0.01) or srs2Δ (†p≤0.05). Strains *srs2::hRTEL1* No Tract (CFY3593) and *srs2::hRTEL1* CAG_{70} (CFY3597) used to replace incorrect data presented in(Frizzell et al., 2014).

We also used PCR to examine expansion frequencies for a $(CAG)_{85}$ tract (Table 1 and Appendix 3.3). The *srs2Δ* strain showed five-fold more expansions than the wild-type control, similar to previously reported values for $(CAG)_{70}$ (Anand et al., 2012; Kerrest et al., 2009). We previously published expression of RTEL1 reduced expansion levels down from *srs2Δ* although not to wildtype levels. In contrast, the expansion frequency was still partly elevated following expression of Fbh1. The partial rescue of $(CAG)_{85}$ expansions by Fbh1 is consistent with its known role in preventing recombination (Chiolo et al., 2007), since expansions of this repeat size were previously shown to occur during a Rad51-dependent

process in *srs2Δ* yeast (Kerrest et al., 2009). Although both helicases can compensate for some Srs2 anti-recombinase functions, RTEL1 is uniquely able to complement Srs2 roles in replication based on rescue of CAG repeat-mediated fragility and instability in a *srs2Δ* mutant. We concluded that expression of RTEL1 in yeast provides similar biochemical functions as Srs2 in DNA damage repair and in inhibiting triplet repeat-mediated chromosome fragility and expansions.

After publication, we discovered issues with two of our strains. There was a point mutation in one of the two strains used for *srs2::hFBH1* $(CAG)_{85}$ (CFY2993) instability data and the s*rs2::hRTEL1* $(CAG)_{85}$ (CFY2995) strain had Srs2 ORF at the SRS2 locus and no RTEL1-HIS3MX6 present in the genome. Both *srs2::hFBH1* $(CAG)_{85}$ (CFY2992) and *srs2::hRTEL1* $(CAG)_{85}$ (2994) were verified to be correct strains through PCR and sequencing. New instability data for *srs2::hFBH1* was obtained with more assays from CFY2992. A new *srs2::hRTEL1* $(CAG)_{85}$ (CFY3604) was constructed and confirmed through junction PCRs as well as sequencing. (Further details on strain issues and checks can be found in Appendix 3.4). We performed additional instability reactions on CYF3604 to combine with CFY2994.

We obtained more instability data for *srs2::hFBH1* $(CAG)_{85}$ (CFY2992) and found expansion frequencies were still elevated 3.9 fold over wild-type and not significantly decreased from *srs2Δ* (Table 1), indicating hFbh1 cannot substitute for Srs2 in preventing CAG expansions. Expression of hRTEL1 led to a nearly significant decrease in expansion frequency compared to *srs2Δ* ($p<0.055$) (Table 1), suggesting hRTEL1 can partially substitute for Srs2 in preventing CAG expansions.

Table 1. $(CAG)_{85}$ Instability on YAC CF1.

		Expansions (Frizzell et al. 2014)				Expansions		
Mutant	No. colonies analyzed	#	%	Fold over WT	No. colonies analyzed	#	%	Fold over WT
Wild-type	299	4	1.3					
srs2Δ	139	10	7.2*	5.4*				
srs2::hFBH1	131	6	4.6	3.4	154	8	5.2*	4.0*
srs2::hRTEL1	210	4	1.9^	1.4^	174	6	3.4†	2.6†

*p<0.05 compared to wild-type, ^p<0.05 compared to *srs2Δ,* †p<0.06 compared to *srs2Δ*

DISCUSSION

Parallels between RTEL1 and yeast Srs2 in inhibiting TNR expansions and fragility

This work identifies RTEL1 as a key human enzyme that inhibits TNR expansions and fragility. Purified RTEL1 readily unwound CTG and CAG hairpin structures *in vitro*, in a manner dependent on its ATPase activity (Figures 1C and 1D). We found expression of RTEL1 in yeast *srs2* mutants efficiently suppressed CAG repeat-dependent chromosomal fragility and expansions, whereas expression of Fbh1 was substantially poorer in reversing these phenotypes (Figure 5, Table 1). We conclude that RTEL1 is an important human factor that blocks triplet repeat expansions and repeat-mediated chromosome fragility, and that its DNA helicase function is likely important in doing so.

In contrast, we found little or no evidence for a role in triplet repeat instability for the alternative Srs2 analog Fbh1 (F-box helicase). Fbh1 was originally identified as a human helicase/F-box protein (Kim et al., 2002) and in fission yeast as a regulator of recombination (Morishita et al., 2005; Osman et al., 2005). Fbh1 was subsequently shown to function at replication forks (Lorenz et al., 2009). In human cells, Fbh1 promotes formation of double-strand breaks in response to replication stress (Fugger et al., 2015; Jeong et al., 2013) and helps avoid crossovers at collapsed replication forks (Kohzaki et al., 2007). A previous study showed that human Fbh1 expressed in budding yeast suppressed recombination defects and MMS sensitivity of an *srs2Δ* mutant, however Fbh1 did not restore MMS hypersensitivity to a *rad5Δ srs2Δ* double mutant (Chiolo et al., 2007), in agreement with our data (Figure 3). Despite some parallels to Srs2, our experiments showed little to no role for Fbh1 at triplet repeats in yeast (Figure 5, Table 1). While we cannot rigorously rule out that Fbh1 imparts protection at TNRs in human cells, the current data do not support this hypothesis.

Potential mechanism of TNR stabilization by RTEL1

Srs2 has been proposed to inhibit expansions through its helicase activity on TNR hairpins (Bhattacharyya and Lahue, 2004, 2005; Daee et al., 2007; Dhar and Lahue, 2008) and/or by unwinding TNR structures to facilitate passage of replication forks (Anand et al., 2012; Kerrest et al., 2009). The results in Figures 1C and 1D indicate that purified RTEL1 is capable of efficiently unwinding $(CTG)_{11}$ hairpins, analogous to Srs2 (Bhattacharyya and Lahue, 2005; Dhar and Lahue, 2008). The ATPase function of both enzymes is important for unwinding TNRs (Anand et al., 2012; Bhattacharyya and Lahue, 2004), consistent with a

requirement for helicase activity. These results support the possibility that RTEL1 unwinds TNR hairpins before they can be converted into full expansion mutations. Our genetic analysis suggests that RTEL1 may work in the same pathway as HTLF and Rad18, based on the requirement for Rad18 and HLTF in expansion assays, the double knockdown data of RTEL1+Rad18 and RTEL1+HLTF, and the similar profiles of expansion sizes in all the knockdowns (Frizzell et al., 2014). Thus RTEL1 function at TNRs could act during post-replication repair or a template-switching event such as fork reversal (Figure 4).

In the PRR model, RTEL1 could conceivably unwind hairpins that initiate PRR at gaps left behind the replication fork, or hairpins that occur during error-free PRR repair synthesis (Figure 6A). This model is strengthened by the similarity of the D-loop structure (lower panel, Figure 6A) to substrates that RTEL1 has been proposed to unwind during processing of intermediates in recombination and T-loops (Uringa et al., 2011; Vannier et al., 2012). In this mode of action, RTEL1 could antagonize any error-prone recombination events that lead to expansions of long TNRs as seen in yeast (Kerrest et al., 2009; Sundararajan et al., 2010). We postulate that RTEL1 is recruited to the TNR by post-replication repair factors Rad18 and/or HLTF, or that these factors modify another target that in turns attracts RTEL1 (Figure 6A). The activity of all three proteins would remove the hairpin and prevent expansions, whereas lack of any one or more of RTEL1, HLTF or Rad18 would result in higher expansion frequencies.

Another potential mode of action is through HLTF-mediated, error-free resolution of TNR replication stress (Figure 6B). HLTF, like Rad5, has been shown to mediate fork reversal of model stalled replication fork substrates through unwinding of the leading and lagging strands, followed by annealing of the

nascent and parental strands to form a chicken-foot structure (Blastyák et al., 2007, 2010). This raises the possibility that replication fork reversal by HLTF could provide a means for stabilizing TNR tracts. In this case, RTEL1 would unwind hairpins at a stalled or reversed fork to allow restart without expansions or fragility. A hairpin on the reversed fork end was previously proposed as a potential expansion intermediate (Mirkin, 2007) and provides a ssDNA-dsDNA junction, proposed to be a good substrate for RTEL1 loading and 5' to 3' unwinding (Uringa et al., 2011; Youds et al., 2010). Similarly, a template switch event occurring at the fork, mediated by HTLF and Rad18, could also require RTEL1 to unwind aberrant structured intermediates that might occur (Kim and Mirkin, 2013; Mirkin, 2007). This unwinding activity of RTEL1 is supported by the facts that Srs2 was shown to excel at unwinding G-rich structured DNA encountered during replication (Anand et al., 2012), and RTEL1 also appears to have *in vivo* roles in unwinding G-rich or structured regions such as found at telomeres and recombination hotspots (Uringa et al., 2011; Vannier et al., 2012). The fork restart model could also explain how the lack of RTEL1, HLTF or Rad18 would lead to excess expansions.

There is emerging evidence that RTEL1 and HLTF help prevent human disease. Polymorphisms in the *RTEL1* gene are susceptibility loci for glioma risk (Shete et al., 2009; Wrensch et al., 2009) and inherited mutations in *RTEL1* cause a severe form of dyskeratosis congenita (Ballew et al., 2013; LeGuen et al., 2013; Walne et al., 2013). RTEL1 effects on risk of these diseases have been attributed to its telomere-stabilizing activity. For HLTF, silencing of its promoter by methylation is associated with colon, gastric and uterine cancers (Debauve et al., 2008; Moinova et al., 2002). Based on our findings in this paper, we suggest

that down-regulation or loss of RTEL1 or HLTF might also lead to genetic predisposition towards TNR expansions.

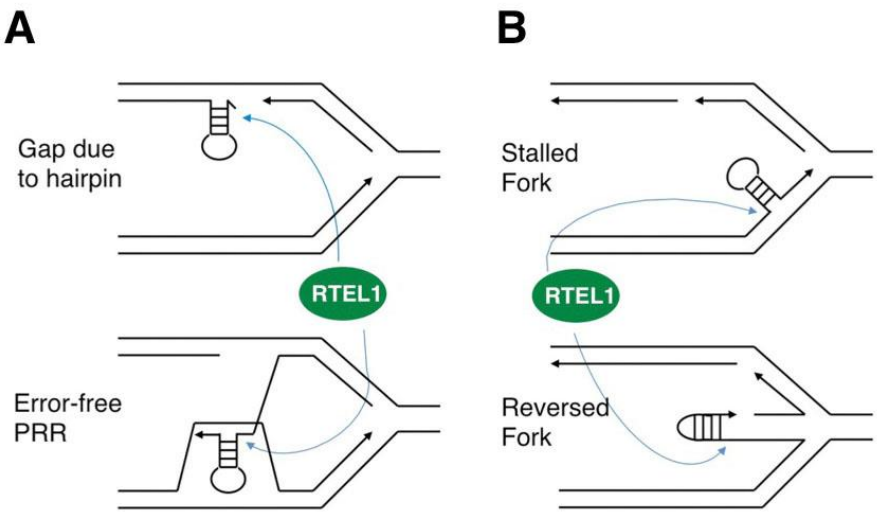

Figure 6. Models for inhibition of expansions by the concerted activities of HLTF, Rad18 and RTEL1. (A) A triplet repeat hairpin is formed by DNA replication (shown) or repair (not shown). HLTF and Rad18 recruit RTEL1 directly to the hairpin, or modify another factor which does so. Once at the hairpin, RTEL1 uses its helicase activity to unwind the hairpin to help avoid an expansion. *Lower panel,* recombinational repair attempts to resolve the hairpin but creates another hairpin in the process. RTEL1 acts to resolve the hairpin(s) and avoid expansion. (B) A hairpin is formed during DNA replication in conjunction with fork stalling. The hairpin could be alleviated directly by RTEL1 (*top panel*), or HLTF in conjunction with Rad18 acts to reverse the stalled fork, which brings RTEL1 to the hairpin for unwinding. For both A and B, loss or

reduced levels of HLTF, Rad18 or RTEL1 preclude hairpin unwinding such that the hairpin is subsequently processed to a triplet repeat expansion.

Potential model based on newly obtained data

We previously published results indicating expression of human RTEL1 in yeast could suppress *srs2Δ* MMS sensitivity and restore MMS hypersensitivity of *srs2Δrad5Δ*. From this, along with work from human cells (Frizzell et al., 2014), we concluded RTEL1 could substitute for Srs2 in post replication repair and suppress potential expansions that could occur during this process. However our newly obtained data showed expression of human RTEL1 in yeast did not suppress *srs2Δ* MMS sensitivity or restore MMS hypersensitivity of *srs2Δrad5Δ*, altering our interpretations.

Since RTEL1 expression did not suppress *srs2Δ* MMS sensitivity or restore MMS hypersensitivity of *srs2Δrad5Δ*, it suggests that it cannot substitute for Srs2 in PRR, at least in yeast. It is believed that *rad5* mutants are sensitive to MMS due to Srs2 preventing recombination to allow bypass of a damaged base. Since RTEL1 expression in yeast in *rad5Δ* did not restore MMS sensitivity, it could be due to the difference between RTEL1 and Srs2 anti-recombination activities. Srs2 prevents recombination by dismantling the Rad51 coated presynaptic filament (Krejci et al., 2003; Veaute et al., 2003) while RTEL1 prevents recombination by disrupting pre-formed D loops (Uringa et al., 2011). Based on our conclusion in chapter 2 that Srs2 is preventing repeat instability through recombination inhibition, we can infer RTEL1 could be reducing repeat expansions in the same manner. Indeed while we see a suppression of repeat

expansions in *srs2Δ* strains when we expressed human RTEL1, it was not down to wild-type levels. Perhaps RTEL1 anti-recombination activity is not as robust as Srs2 and therefore we still see increased levels of expansions compared to wild-type. This could suggest that recombination is occurring in these strains enough to rescue growth after MMS treatment.

We previously published results indicating expression of human RTEL1 in yeast strains could suppress *srs2Δ* fragility rates. Our conclusion from chapter 2 was that Srs2 was preventing repeat fragility at the replication fork through hairpin unwinding. Based on our data in this chapter and chapter 2, we believed both Srs2 and RTEL1 helicase mediated hairpin unwinding activity is needed to prevent repeat fragility. Our newly obtained data still supports this conclusion.

Altogether we show that RTEL1 can mostly substitute Srs2 in some of its cellular functions. Expression of RTEL1 in yeast reduced *srs2Δ* expansions either through its anti-recombination or hairpin unwinding activity. Expression of RTEL1 also reduced *srs2Δ* fragility most likely via hairpin unwinding. Since RTEL1 doesn't rescue MMS sensitivity of *srs2Δ* or restore hypersensitivity of *srs2Δrad5Δ*, this suggests Srs2 plays a more anti-recombinase role in post replication repair that RTEL1 cannot fully complement. Since we know RTEL1 helicase activity can substitute for Srs2 to prevent repeat fragility, this indicates that damaged bases and hairpin structures are repaired by different mechanisms.

Appendix 3.1

RT-PCR to confirm hRTEL1 and hFbh1 expression in yeast

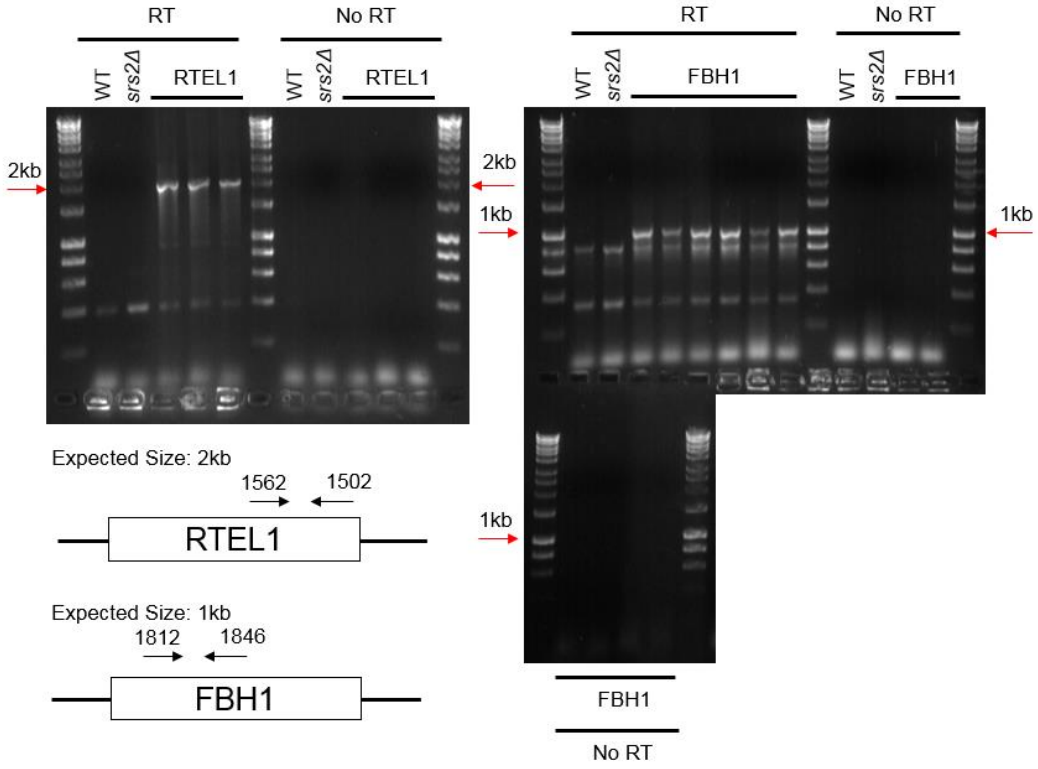

Gels depict PCR products using cDNA template generated by RT-PCR from *srs2::RTEL1* and *srs2::hFbh1* strains using primers shown in the diagram

Appendix 3.2

Raw fragility data for YAC CF1

	No tract			
	WT	*srs2Δ*	*srs2::hFBH1*	*srs2::hRTEL1*
	1.73	1.33	4.13	1.46
	2.62	1.41	2.29	4.03
	2.10	2.27	2.67	2.12
	2.07	1.41	4.12	
	2.59	1.95	5.29	
	2.78	3.34	4.11	
	1.32	1.47		
		3.89		
		2.65		
Average Rate of FOA^R x 10^{-6}	2.17	2.19	3.77	2.54
SEM	0.20	0.31	0.45	0.77
p-value compared to wild-type		0.9639	0.0057	0.5351
p-value compared to *srs2Δ*			0.0104	0.6261

	CAG_{70}			
	WT	*srs2Δ*	*srs2::hFBH1*	*srs2::hRTEL1*
	13.37	18.98	33.20	15.94
	14.04	17.84	18.53	27.32
	12.19	29.70	24.25	9.78
	12.58	22.03	15.43	8.12
	4.24	25.36		4.09
	5.15	17.98		8.45
	8.49	26.55		
	7.40	19.75		
	7.03	26.94		
		63.35		
		37.16		
		32.05		
		34.61		
		22.00		
		30.81		

		55.56		
Average Rate of FOA^R x 10^{-6}	9.39	30.04	22.85	12.28
SEM	1.24	3.25	3.90	3.39
p-value compared to wild-type		0.0001	0.0012	0.37
p-value compared to *srs2Δ*			0.3088	0.0057

Appendix 3.3

Raw instability data for CAG_{85} YAC CF1

Contractions

Mutant	No. of colonies	#	%	Fold over WT	p-value compared to WT	p-value compared to *srs2Δ*
Wild-type	299	33	11.04			
srs2Δ	139	4	2.88	0.26		
srs2::hFBH1	154	21	13.64	1.24	0.4456	0.0012
srs2::hRTEL1	174	12	6.90	0.62	0.1476	0.1238

Expansions

Mutant	No. of colonies	#	%	Fold over WT	p-value compared to WT	p-value compared to *srs2Δ*
Wild-type	299	4	1.34			
srs2Δ	139	10	7.19	5.38	0.0002	
srs2::hFBH1	154	8	5.19	3.88	0.0262	0.6273
srs2::hRTEL1	174	6	3.45	2.58	0.1826	0.0547

Appendix 3.4

Strain corrections

srs2::hRTEL1 No Tract (previously CFY2804, 2805. Remade: CFY3593)

- Strain issues
    - Srs2 ORF present at SRS2 locus; Confirmed by 5' and 3' junction PCRs and sequencing the 5' junction
    - CFY2804 had hRTEL1 ORF present somewhere within the genome (maybe extra-chromosomally). Confirmed by PCR with primers internal to hRTEL1-HIS3MX6 cassette; isoform 1. hRTEL1 ORF not present in CFY2805
- Strain remake and check
    - RTEL1 ORF and HIS3MX6 marker for co-transformation into CFY1626. Transformants PCR checked at 5' end to confirm Srs2 ORF absence and 3' end to confirm RTEL-HIS3MX6 presence. Correct transformants further checked with PCR across Srs2 locus and sequenced across the entire RTEL1 gene to confirm proper integration and no amino acid changes

srs2::hRTEL1 $(CAG)_{70}$ (previously CFY2806, 2807. Remade: CFY3597)

- Strain issues
    - Srs2 ORF present at SRS2 locus; Confirmed by 5' and 3' junction PCRs and sequencing the 5' junction
    - hRTEL1 ORF not present in CFY2806. CFY2807 had hRTEL1 ORF present somewhere within the genome (maybe extra-chromosomally). Confirmed by PCR with primers internal to hRTEL1-HIS3MX6 cassette; isoform 1
- Strain remake and check
    - PCR amplify RTEL1-HIS3MX6 at SRS2 locus from CFY3593 for transformation into CFY1628. Transformants PCR checked at 5' end to confirm Srs2 ORF absence and 3' end to confirm RTEL-HIS3MX6 presence. Correct transformants further checked with PCR across Srs2 locus and sequenced across the entire RTEL1 gene to confirm proper integration and no amino acid changes

srs2::hRTEL1 $(CAG)_{85}$ (previously CFY2994, 2995. Remade: CFY3604)

- CFY2994 was confirmed by 5' and 3' junction PCRs and sequencing to have Srs2 ORF absent at the SRS2 locus and RTEL1 present at the SRS2 locus (instability included reactions from this strain)
- Strain issues
    - Srs2 ORF present at SRS2 locus in CFY2995; Confirmed by 5' and 3' junction PCRs and sequencing the 5' junction
    - hRTEL1 ORF not present in CFY2995
- Strain remake and check
    - PCR amplify RTEL1-HIS3MX6 at SRS2 locus from CFY3593 for transformation into CFY810. Transformants PCR checked at 5' end to confirm Srs2 ORF absence and 3' end to confirm RTEL-HIS3MX6 presence. Correct transformants further checked with PCR across Srs2 locus and sequenced across the entire RTEL1 gene to confirm proper integration and no amino acid changes

srs2::hRTEL1 rad5Δ $(CAG)_{70}$ (previously CFY2949, 2950. Remake: CFY3654)

- Strain issue
    - Parent strains 2806, 2807. Rad5 confirmed knockout by PCR using primers to check Rad5 ORF absence and KANMX6 presence
- Strain remake and check
    - *rad5::KANMX6* knock out in CFY3597; junction PCRs to confirm proper marker integration and internal PCR to confirm loss of Rad5 ORF

srs2::hFBH1 $(CAG)_{85}$ (previously CFY2992, 2993)

- CFY2992 was confirmed by PCR to have Srs2 ORF absent at SRS2 locus and by sequencing to have FBH1 at Srs2 locus. More instability reactions were performed on this strain to add to previous data from this strain
- Strain issue
    - Point mutation in the FBH1 gene resulting in an amino acid change in CFY2993

Appendix 3.5

Strain table

Strain	Background	Genotype	Reference
CFY-1626 **CFY-1627**	BY4705	*ade2Δ::hisG, his3Δ200, leu2Δ0, lys2Δ0, met15Δ0, trp1Δ63, ura3Δ0, can^R, MATa* YAC: *URA3 LEU2* No Tract	Sundararajan et al. (2010)
CFY-1628	BY4705	*ade2Δ::hisG, his3Δ200, leu2Δ0, lys2Δ0, met15Δ0, trp1Δ63, ura3Δ0, can^R, MATa* YAC: *URA3 LEU2* CAG-70	Sundararajan et al. (2010)
CFY-810	BY4705	*ade2Δ::hisG, his3Δ200, leu2Δ0, lys2Δ0, met15Δ0, trp1Δ63, ura3Δ0, can^R, MATα* YAC: *URA3 LEU2* CAG-85	House et al. (2014)
CFY-766	BY4705	*ade2Δ::hisG, his3Δ200, leu2Δ0, lys2Δ0, met15Δ0, trp1Δ63, ura3Δ0, can^R, MATα* YAC: *URA3 LEU2* CAG-70	Kerrest et al. (2009)
CFY-925 **CFY-926**	BY4705	*his3Δ1, leu2Δ0, lys2Δ0, ura3Δ0, can^R, MATα , srs2::KAN* YAC: URA3 LEU2 No Tract	Kerrest et al. (2009)
CFY-928	BY4705	*his3Δ1, leu2Δ0, lys2Δ0, ura3Δ0, can^R, MATα , srs2::KAN* YAC: *URA3 LEU2* CAG-70	Kerrest et al. (2009)
CFY-2623	BY4705	*ade2Δ::hisG, his3Δ200, leu2Δ0, lys2Δ0, met15Δ0, trp1Δ63, ura3Δ0, can^R, MATα, srs2::TRP* YAC: *URA3 LEU2* CAG-70	This study
CFY-2990 **CFY-2991**	BY4705	*ade2Δ::hisG, his3Δ200, leu2Δ0, lys2Δ0, met15Δ0, trp1Δ63, ura3Δ0, can^R, MATα srs2::TRP* YAC: *URA3 LEU2* CAG-85	This study
CFY-1665	BY4705	*ade2Δ::hisG, his3Δ200, leu2Δ0, lys2Δ0, met15Δ0, trp1Δ63, ura3Δ0, can^R, MATα, rad5::KAN* YAC: *URA3 LEU2* No Tract	This study
CFY-1666	BY4705	*ade2Δ::hisG, his3Δ200, leu2Δ0, lys2Δ0, met15Δ0, trp1Δ63, ura3Δ0, can^R, MATα, rad5::KAN* YAC: *URA3 LEU2* CAG-70	This study

CFY-2773		*ade2Δ::hisG, his3Δ200, leu2Δ0, lys2Δ0, met15Δ0, trp1Δ63, ura3Δ0, can^R, MATα, srs2::hFBH1*	
CFY-2774	BY4705	YAC: *URA3 LEU2* No Tract	This study
CFY-2775		*ade2Δ::hisG, his3Δ200, leu2Δ0, lys2Δ0, met15Δ0, trp1Δ63, ura3Δ0, can^R, MATα, srs2::hFBH1*	
CFY-2776	BY4705	YAC: *URA3 LEU2* CAG-70	This study
CFY-2992	BY4705	*ade2Δ::hisG, his3Δ200, leu2Δ0, lys2Δ0, met15Δ0, trp1Δ63, ura3Δ0, can^R, MATα, srs2::hFBH1* YAC: *URA3 LEU2* CAG-85	This study
CFY-3593	BY4705	*ade2Δ::hisG, his3Δ200, leu2Δ0, lys2Δ0, met15Δ0, trp1Δ63, ura3Δ0, can^R, MATα, srs2::hRTEL (isoform 1)* YAC: *URA3 LEU2* No Tract	This study
CFY-3597	BY4705	*ade2Δ::hisG, his3Δ200, leu2Δ0, lys2Δ0, met15Δ0, trp1Δ63, ura3Δ0, can^R, MATα, srs2::hRTEL (isoform 1)* YAC: *URA3 LEU2* CAG-70	This study
CFY-3604	BY4705	*ade2Δ::hisG, his3Δ200, leu2Δ0, lys2Δ0, met15Δ0, trp1Δ63, ura3Δ0, can^R, MATα, srs2::hRTEL (isoform 1)* YAC: *URA3 LEU2* CAG-85	This study
CFY-2982		*ade2Δ::hisG, his3Δ200, leu2Δ0, lys2Δ0, met15Δ0, trp1Δ63, ura3Δ0, can^R, MATα, srs2::TRP, rad5::KAN*	
CFY-2983	BY4705	YAC: *URA3 LEU2* No Tract	This study
CFY-2984		*ade2Δ::hisG, his3Δ200, leu2Δ0, lys2Δ0, met15Δ0, trp1Δ63, ura3Δ0, can^R, MATα, srs2::TRP, rad5::KAN*	
CFY-2985	BY4705	YAC: *URA3 LEU2* CAG-70	This study
CFY-2986		*ade2Δ::hisG, his3Δ200, leu2Δ0, lys2Δ0, met15Δ0, trp1Δ63, ura3Δ0, can^R, MATα, srs2::hFbh1, rad5::KAN*	
CFY-2987	BY4705	YAC: *URA3 LEU2* No Tract	This study

CFY-2988		*ade2Δ::hisG, his3Δ200, leu2Δ0, lys2Δ0, met15Δ0, trp1Δ63, ura3Δ0, can^{R}, MATα, srs2::hFbh1, rad5::KAN*	
CFY-2989	BY4705	YAC: *URA3 LEU2* CAG-70	This study
CFY-3654	BY4705	*ade2Δ::hisG, his3Δ200, leu2Δ0, lys2Δ0, met15Δ0, trp1Δ63, ura3Δ0, canR, MATα, srs2::hRTEL (isoform 1),rad5::KAN YAC: URA3 LEU2 CAG-70*	This study

Appendix 3.6

Primer table

#	Primer Name	Purpose	Sequence
2076	newCAGfor	Anneals 42bp from CAG repeat, on centromeric side; tract check	CCTCAGCCTGGCCG AAAGAAAGAAA
2077	newCAGrev	Anneals 117bp from CAG repeat, on the telomeric side; tract check	CAGTCACGACGTTGT AAAACGACGG
499	200bp upstream Srs2 ORF	To amplify across *SRS2* ORF to check proper integration of human ORFS; to amplify *srs2::hFBH1-HIS3MX6*	ctccagctatcctgatacta
500	200bp downstream Srs2 ORF	To amplify across SRS2 ORF to check proper integration of human ORFS; to amplify srs2::hFBH1-HIS3MX6	catactgctcattcatagct
853	Srs2_1943-1963R	To confirm absence of Srs2 ORF	gacctttggcaccgtgaattg
678	Srs2_225upstream	5' junction check for human gene integration	agaataggagcgagtttagagttac
1064	Fbh1_962-981R	Internal Fbh1 primer to confirm knock in	gatgttaatccccttctccc
1065	Fbh1_1339-1356F	Internal Fbh1 primer to confirm knock in	cggaagtaccagtcaaag
842	His3 for RTEL	Amplify HIS3MX6 from pFa for tagging*srs2::hRTEL1*; has homology to 845, includes stop codon	AGCTTGCCTCGTCC CCGCCGGGTCACCC GGC
843	His3 rev RTEL	Amplify HIS3MX6 from pFa for taggingsrs2::hRTEL1; homology to 3' end of Srs2 locus	CCGCCTCCAATAGTT GACGTAGTCAGGCA GAAAGTGCTACGTTA GTATCGAATCGACAG
844	Srs2::hRTEL for	Creation of RTEL fragment for *srs2::hRTEL1*; homology to 3' end of Srs2 promoter	CCAATTTGATCTTTC TTCTACCGGTACTTA GGGATAGCAA
845	Srs2::hRTEL rev	Creation of RTEL fragment for *srs2::hRTEL1*; has	ATGTCGCTGGCCGG GTGACCCGGCGGGG ACGAGGCAAGCTTTA

		homology to 842; includes stop codon	CAGATCCTCTTCTGAGA
1502	Rtel C term reverse	For RT PCR to confirm expression	gttcgaaagggtgacctcgag
1557	Rtel_518rev	5' check RTEL integration	ggcacaagtggatctgtagatg
1558	Rtel_518for	Used to sequence RTEL	caggagcgacttgccaccttctac
1576	Rtel_623for	Used to sequence RTEL	cttactacctgtcccggaacctgaag
1559	Rtel_1048for	Used to sequence RTEL	gagctgtttgctgaagcccagatcac
1560	Rtel_1490for	Used to sequence RTEL	cagtctgcctggagaacccacacatc
1561	Rtel_1890for	Used to sequence RTEL	gctggacttctcagacacgaatggc
1562	Rtel_2239for	Used to sequence RTEL; For RT PCR to confirm expression	cagttcttccgtgttgccgagcgaac
1577	Rtel_3055for	Used to sequence RTEL	caagagcacctgaaccagggcagg
1563	Rtel_4208for	Used to sequence RTEL	ctcgaggtcacccttcgaac
1812	Fbh1_471-493 for	Used to sequence FBH1;For RT PCR to confirm expression	CCT CTA TTG GAA CCT GAG CTT GG
1813	Fbh1_901-920 for	Used to sequence FBH1	GTG ACC ATG CCA GAT GTC AC
1814	Fbh1_1337-1356 for	Used to sequence FBH1	GGC GGA AGT ACC AGT CAA AG
1815	Fbh1_1756-1775 for	Used to sequence FBH1	GTT CTG TCT CAG CCA TGT GG
1816	Fbh1_2266-2286 for	Used to sequence FBH1	GAC AAG GAG CTT GAA GCC AAG
1817	Fbh1_2696-2715 for	Used to sequence FBH1	CTG TTG ACA CCG TCC TTA CC
1846	Fbh1_1477-1498rev	For RT PCR to confirm expression	CAA TGG TCA GCT CTT CGT CAG C

Chapter 4

Ctf18 and Srs2 but not DNA damage tolerance pathways are needed to prevent chromosomal breakage at structure-forming CAG/CTG repeats

Jennifer Nguyen^, Lionel Gellon^, Katherine Wu^, Catherine Freudenreich^

^Department of Biology, Tufts University, Medford MA 02155, USA

Author contributions:

Jennifer Nguyen: performed all CAG_{70} fragility assays except those listed below, sister chromatid recombination assay, tetrad dissections, growth curve, and ChIP

Lionel Gellon: performed *ctf18Δ, rad5Δctf18Δ, srs2Δctf18Δ,* CAG_{70} fragility assays

Katherine Wu: contributed to TLS CAG_{70} fragility assays

Jennifer Nguyen and Catherine H. Freudenreich analyzed data

Jennifer Nguyen wrote chapter

Catherine Freudenreich provided edits and comments to chapter

ABSTRACT

CAG/CTG repeats can be source of DNA damage because they have a propensity to form secondary structures that can impede important cellular processes such as replication, which can lead to instability of the repeats, replication fork stalling, or chromosomal breakage (fragility). Replication is a tightly regulated process requiring the coordination of various proteins to maintain fidelity. One important replication protein is the DNA clamp, PCNA. PCNA increases polymerase processivity to allow longer stretches of synthesis during replication and serves as a scaffold for binding of various proteins involved in replication and repair. Under normal replication conditions, PCNA can be SUMOylated at Lys164 (K164), which recruits the Srs2 helicase. When the replication fork stalls at a site of DNA damage, PCNA is ubiquitinated at K164 to signal the DNA damage tolerance (DDT) repair pathway (also called post replication repair). We have determined that under normal conditions, rendering PCNA unmodifiable by either ubiquitination or SUMOylation (K164R) minimally affects repeat fragility. However, PCNA modification becomes important in the absence of the alternative clamp loader Ctf18. In this study, we have identified a role for PCNA SUMOylation in response to secondary structure formation by the CAG/CTG repeats. Specifically in the absence of Ctf18, Srs2 recruitment to PCNA is especially needed to prevent a further increase in repeat fragility. We hypothesize three pathway choices by which a stalled replication fork can bypass a hairpin structure: bypass of the lesion through DDT, Ctf18 mediated hairpin bypass via PCNA unloading/loading, and Srs2 recruitment to unwind the hairpin. Our data shows that the latter two pathways are specifically needed at a DNA structure whereas DDT pathways are primarily used for base damage. This work

implicates Ctf18 and Srs2 in prevention of breakage specifically at a DNA structure

INTRODUCTION

Replication needs to occur with minimal error in every dividing cell. During replication, there are many opportunities for DNA mutations to arise. One such opportunity is replication through a natural pause site such as a repetitive sequence, for example CAG/CTG trinucleotide repeats. These are common in the genome and long tracts of these repeats have been linked to several neurodegenerative diseases such Huntington's disease and several spinocerebellar ataxias, with affected individuals with Huntington's disease having 40+ and spinocerebellar ataxias ranging from 20-61+ CAG repeats (López Castel et al., 2010; Usdin et al., 2015). When unwinding occurs for replication, repetitive sequences have a propensity to form secondary structures which can impede replication progression and cause forks to stall (Mirkin, 2007; Mirkin and Mirkin, 2007). Polymerase stalling at a difficult to replicate region could lead to the uncoupling of the replicative MCM helicase from the polymerases, allowing it to expose ssDNA ahead of the replication fork (Berti and Vindigni, 2016; Byun et al., 2005; Sogo et al., 2002), which can be prone to nucleolytic attack leading to breakage (Froget et al., 2008; Kai et al., 2005; Seigneur et al., 1998). RPA coating of the ssDNA can recruit Rad18 to modify PCNA and signal the DNA damage response to prevent breakage from occurring (Davies et al., 2008). The $(CAG/CTG)_{55\text{-}98}$ as well as $(CGG/CCG)_{40}$ repeats have been shown to cause increased fork stalling and chromosomal fragility (Chapter 2, (Anand et al., 2012; Kerrest et al., 2009)), providing a natural impediment for

studying the mechanisms cells use to coordinate replication and repair to protect against damage.

PCNA serves as a platform for various proteins involved in replication as well as repair. PCNA, an evolutionarily conserved homotrimer, is a DNA sliding clamp that forms a ring shape and is loaded onto DNA by replication factor C (RFC) (Majka and Burgers, 2004; Moldovan et al., 2007). RFC is a ring-like protein complex composed of the subunits RFC1, RFC2, RFC3, RFC4, RFC5, which have homology to the *E. coli β* clamp loader (Hedglin et al., 2013). In addition to RFC, there are also alternative clamp loaders, which share the small RFC2-5 subunits but have Ctf18, Elg1, or Rad24 in place of Rfc1 (Majka and Burgers, 2004). Each of these alternative clamps have a role in specific pathways in cellular processes: Rad24-RFC interacts with the 9-1-1 complex (in yeast Rad17–Mec3–Ddc1; in humans Rad9, Rad1, Hus1) during the DNA damage checkpoint (Bermudez et al., 2003a; Majka and Burgers, 2003), Elg1 can unload unmodified and SUMOylated PCNA from DNA to protect genome integrity (Kubota et al., 2013a, 2015), and Ctf18 establishes cohesion between sister chromatids and has been shown to biochemically both load and unload PCNA (Bermudez et al., 2003b; Bylund and Burgers, 2005). Interestingly, Ctf18 but not Rad24 or Elg1 was found to have a novel role in protecting repeat integrity (Gellon et al., 2011). Temperature sensitive sister chromatid cohesion mutants did not show increased repeat fragility or instability suggesting Ctf18's protective role to be occurring independently of its role in cohesion (Gellon et al., 2011), however the mechanism by which Ctf18 protects CAG repeats has not been fully identified.

Ctf18 plays an important role in genome maintenance and various genome defects arise in its absence. In addition to interacting with PCNA, Ctf18 has been shown to interact with RPA and pol ε, positioning it for replication involvement (Kim and Brill, 2001; Murakami et al., 2010). Indeed studies have shown that replication is impeded in the absence of Ctf18. When cells are treated with hydroxyurea (HU) to stall replication forks, Ctf18 is needed to prevent slowed fork speed and asymmetrical fork progression during replication (Crabbé et al., 2010), indicating Ctf18 is needed to facilitate fork progression and prevent fork stalling. Absence of Ctf18 in the presence of HU results in de-repression of late origin firing, indicating Ctf18 has a role in the DNA replication checkpoint pathway (Crabbé et al., 2010). An accumulation of replication machinery on chromatin was seen in *ctf18Δ* supporting firing of more origins (Kubota et al., 2011). This role is independent of its role in cohesion and is specific to Ctf18 since *rad24Δ* and *elg1Δ* did not show this same level of late origin de-repression (Crabbé et al., 2010). Ctf18 may also have a role in repair since in its absence, pol ε loading onto PCNA for nucleotide excision repair after UV damage was defective (Ogi et al., 2010).

Ctf18-RFC is unique among the clamp loaders in having seven subunits instead of five. Along with Ctf18 and the shared RFC2-5 subunits, Ctf8 and Dcc1 comprise the heptamer complex (Mayer et al., 2001). Ctf18 and Dcc1 were originally identified in two independent screens implicating a role for the Ctf18-RFC in repeat maintenance (Gellon et al., 2011; Razidlo and Lahue, 2008). Further analysis showed a significant increase in repeat fragility and instability in the absence of the Ctf18-RFC (Gellon et al., 2011). Additionally, even without repeats *ctf18* strains had an increase in Rad52 foci in S and G2 phases and *dcc1*

strains had slower division time with an extended G2/M phase although repeat tracts exacerbated these phenotypes (Gellon et al., 2011). Since Rad52 foci in S phase is indicative of repair (Lisby et al., 2001), we hypothesized that in the absence of Ctf18-RFC, the increase in Rad52 foci is a result of DNA damage occurring during S phase that requires repair. If not properly repaired during S phase, the damage persists into G2.

The DNA damage tolerance pathway (DDT; also known as post replication repair (PRR)) is utilized in cells to bypass lesions that could impede replication during S phase. DDT is coordinated by post-translational ubiquitination of PCNA. Monoubiquitination is mediated by the E2/E3 Rad6/Rad18 complex, which ligates a ubiquitin moiety to the Lys164 of PCNA (Hoege et al., 2002; Stelter and Ulrich, 2003; Ulrich, 2009). Monoubiquitination leads to the recruitment of specialized translesion synthesis (TLS) polymerases (Hoege et al., 2002; Lehmann et al., 2007; Stelter and Ulrich, 2003), capable of adding bases opposite a damaged template to allow replication past a lesion (Lehmann et al., 2007; Waters et al., 2009). In yeast, the TLS polymerases are coded by Rad30 (Pol η), Rev3/7 (Pol ζ), and Rev1 (REV1) (Waters et al., 2009). Polyubiquitination is facilitated by the E2 conjugator Mms2/Ubc13 and E3 ligase Rad5 , which is responsible for creating a polyubiquitin Lys63 linked chain off the same residue and it is known that this signals an error-free bypass pathway that can utilize the sister chromatid as a template for synthesis (Hoege et al., 2002; Torres-Ramos et al., 2002; Unk et al., 2010). PCNA SUMOylation can also occur at the Lys164 residue although both of these modifications are not antagonistic to each other (Hoege et al., 2002). PCNA SUMOylation is performed by E2/E3 Ubc9/Siz1 and occurs independently from DNA damage, although PCNA SUMOylation can occur under

lethal concentrations of the alkylating chemical methyl methanesulphonate (MMS) (Hoege et al., 2002). PCNA SUMOylation is stimulated by PCNA loading onto DNA (Parker et al., 2008). SUMOylated PCNA is known to recruit the anti-recombinase helicase Srs2 (Papouli et al., 2005; Pfander et al., 2005).

When the replication fork encounters DNA damage, PCNA ubiquitination occurs in S phase to signal DDT and PCNA modification can persist into G2 if more time for repair is required (Daigaku et al., 2010; Karras and Jentsch, 2010). This signaling matches the timing of increased Rad52 foci observed in *ctf18* cells and coincides with the extended G2 phase seen in *dcc1* cells (Gellon et al., 2011). We hypothesized in the absence of the Ctf18-RFC, damage is occurring in S phase and persisting into G2 due to untimely repair, which could be repaired by DDT. In this study, we found that in the absence of Ctf18-RFC, PCNA modification on Lys164 is needed to prevent repeat fragility. Specifically, absence of Srs2 recruitment through SUMOylated PCNA is especially important in cells without Ctf18-RFC. We propose a model wherein there are three pathways by which a stalled fork can bypass a hairpin to continue replication: PCNA ubiquitination to enact TLS or error-free bypass via template switch, Srs2 recruitment to SUMOylated PCNA to unwind the hairpin, and Ctf18 mediated hairpin bypass by unloading/loading of PCNA. Our data indicate Ctf18 mediated bypass and Srs2 recruitment are most important at a DNA structure whereas the TLS and error-free bypass pathways are primarily used for base damage.

MATERIALS AND METHODS

Strains

Strains used for fragility and instability assays were the isogenic BY4705 background, contained a yeast artificial chromosome with CAG-70 repeats, LEU2, and URA3 markers as previously described (–LEU2-G_4T_4-CAG_{70}-URA3, referred to YAC CF1) (Callahan et al., 2003; Sundararajan and Freudenreich, 2011). Strains used for the SCR assays and RPA ChIP were the W303 background. Gene knockouts were generated through PCR-directed gene replacement (Longtine et al., 1998) except *srs2Δctf18Δ, srs2Δrad5Δctf18Δ*, and *srs2Δrad18Δctf18Δ* which were generated through mating and tetrad dissection. Mutants were confirmed by PCR to have target gene absence and marker gene presence at the current locus. *pol30K164R* was obtained from the R. Lahue lab and saved as CFY2151. Two methods were used to generate *pol30K164R* CAG_{70}: (1) kar-crossed CAG_{70} YAC CF1 into the Lahue strain (CFY2638 and CFY2639), (2) PCR amplified across the POL30 locus (CFY2638) and co-transformed that fragment with HIS3MX6 to create *polK164R* in BY4705 background already containing CAG_{70} YAC CF1 (CFY3922 and CFY 3923). Transformants were sequenced to confirm the point mutation. RFA1-myc-TRP was PCR amplified from a previously constructed strain (Papamichos-Chronakis and Peterson, 2008) using primers flanking the RFA1 locus. The fragment was transformed into the W303 background strain with CAG_{130} 7kb from ARS607 on Chr VI (CFY3566) and integration was confirmed by PCR. Strains used for 2D analysis contain either YEP24 plasmids carrying $(CGG/CCG)_{40}$ or $(CAG/CTG)_{130}$ repeats were previously described (Anand et al., 2012; Pelletier et al., 2003)

Fragility and instability assays

Assays were done as previously described (Kerrest et al., 2009). Briefly, cells having confirmed tract lengths were grown at 30^{o}C in yeast complete (YC) media -Leu for 6-8 divisions to allow breakage to occur. Assays were performed with either the 1 colony or 10 colony method with a minimum of 3 experiments per mutant. Cells were plated on 5-FOA-Leu to select for breakage events and YC –Leu for total cell count. Rate of breakage per 100μL was calculated using the Maximum Likelihood Method (FALCOR).

Instability was determined via PCR across the repeats of at least 150 colonies from cells grown on YC –Leu plates as part of the fragility assay. PCR products were visualized on a high resolution 2% Metaphor gel (Lonza), which can accurately resolve +/- 9 bp (3 repeats) in the 0-200 bp size range. Tracts were sized using Photoshop and drawing a line between two markers. Primers used were either 2076/2077 or 1533/1534, which resulted in products with 159bp or 95bp of unique sequence in addition to the length, respectively. Sizes were estimated by subtracting out unique sequence and dividing by three.

Tetrad Dissection

MATa and MATα strains were mated for 16 hours on YC –Leu-Ura and then plated on media selecting for diploids. Diploids were resuspended in liquid sporulation media (1% KoAC) and incubated at 30^{o}C for 7-10 days. Cells were treated with Zymolyase 100T for 2 minutes before plating on YPD for dissections. After 7 days of growth, spores were genotyped by pinning onto single drop out plates. Mutants of interest were PCR confirmed for target gene absence and marker gene presence.

Growth Curve

Strains were grown to saturation in 5mL YC –Leu-Ura and then diluted down to OD_{600} 0.06 in 20mL in YC –Leu-Ura. Strains were grown at 30^{o}C with constant agitation. OD_{600} readings were taken at the time points indicated. Each data point represents the average of two independent tubes.

RESULTS

PCNA modification is needed in the absence of Ctf18-RFC

We hypothesized that Ctf18-RFC had a role in DDT to facilitate replication through hairpin structures. To test this, we used a genetic approach to determine the relationship between Ctf18-RFC and PCNA modification. We utilized a strain with the Lysine 164 (K164) on PCNA mutated to Arginine (*pol30K164R)*, rendering the residue unmodifiable and unable to signal DDT or to recruit Srs2 (Figure 1A) (Daee et al., 2007). If Ctf18-RFC, DDT and/or Srs2 recruitment are in the same pathway, we would expect to see epistasis and similar levels of chromosomal breakage (fragility) in the single and double mutants.

We tested chromosomal fragility using a yeast artificial chromosome (YAC) breakage assay as previously described (Figure 1B) (Kerrest et al., 2009). Strains carried a YAC containing CAG-70 repeats (nomenclature refers to sequence on the lagging strand template) and were grown in non-selective conditions to allow breakage to occur. We can correlate breakage with the number of colony forming units (CFUs) grown on FOA media, selecting for loss of the URA3 gene on the right arm of the YAC. We investigated the effect of unmodifiable PCNA on the rate of FOA^{R} in two strain backgrounds, BY4705 and

BL0035, and found differing rates of FOA^R for *pol30K164R* (Figure 1C and 1D). In the BY4705 background, *pol30K164R* did not show a significant increase in rate of FOA^R compared to wild-type (Figure 1C), suggesting PCNA modification is not needed to prevent repeat fragility. In the BL0035 background, *pol30K164R* has a significant increase in rate of FOA^R compared to wild-type (Figure 1D), which suggests PCNA modification is needed to prevent repeat fragility. Other work has shown *pol30K164R* BL0035 resulted in a 45-fold increase in expansion frequency in short CAG repeats (Daee et al., 2007), supporting the need for PCNA modification in repeat maintenance in that strain background. Interestingly, when the *pol30K164R* mutant was combined with *ctf18Δ*, a synergistic increase in the rate of FOA^R was seen compared to either single mutant in BY4705 and compared to *pol30K164R* in BL0035 (Figure 1C and 1D). While the absolute numbers are different, the fold changes of *pol30K164Rctf18Δ* over *pol30K164R* are comparable (24-fold and 41-fold for BY4705 and BL0035 respectively). Taken together, this suggests that in the absence of the Ctf18-RFC, PCNA modification is needed to prevent repeat fragility.

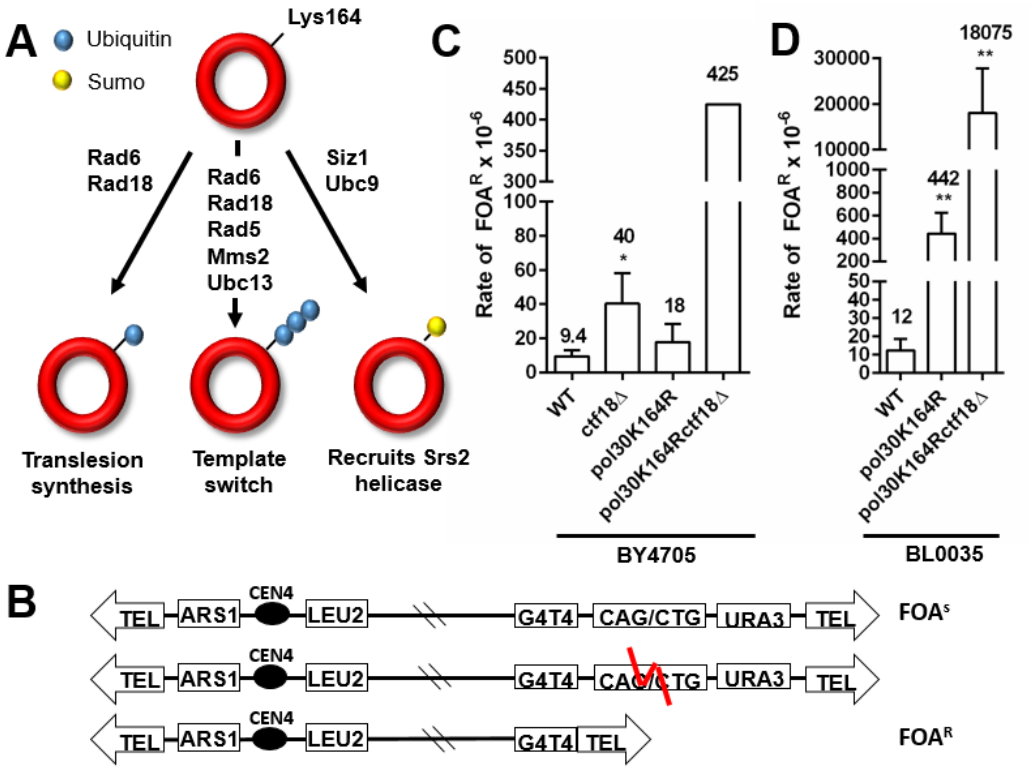

Figure 1. PCNA modification is needed to prevent repeat fragility in the absence of Ctf18 (A) PCNA is modified on Lysine 164 to coordinate DDT. Monoubiquitination by Rad6/Rad18 recruits translesion polymerases, polyubiquitination by Rad5/Mms2/Ubc13 promotes error-free template switch, SUMOylation by Siz1/Ubc9 recruits the Srs2 helicase. (B) Schematic of the YAC system. A breakage event that occurs within/near the repeats can lead to loss of the right arm and result in cells resistant to 5-FOA. (C) The rate of FOA^R x 10^{-6} is shown for the BY4705 strain background. Data represents the average of at least three experiments except *pol30K164R ctf18Δ*, which represents one 5-plate assay. Error bars represent SEM. Student's t-test *p<0.05 compared to WT. (D) Rate of FOA^R x 10^{-6} is shown for the BL0035 strain background. Data represents the average of at least three experiments. Error bars represent SEM. Student's t-test **p<0.01 compared to WT

TLS and template switch pathways are not required to prevent repeat fragility in the absence of Ctf18-RFC

We reasoned that *pol30K164R* abolishes the ability to go through DDT to invoke TLS or template switch, or to recruit Srs2. We wanted to test how each of these mechanisms individually contributed to preventing repeat fragility in the absence of Ctf18-RFC.

To determine if polyubiquitination of PCNA, and thus the error-free template switch pathway, was needed in the absence of Ctf18-RFC, we investigated Rad5, a DNA-dependent ATPase and E3 ubiquitin ligase. Deletion of *RAD5* had wildtype levels of repeat fragility (Figure 2A), suggesting error-free bypass via a template switch doesn't prevent repeat fragility. The *rad5Δctf18Δ* mutant had a significant increase in FOA^R but only to the level of *ctf18Δ* (Figure 2A), which could indicate Ctf18-RFC works upstream of the error-free pathway and/or that pathway is not important in the absence of Ctf18-RFC to prevent fragility. We see similar results for *mms2Δctf18Δ* (Appendix 4.3). To further address whether Ctf18-RFC might have a role in error-free bypass, we utilized a strain which uses *ADE2* function as a readout for spontaneous unequal sister chromatid recombination as a proxy for template switch (Figure 2B, (Mozlin et al., 2008)). Spontaneous or MMS-induced sister chromatid recombination and template switch are both dependent on recombination proteins Rad51, Rad55, Rad57, which mediates strand invasion to replicate past a lesion (Vanoli et al., 2010). We found the rates of recombination between wildtype and *ctf18Δ* are indistinguishable (Figure 2C). Taken together, the error-free template switch

pathway does not seem to have an important role in repeat maintenance in the absence of Ctf18-RFC.

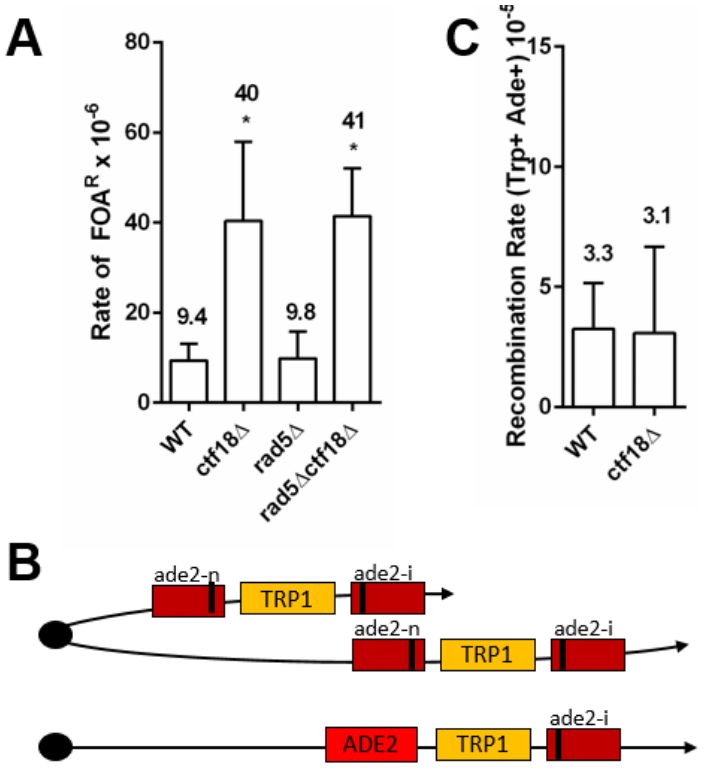

Figure 2. Error-free template switch does not have a role in preventing repeat fragility in the absence of Ctf18 and Ctf18 does not function in template switch during sister chromatid recombination. (A) Rate of FOA^R x 10^{-6} is shown. Data represents the average of at least three experiments. Error bars represent SEM. Student's t-test *p<0.05 compared to wildtype. (B) Schematic for sister chromatid recombination (SCR) assay, testing for effect of *ctf18Δ* on SCR/template switching. Unequal sister chromatid recombination leading to ADE2+ TRP+ strains is used to determine a rate of SCR. (C) Rate of recombination x 10^{-5} is shown. Data represents the average of at least two experiments. Error bars represent SEM

Next, to address whether TLS was needed in the absence of Ctf18-RFC, we tested the effect of Rad18, the RING-finger containing E3 ubiquitin ligase responsible for monoubiquitination of PCNA. We see a significant 2-fold increase in *rad18Δ* repeat fragility compared to wildtype (Figure 3). To specifically address TLS, we looked at strains lacking the TLS polymerases. *rev1Δrev3Δrad30Δ* strains do not show an increase in fragility (Figure 3), suggesting the increase we see in *rad18Δ* may be due to either loss of both TLS and template switch, or its other functions in the cell. Rad18 has been shown to coordinate the Fanconi Anemia pathway to repair cross-links in DNA in HeLa cells (Geng et al., 2010) and homologous recombination in MEF cells (Huang et al., 2009). We see a significant increase in FOA^R in *rad18Δctf18Δ*, although this is not significantly different from *ctf18Δ* due to the large spread of data (Figure 3) (Appendix table 4.3). To determine if this increase in fragility was due to a lack of TLS, we investigated *rev1Δrev3Δrad30Δctf18Δ* strains and found there was no significant increase in fragility compared to *ctf18Δ* (Figure 3). Taken together, these data indicate Rad18 might play a role in preventing repeat fragility in the absence of Ctf18-RFC, although we cannot distinguish if this is due to Rad18's other cellular functions or the lack of signaling of both TLS and template switch.

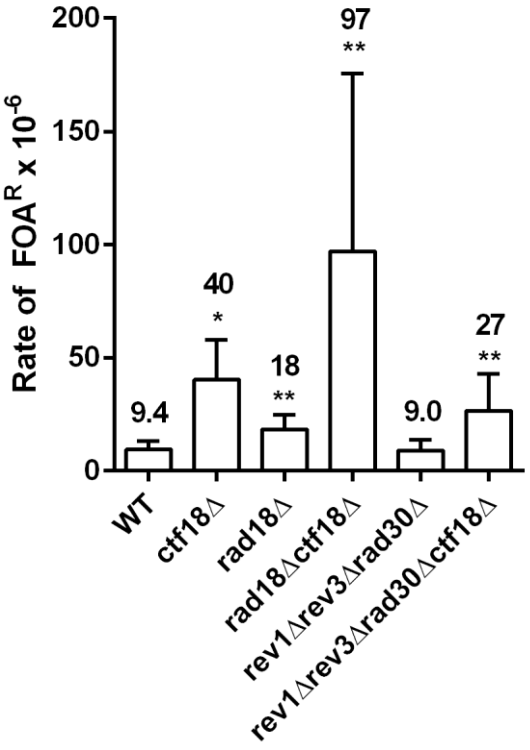

Figure 3. Deletion of the TLS pathway in *ctf18Δ* does not lead to synergistic increase in fragility. (A) Rate of FOA^R x 10^{-6} is shown. Data represents the average of at least three experiments. Error bars represent SEM. Student's t-test *p<0.05, **p<0.01 compared to WT.

In the absence of Ctf18, Srs2 recruitment via PCNA interaction is necessary to protect repeat fragility

We next addressed whether the SUMOylation pathway was important in the absence of Ctf18. PCNA is normally SUMOylated during DNA replication and when the cell is exposed to high amounts of DNA damage (Hoege et al., 2002). It is well known that SUMOylated PCNA recruits Srs2, a helicase and anti-recombinase (Papouli et al., 2005; Pfander et al., 2005). Srs2 has been shown to

have a specialized role in preventing repeat instability and fragility (Anand et al., 2012; Bhattacharyya and Lahue, 2004, 2005; Kerrest et al., 2009). We have previously shown that Srs2 requires its helicase activity and PCNA interaction, but not anti-recombinase activity, to prevent $(CAG/CTG)_{70}$ and $(CGG/CCG)_{40}$ repeat fragility as well as to prevent fork stalling as observed through 2D gel electrophoresis (Nguyen, et al. in prep; (Anand et al., 2012)). Altogether these data suggest Srs2 is recruited to the replication fork to unwind hairpins and allow replication to continue, preventing fork stalling and eventually breakage.

Separately, ***ctf18Δ*** and ***srs2Δ*** both have high rates of repeat fragility but when combined, we see a synergistic increase in rate of FOA^R in ***srs2Δctf18Δ*** (Figure 4), indicating a need for Srs2 in the absence Ctf18 to prevent further repeat fragility. We hypothesized this is due to a lack of Srs2 recruitment to PCNA. To test this, we utilized a Srs2 truncation mutant, *srs2 (1-998)*, where the last 176 residues of Srs2 are absent, which abolishes the PCNA interaction but maintains both helicase and Rad51 displacement activities (Le Breton et al., 2008; Colavito et al., 2009; Pfander et al., 2005). Indeed we see the same degree of synergistic increase in FOA^R in *srs2 (1-998) ctf18Δ* (Figure 4), supporting the vital need for Srs2 recruitment to PCNA to prevent repeat fragility in the absence of Ct18-RFC. These rates mirror the rate of FOA^R seen in ***pol30K164Rctf18Δ*** BY4705, suggesting Srs2 recruitment to PCNA could be the main pathway to prevent repeat fragility in the absence of Ctf18.

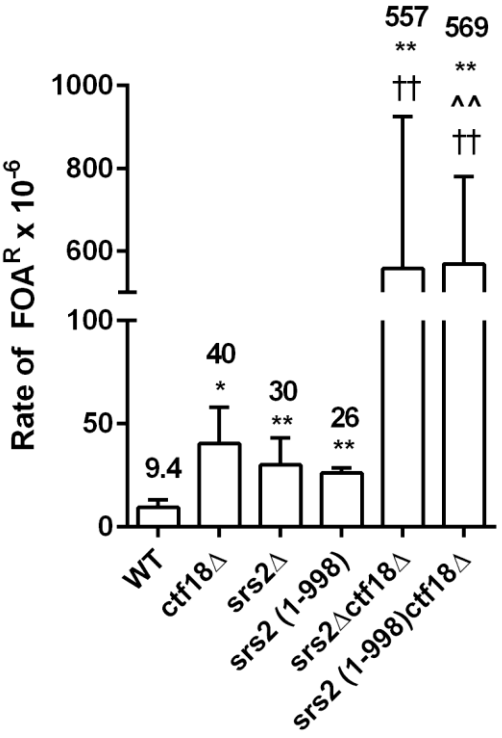

Figure 4. Srs2 recruitment to SUMOylated PCNA is needed to prevent synergistic fragility. Rate of FOA^R x 10^{-6} is shown. Data represents the average of at least three experiments. Error bars represent SEM. Student's t-test *p<0.05, **p<0.01 compared to WT; ^^p<0.01 compared to *ctf18Δ*; ††p<0.05 compared to *srs2Δ* or *srs2 (1-998)*, respectively

DDT and Srs2 recruitment is important for cell survival in the absence of Ctf18

Unlike *pol30K164Rctf18Δ*, which prevents DDT and Srs2 recruitment in the absence of Ctf18, our genetic approach thus far has only affected one or two pathways (TLS, template switch, TLS and template switch, Srs2 recruitment) rather than affecting all three at once in the absence of Ctf18. Our data suggests

Srs2 recruitment to PCNA is the major pathway needed to prevent further fragility in the absence of Ctf18. To determine whether TLS or template switch is needed to prevent fragility in the absence of both Srs2 and Ctf18 we created two triple mutants, *srs2Δrad5Δctf18Δ* and *srs2Δrad18Δctf18Δ*. Tetrad dissection was necessary to obtain these mutants after several unsuccessful attempts to obtain them by transformation. The frequency of genotypes between two crosses, *srs2Δrad5Δ* x *ctf18Δ* and *srs2Δrad18Δ* x *ctf18Δ* indicate that these mutants are very sick and not easily recovered (Figure 5A).

srs2Δrad5Δctf18Δ strains have loss polyubiquitination of PCNA and cannot promote error-free bypass in the absence of Srs2 and Ctf18. We see a synergistic increase in the rate of FOA^R in *srs2Δrad5Δctf18Δ* but only approximately to the level of *srs2Δctf18Δ*, supporting our previous results indicating no need for template switch in this mode of repair (Figure 5B). *srs2Δrad18Δctf18Δ* strains have loss monoubiquitination of PCNA and cannot signal TLS or error-free bypass in the absence of Srs2 and Ctf18. We saw a decrease in rate of FOA^R compared to *srs2Δctf18Δ* (Figure 5B), suggesting the loss of DDT signaling in the absence of Srs2 and Ctf18 leads to a decrease in fragility, contradictory to the *pol30K164Rctf18Δ* results. However, it should be noted that both of these triple mutants have a severe growth defect phenotype, requiring roughly five times longer to grow compared to wildtype strains. Two possibilities could result in the decrease in FOA^R: 1) since the triple mutants are very sick, only survivors resulting from suppressor mutations are able to proliferate and overtake growth in cultures, or 2) most cells with a broken chromosome undergo irreversible arrest and are not recovered. Either possibility

would result in a low rate of FOA^R that does not reflect the triple mutant phenotype.

We performed a growth curve to determine what effect loss of the various proteins have in the absence of Ctf18-RFC. Strains were normalized to the same OD and grown in yeast complete media selecting for the YAC (YC-Leu-Ura). It was previously demonstrated that compared to wildtype, *ctf18Δ* has a slow growth phenotype (Gellon et al., 2011). Generally, we see that most mutants previously tested for fragility grow similar to *ctf18Δ* with the exception of *rad18Δctf18Δ* which grew slower, but was eventually able to reach the target OD. However, *srs2Δctf18Δ*, *srs2Δrad5Δctf18Δ*, and *srs2Δrad18Δctf18Δ* exhibit extremely slow growth (Appendix 4.2). This slow growth phenotype could be attributed to failure to promote checkpoint recovery due to deletion of Srs2p (Vaze et al., 2002). Supporting this interpretation, *srs2(1-998) ctf18Δ* doesn't grow as slowly as *srs2Δctf18Δ*, fitting with previous data that identifies the need for Srs2 Rad51 displacement activity to lead to checkpoint recovery (Yeung and Durocher, 2011), which is still intact in *srs2(1-998)*. We conclude we are likely underestimating fragility in mutant strains missing both Ctf18 and Srs2 because of their inability to properly progress through the cell cycle and deleting Rad18 in the *srs2Δctf18Δ* double appears to further exacerbate the problem (Figure 6B). On the other hand, the *pol30K164Rctf18Δ* mutant in both strain backgrounds did not display the slow growth phenotype (growth was similar to *ctf18Δ*) despite the difference in rate of FOA^R, indicating recovery of the cells with broken and healed chromosomes is occurring.

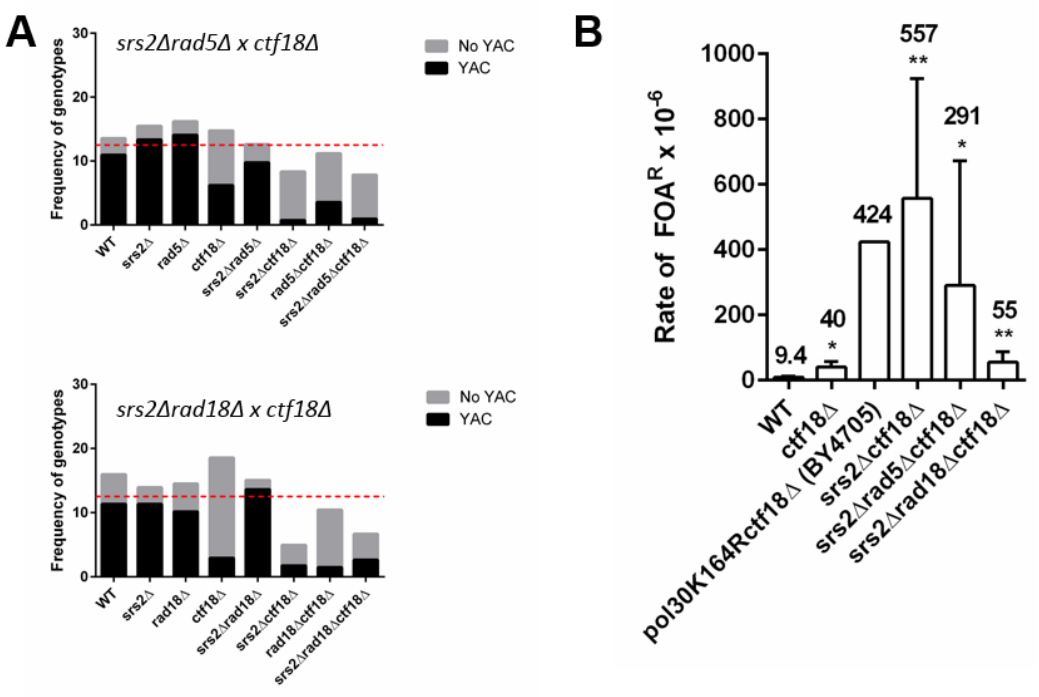

Figure 5. (A) Frequency of specified genotypes from tetrad dissection are shown. n=325 spores for *srs2Δrad5Δ x ctf18Δ* cross, n=201 *srs2Δrad18Δ x ctf18Δ* cross. Red dotted line indicates expected frequency of the 8 genotypes (12.5%) (B) Rate of FOA^R x 10^{-6} is shown. Data represents the average of at least three experiments except *pol30K164rctf18Δ*, which only has one experiment. Error bars represent SEM. *p<0.05, p**<0.01 compared to wildtype;

DISCUSSION

It was previously found that the alternative clamp loader Ctf18-RFC has a specialized role in protecting repeats independent of its role in cohesion (Gellon et al., 2011). In this study we determine that while Ctf18-RFC is needed to prevent repeat fragility, cells lacking Ctf18 rely on PCNA modification to protect against further increase in fragility (Figure 1B). Specifically, it is recruitment of Srs2 to SUMOylated PCNA that is the major pathway utilized in the absence of

Ctf18-RFC (Figure 4). Even in CTF18+ strains, Srs2 has been shown to be important in preventing repeat fragility. Srs2 is recruited to SUMOylated PCNA to unwind hairpin structures to prevent repeat fragility (Nguyen, et al. in prep; (Anand et al., 2012)), suggesting Ctf18 and Srs2 are working in parallel but distinct pathways to prevent repeat fragility.

The *pol30K164R* mutant prevents ubiquitination and SUMOylation on that residue. This would suggest *pol30K164R* results in loss of Srs2 recruitment since Srs2 is recruited by SUMOylated PCNA. However it has been shown that Srs2 has two independent motifs that facilitate SUMOylated PCNA interaction: a PCNA interacting domain (PIM) and a SUMO interacting domain (SIM) (Kolesar et al., 2016). We see a modest increase in FOA^R in *pol30K164R* (Figure 1), although this is not equivalent to *srs2Δ* FOA^R rates (Figure 4), suggesting that Srs2 could still be interacting with PCNA without modification, although not as efficiently, to prevent repeat fragility. To confirm this, we could observe fragility rates in *srs2-ΔSIM* and expect to see similar rates as *pol30K164R*.

The increased rate of FOA^R in *rad18Δctf18Δ* indicates in the absence of Ctf18, either the lack of both TLS and template switch (since Rad18 is required for both of these pathways) or one of Rad18's other functions (such as coordinating homologous recombination) is needed to prevent fragility. We can distinguish between the two by testing whether the increased rate of FOA^R in *rad18Δctf18Δ* is due to Rad18's role in DDT with *rad5Δrev1Δrev3Δrad30Δctf18Δ*, which would knock out both template switch and translesion synthesis in the absence of Ctf18. If the increased rate of FOA^R in *rad18Δctf18Δ* is due to loss of both of these pathways, we expect to get the same rate with *rad5Δrev1Δrev3Δrad30Δctf18Δ*. If the rate of FOA^R only increases to the level of

the *ctf18Δ* single, then that would indicate template switch and translesion synthesis are not needed and it is one of Rad18's other cellular functions that is needed to prevent fragility in the absence of Ctf18.

Our growth curve suggests Srs2's role in promoting checkpoint recovery is important in *ctf18Δ* cells to prevent cell cycle arrests after DNA damage induced checkpoint activation. If this is true, Rad53 phosphorylation status in strains lacking both Ctf18 and Srs2 should be elevated (Liberi et al., 2000b). Future analysis of instability could also provide insight on how these pathways function to prevent repeat expansion and contraction. Our data do not provide a clear mechanism as of yet though expansions and contractions appear to be additive in the *srs2Δctf18Δ* double mutant compared to each single (Appendix 4.7).

Ctf18 has been shown to localize to HU-stalled replication forks (Lengronne et al., 2006) and can interact with pol ε in both yeast and human cells (Gavin et al., 2006; Murakami et al., 2010), poising it perfectly to facilitate replication at challenged forks. Ctf18-RFC has been shown to be capable of unloading/loading PCNA off/on a DNA substrate (Bermudez et al., 2003b; Bylund and Burgers, 2005) and in its absence, there is a decrease in PCNA signal at HU-stalled replication forks (Lengronne et al., 2006). Some groups have suggested that Ctf18-RFC may be facilitating replication through the cohesin ring (Lengronne et al., 2006; Terret et al., 2009). In contrast, another group found that Elg1, another alternative clamp loader, was responsible for the majority of PCNA unloading and found no change in PCNA chromatin bound signal in *ctf18Δ* strains in the absence of HU (Kubota et al., 2013a). Since unloading of PCNA by Ctf18-RFC is slow (Majka and Burgers, 2004), it may be that Ctf18-RFC can unload or load PCNA at specific sites in the genome, like at stalled replication forks or at repeat

sequences. Ctf18-RFC was shown to stimulate pol η (a translesion synthesis polymerase) activity, suggesting Ctf18 may be involved with repair at aberrant DNA structures formed during fork stalling or sites of damage (Shiomi et al., 2007).

In the future, a 2D gel should be performed to determine if there is an increase in fork stalling at repeat sequences in the absence of Ctf18. This would confirm that Ctf18-RFC is needed to facilitate replication through repetitive sequences. Another way to confirm fork stalling in *ctf18Δ* strains would be to use chromatin immunoprecipitation (ChIP) for RPA or pol ε at the repeats. RPA is known to accumulate at stalled forks due to the increase in ssDNA (Petermann and Helleday, 2010), therefore we expect to see an increase in RPA signal in the absence of Ctf18 if forks are stalling. We can additionally ChIP PCNA specifically at the repeats in *ctf18Δ* mutants to determine if there is an accumulation or reduction of PCNA signal, shedding light on whether Ctf18-RFC is needed to unload or load PCNA to bypass a repeat sequence to prevent replication fork stalling. Perhaps Ctf18-RFC alone is needed to facilitate replication through a repeat sequence or it is the preferred clamp loader but the other clamp loaders could compensate in the absence of Ctf18-RFC. Perhaps Ctf18-RFC could be working with Elg1, where Elg1 is responsible for unloading PCNA when it encounters a stall and Ctf18 is required to reload it past the hairpin to allow replication to continue. Work in *S. pombe* showed synthetic lethality of *rfc1 ctf18* was rescued with *elg1*, which supports opposing roles for both of these clamps (Kim et al., 2005). Two attempts at ChIP, one for PCNA at CAG_{70} on YAC CF1 and one for RPA at CAG_{130} on Chr VI, have both been inconclusive thus far (Appendix 4.7 and 4.8, respectively).

We propose a model wherein when a replication fork encounters a hairpin structure that could stall the fork, there can be three pathways to continue normal replication: ubiquitinate PCNA to lead to TLS or error-free bypass, SUMOylate PCNA to recruit Srs2 to unwind the hairpin, or utilize Ctf18-RFC mediated hairpin bypass. When one or more of these pathways are perturbed, the others are more heavily relied upon. In our model, if Ctf18-RFC is absent, hairpin bypass via unloading/loading of PCNA is perturbed, which leads to an increase of fragility (Figure 7, pathway B). However, cells can still recruit Srs2 or utilize DDT to bypass the hairpin (Figure 7, A and C) preventing a greater increase in fragility. The synergistic increase in *srs2Δctf18Δ* and *srs2(1-998) ctf18Δ* does indicate Srs2 activity to be primarily utilized in the absence of Ctf18-RFC. Since both Ctf18 and Srs2 localize to the replication fork, they are both optimally located to work at DNA structures that can form during replication. Although TLS and template switch have been shown to efficiently bypass base damage, our work indicates these pathways play a minor role in bypassing a hairpin structure. Previous studies have shown that expressing proteins involved in ubiquitinating PCNA in G2 (Rad18p, Rad5p, and Ubc13p) can rescue the MMS sensitivities of those deletion mutants, suggesting that DDT can operate after S phase (Karras and Jentsch, 2010). This could put TLS and template switch as a backup repair mechanism if neither hairpin bypass nor unwinding were accomplished in S phase.

Conservation of the DDT proteins and Ctf18-RFC up to higher eukaryotes could indicate the importance of these repeat maintenance pathways. RTEL1 has recently been identified as a potential human Srs2 ortholog, capable of rescuing increased levels in fragility (Frizzell et al., 2014). It would be interesting to study

whether there is the same level of impact on fork stability at DNA structure barriers in higher eukaryotes if any of these repair pathways are perturbed. RTEL1 has been shown to unwind T loops at telomeres to prevent telomere fragility (Vannier et al., 2012). It has been suggested Ctf18 is needed to protect telomere length by maintaining cohesion to facilitate replication through the telomere (Hanna et al., 2001). Perhaps the same balance between RTEL1 and Ctf18-RFC would be needed to protect telomeres and other repetitive DNA in higher eukaryotes. Altogether, our data suggests bypass via re-loading of PCNA past a DNA structure could be an alternative method to prevent repeat fragility if helicase unwinding of structure fails or cannot be utilized. This study indicates that Ctf18-RFC and Srs2 work in parallel pathways to prevent repeat fragility and maintain genome integrity.

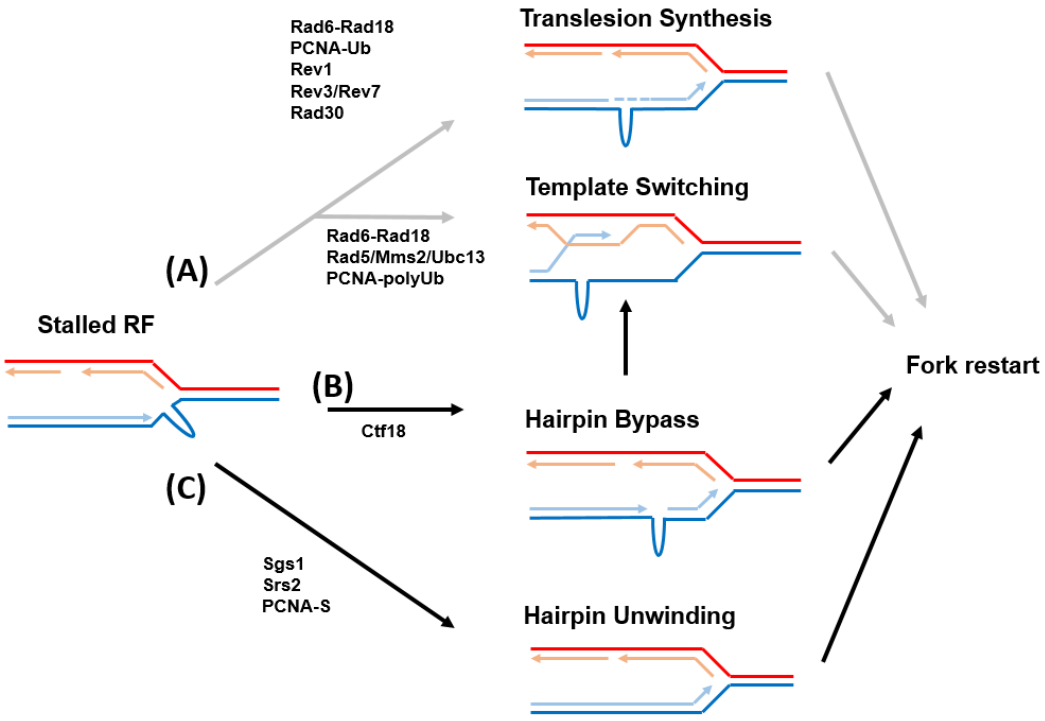

Figure 7. Proposed model for role of Ctf18 in preventing repeat fragility. When a replication fork (RF) is stalled, there can be three pathways that can allow bypass, or unwinding of the hairpin can occur: (A) Monoubiquitination by Rad6/Rad18 to recruit TLS polymerases or further polyubiquitination by Rad5/Mms2/Ubc13 to promote template switching. This is a minor pathway at a CAG/CTG hairpin (B) Ctf18 mediated hairpin bypass via unloading/loading of PCNA past the hairpin structure (C) Srs2 recruitment to SUMOylated PCNA to unwind the hairpin.

Appendix 4.1

Supplemental methods

Chromatin Immunoprecipitation

ChIP was performed as previously described (House et al., 2014). Briefly, cells were isolated from log phase (OD ~0.4) and treated with 30μM alpha factor for 1.5 hours to synchronize. Cells were released into S phase in YPD and time points were taken as indicated in graphs. Cells were cross-linked with 1% formaldehyde for 20 minutes and lysed with FA-lysis buffer (Aparicio et al., 2005) . Isolated chromatin was incubated with either 2μg anti-PCNA 5E6/2 (Abcam, ab70472) or 2μg anti-myc (Thermo Fisher Scientific, MA1-21316) antibody for 16 hours at 4°C. Protein G Dynabeads (Thermo Fisher Scientific, 10004D) were used for immunoprecipitation and washed in FA lysis buffer with 1M NaCl. qPCR with SYBR green PCR master mix (Roche, 04913850001) was used to determine DNA levels. qPCR reactions were performed in duplicate. Primers 99998/99999, spanning the CAG repeats on YAC CF1 resulting in a 369bp amplicon, were used for PCNA ChIP, primers 1227/1228, located 92bp from the CAG repeats on Chr VI generating a 168bp amplicon, were used for RFA1 ChIP (sequences found in Appendix Table 4.10).

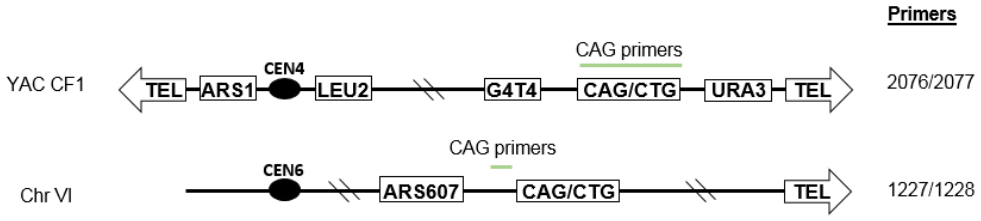

Figure 1. Schematic of primer locations on either YAC CF1 or Chr VI in relation to the CAG repeat with associated primer numbers on the right.

2D Gels

For CGG/CCG repeats, small volume cultures were grown in YC-Ura to saturation then diluted down to OD 0.2 in 500mL cultures and grown to mid-log phase, ~OD 0.4. Isolation of replication intermediates was performed as previously described (Wu and Gilbert 1995), using a G/100 Qiagen column. 10ug

of DNA was digested with 20U of XbaI and SalI for 16 hours at 37^{o}C. After digestion, DNA was precipitated with 5M KAc and 100% EtOH. Roughly 10ug of DNA was loaded in the 1st dimension in 0.4% agarose gels and run in 1x TBE for 15 hours at 1V/cm. Lanes were cut from 10kb to 1kb; the fragment size including the repeats was expected to be 4412 bp. The 2nd dimension 1% agarose gel was run at 4^{o}C in 1X TBE with 0.3g/ml of EtBr at 5V/cm for 16 hours. DNA from the agarose gel was transferred to a HybondXL membrane (Amersham) with 10X SSC and hybridized with ^{32}P-labled probe, which was PCR amplified from yEP24 plasmid CFY329. The probe contains a portion of the Amp gene immediately adjacent to the CGG/CCG repeats, nucleotide positions 6952–7581.

Semi-quantitative analysis of 2D gels was done using BioRad Pharos FX PhosphorImager using Quantity One software (two attempts have been unsuccessful thus far).

Appendix 4.2

Growth curve for *ctf18Δ* mutants and raw OD_{600} readings

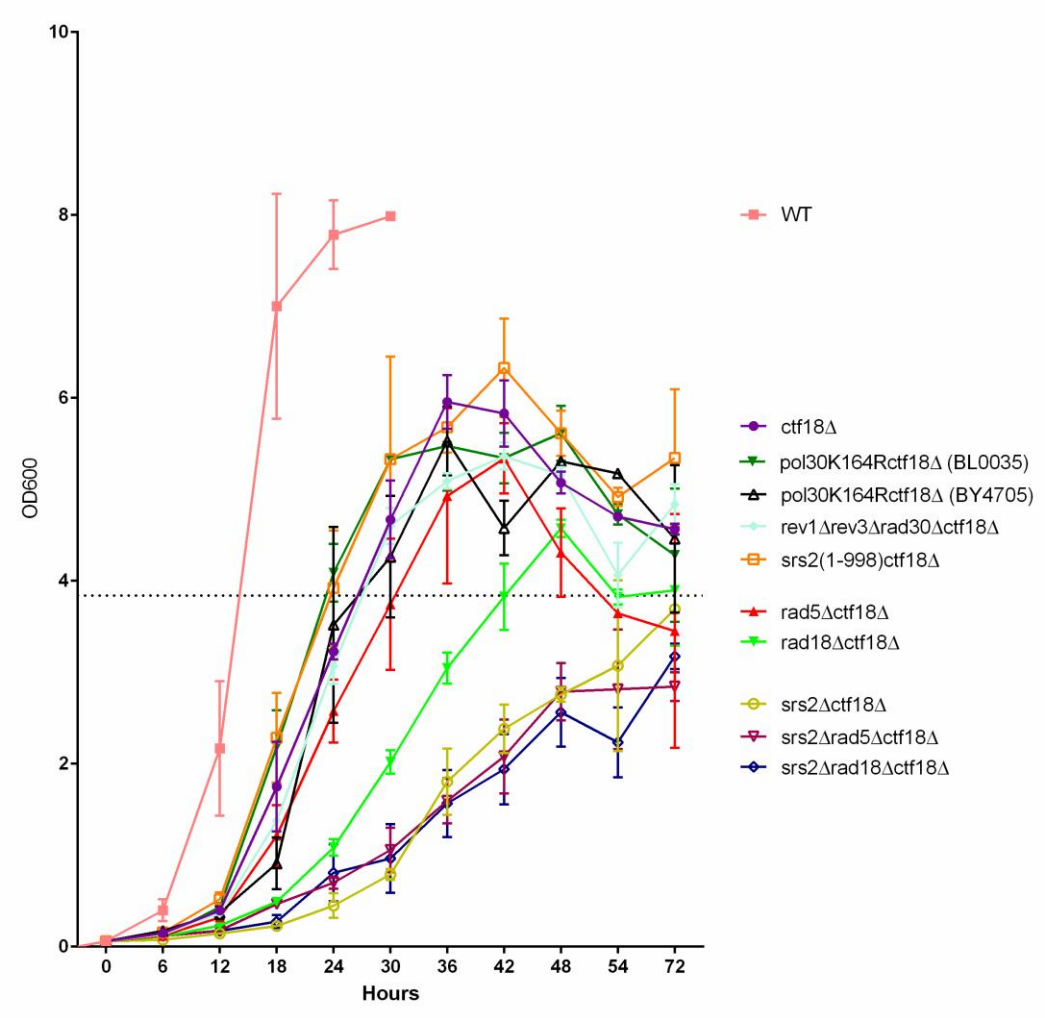

Appendix 4.1. Strains containing CAG_{70} YAC CF1 were normalized to OD 0.06 and grown in 20mL of YC –Leu-Ura at 30°C. Dotted line drawn at OD 3.84 (6 divisions) at which point cells would be plated for fragility assays. All strains containing *ctf18Δ* have a slow growth phenotype compared to wildtype. The most severe growth defect is seen in strains missing both Srs2 and Ctf18

Appendix 4.3

Raw Fragility Data CAG_{70} YAC CF1

	WT	*ctf18Δ*	*pol30K164R* (BY4705)	*pol30K164R* (BY4705)
	13.37	60.40	374.91	10.93
	14.04	33.20	254.50	30.44
	12.19	27.40	308.80	7.44
	12.58		625.46	22.23
	4.24		650.26	
	5.15			
	8.49			
	7.40			
	7.03			
Average Rate of FOA^R x 10^{-6}	9.39	40.33	442.79	17.76
SEM	1.24	10.17	81.98	5.28
p-value compared to wild-type		0.0003	<0.0001	0.0508

	pol30K164Rctf18Δ (BL0035)	*pol30K164Rctf18Δ* (BY4705)
	8955.36	424.75
	17797.45	
	6109.61	
	26548.24	
	31162.20	
	17874.65	
Average Rate of FOA^R x 10^{-6}	18075.00	424.75
SEM	3956.00	
p-value compared to wild-type	< 0.0001	
p-value compared to *ctf18Δ*	0.017	

	srs2Δctf18Δ	*srs2 (1-998) ctf18Δ*	*siz1Δ*	*ctf18Δsiz1Δ*
	167.13	275.33	5.37	7.69
	1062.10	564.04	4.25	15.60
	265.48	756.20	5.11	18.57
	771.57	679.11	9.09	23.95
	520.65		7.36	
			7.75	
			18.68	
Average Rate of FOA^R x 10^{-6}	557.40	568.70	8.23	16.45
SEM	164.20	105.50	1.86	3.39
p-value compared to wild-type	0.0006	< 0.0001	1.856	3.39
p-value compared to *ctf18Δ*	0.0563	0.0083		0.052
p-value compared to *srs2Δ*	< 0.0001	< 0.0001		

	rad5Δ	*rad5Δctf18Δ*	*mms2Δ*	*mms2Δctf18Δ*
	5.49	35.76	14.82	101.89
	7.35	46.90	16.58	30.09
	16.59	53.30	17.98	52.12
		29.70		33.6
Average Rate of FOA^R x 10^{-6}	9.81	41.42	16.46	54.43
SEM	3.43	5.33	0.91	16.54
p-value compared to wild-type	0.8848	< 0.0001	0.0108	0.0013
p-value compared to *ctf18Δ*		0.9226		0.5383

	rad18Δ	*rad18Δctf18Δ*
	9.94	184.10
	17.74	221.23
	23.32	93.44
	11.26	27.22
	23.43	31.29
	24.17	48.66
		24.27
		186.74
Average Rate of FOA^R x 10^{-6}	18.31	97.05
SEM	2.62	26.23
p-value compared to wild-type	0.0044	0.0042
p-value compared to *ctf18Δ*		0.2573

	rev1Δ	***rev3Δ***	***rad30Δ***	***rev1Δ rad30Δ***	***rev3Δ rad30Δ***	***rev1Δ rev3Δ rad30Δ***
	2.59	7.10	13.85	6.05	10.42	14.33
	11.46	17.36	12.00	6.65	28.47	6.84
	7.69	11.50	12.47	13.65		5.92
	7.13	3.26	15.45	6.49		
				5.90		
Average Rate of FOA^R x 10^{-6}	7.22	9.81	13.44	7.75	19.44	9.03
SEM	1.82	3.03	0.78	1.48	9.02	2.66
p-value compared to wild-type	0.3492	0.8796	0.0635	0.4281	0.0445	0.8934

	rev1Δ ctf18Δ	*rev3Δ ctf18Δ*	*rev1Δ rad30Δ ctf18Δ*	*rev3Δ rad30Δ ctf18Δ*	*rev1Δrev3Δ rad30Δctf18Δ*
	28.71	24.05	6.23	69.71	37.55
	71.98	96.54	34.53	34.17	17.62
	43.33	31.20		53.40	20.60
	57.37	50.19		34.36	22.28
				9.49	53.57
				64.52	
				23.65	
				38.93	
Average Rate of FOA^R x 10^{-6}	50.35	50.50	20.38	41.03	30.32
SEM	9.29	16.31	14.15	7.22	6.758
p-value compared to wild-type	< 0.0001	0.0023	0.0948	0.0004	0.0016
p-value compared to *ctf18Δ*	0.5035	0.6502	0.3215	0.96	0.4243

	srs2Δrad5Δctf18Δ	*srs2Δrad18Δctf18Δ*
	19.56	42.06
	76.45	26.24
	217.62	99.83
	849.50	52.68
Average Rate of FOA^R x 10^{-6}	290.80	55.20
SEM	190.80	15.84
p-value compared to wild-type	0.0386	0.0009
p-value compared to *ctf18Δ*	0.3181	0.5024

Appendix 4.4

CAG_{70} YAC CF1 status check (PCR method)

CAG_{70} Strain	# FOA^R colonies	% YAC end loss
Wild-type (JN, AS)*	32	100
srs2Δ	30	100
ctf18Δ	30	100
rad18Δ	30	100
***pol30K164R* (BL0035)**	28	100
***ctf18Δ pol30K164R* (BL0035)**	20	100
***pol30K164R* (BY4705)**	30	100
***ctf18Δ pol30K164R* (BY4705)**	30	100

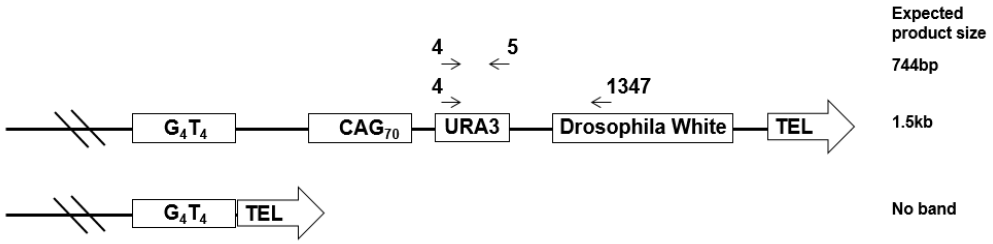

Schematic of PCR performed on a subset of FOA^R colonies to confirm FOA^R was due to YAC end loss and not due to point mutation in URA3. PCRs performed with primers 4/1347. *12 PCR reactions with primers 4/1347, 20 PCR reactions with primers 4/5

Appendix 4.5

Raw sister chromatid recombination data

	WT	*ctf18Δ*
	1.92	2.59
	4.60	8.29
		0.83
		0.57
Recombination Rate (Trp+ Ade+) 10^{-5}	3.26	3.07
SEM	1.34	1.80

Appendix 4.6

Raw genotype distribution of tetrad dissections CAG_{70} YAC CF1

srs2Δrad5Δ* x *ctf18Δ		
Possible Genotype	#	Frequency
Wild-type	11	2.62%
srs2Δ	9	2.14%
rad5Δ	9	2.14%
ctf18Δ	36	8.57%
srs2Δrad5Δ	12	2.86%
srs2Δctf18Δ	32	7.62%
rad5Δctf18Δ	32	7.62%
srs2Δrad5Δctf18Δ	29	6.90%
Wild-type +YAC	46	10.95%
srs2Δ +YAC	56	13.33%
rad5Δ +YAC	59	14.05%
ctf18Δ +YAC	26	6.19%
srs2Δrad5Δ +YAC	41	9.76%
srs2Δctf18Δ +YAC	3	0.71%
rad5Δctf18Δ +YAC	15	3.57%
srs2Δrad5Δctf18Δ +YAC	4	0.95%
Total spores	420	

srs2Δrad18Δ* x *ctf18Δ		
Possible Genotype	#	Frequency
Wild-type	16	4.64%
srs2Δ	9	2.61%
rad18Δ	15	4.35%
ctf18Δ	54	15.65%
srs2Δrad18Δ	5	1.45%
srs2Δctf18Δ	11	3.19%
rad18Δctf18Δ	31	8.99%
srs2Δrad18Δctf18Δ	14	4.06%
Wild-type +YAC	39	11.30%
srs2Δ +YAC	39	11.30%
rad18Δ +YAC	35	10.14%
ctf18Δ +YAC	10	2.90%
srs2Δrad18Δ +YAC	47	13.62%
srs2Δctf18Δ +YAC	6	1.74%
rad18Δctf18Δ +YAC	5	1.45%
srs2Δrad18Δctf18Δ +YAC	9	2.61%
Total spores	345	

Appendix 4.7

Raw Instability Data for CAG_{70} YAC CF1

		Contraction			
CAG_{70} Strain	**No. colonies tested**	**#**	**%**	**Fold over WT**	**p-value to WT**
Wildtype	269	7	2.6	-	-
ctf18Δ	101	29	28.7	11	0.0001
srs2Δ	231	15	6.5	2.5	0.0474
srs2 (1-998)	122	4	3.3	1.5	0.7454
srs2Δctf18Δ	260	150	42.3	16.3	0.0001
srs2 (1-998) ctf18Δ	155	44	28.4	10.9	0.0001
rad5Δctf18Δ	175	58	33.1	12.7	0.0001
srs2Δrad5Δctf18Δ	86	16	18.6	7.2	0.0001
***pol30K164Rctf18Δ* (BL0035)**	106	43	39.8	15.3	0.0001

		Expansion			
CAG_{70} Strain	**No. colonies tested**	**#**	**%**	**Fold over WT**	**p-value to WT**
Wildtype	269	3	1.1	-	-
ctf18Δ	101	7	6.9	6.2	0.0054
srs2Δ	231	13	5.6	5.0	0.0047
srs2 (1-998)	122	2	1.6	1.5	0.6493
srs2Δctf18Δ	260	41	15.8	14.4	0.0001
srs2 (1-998) ctf18Δ	155	6	3.9	3.5	0.0796
rad5Δctf18Δ	175	11	6.3	5.6	0.0049
srs2Δrad5Δctf18Δ	86	10	11.6	10.4	0.0011
***pol30K164Rctf18Δ* (BL0035)**	106	0	0	0	0.5606

Appendix 4.8

Raw data for ChIP PCNA at CAG_{70} repeats on YAC CF1

ΔCT	%Input	ΔΔCT	Fold Enrichment
ΔCT= IP - (Input -log2(x)) [x= the input dilution factor relative to the IP]	2^(ΔCT)	ΔCT of IP CAG - ΔCT IP ACT1	2^(-ΔΔCT)

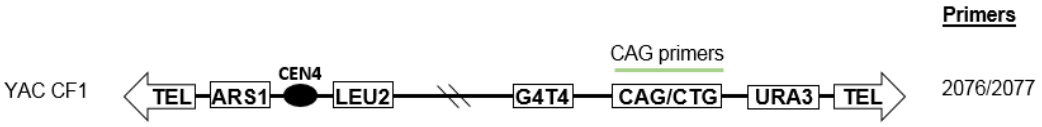

(Primers flanking the repeat and will result in a 369bp amplicon)

		Sample	Mean CT	ΔCT	%Input	ΔΔCT	Fold Enrichment
Wildtype CAG_{70}	CAG primers	IP 0 min	21.28	4.00	0.06	-2.82	7.04
		IP 20 min	17.65	2.11	0.23	-5.16	35.72
		IP 40 min	18.57	3.60	0.08	-2.90	7.48
		IP 60 min	19.89	5.43	0.02	-2.77	6.82
		Input 0 min	21.60				
		Input 20 min	19.86				
		Input 40 min	19.29				
		Input 60 min	18.79				
	ACT1 primers	IP 0 min	22.81	6.82	0.0089		
		IP 20 min	21.33	7.27	0.0065		
		IP 40 min	20.23	6.50	0.0110		
		IP 60 min	21.67	8.20	0.0034		
		Input 0 min	20.31				
		Input 20 min	18.38				
		Input 40 min	18.05				
		Input 60 min	17.80				

		Sample	Mean CT	ΔCT	%Input	ΔΔCT	Fold Enrichment
ctf18Δ CAG_{70}	CAG primers	IP 0 min	23.07	2.91	0.13	-5.86	57.94
		IP 40 min	23.09	3.26	0.10	-5.06	33.42
		IP 80 min	22.36	1.97	0.26	-5.66	50.39
		IP 120 min	22.35	2.37	0.19	-5.10	34.32
		Input 0 min	24.48				
		Input 40 min	24.15				
		Input 80 min	24.71				
		Input 120 min	24.30				
	ACT1 primers	IP 0 min	28.01	8.77	0.00229		
		IP 40 min	27.35	8.32	0.00312		
		IP 80 min	27.55	7.62	0.00507		
		IP 120 min	27.10	7.47	0.00564		
		Input 0 min	23.56				
		Input 40 min	23.35				
		Input 80 min	24.25				
		Input 120 min	23.95				

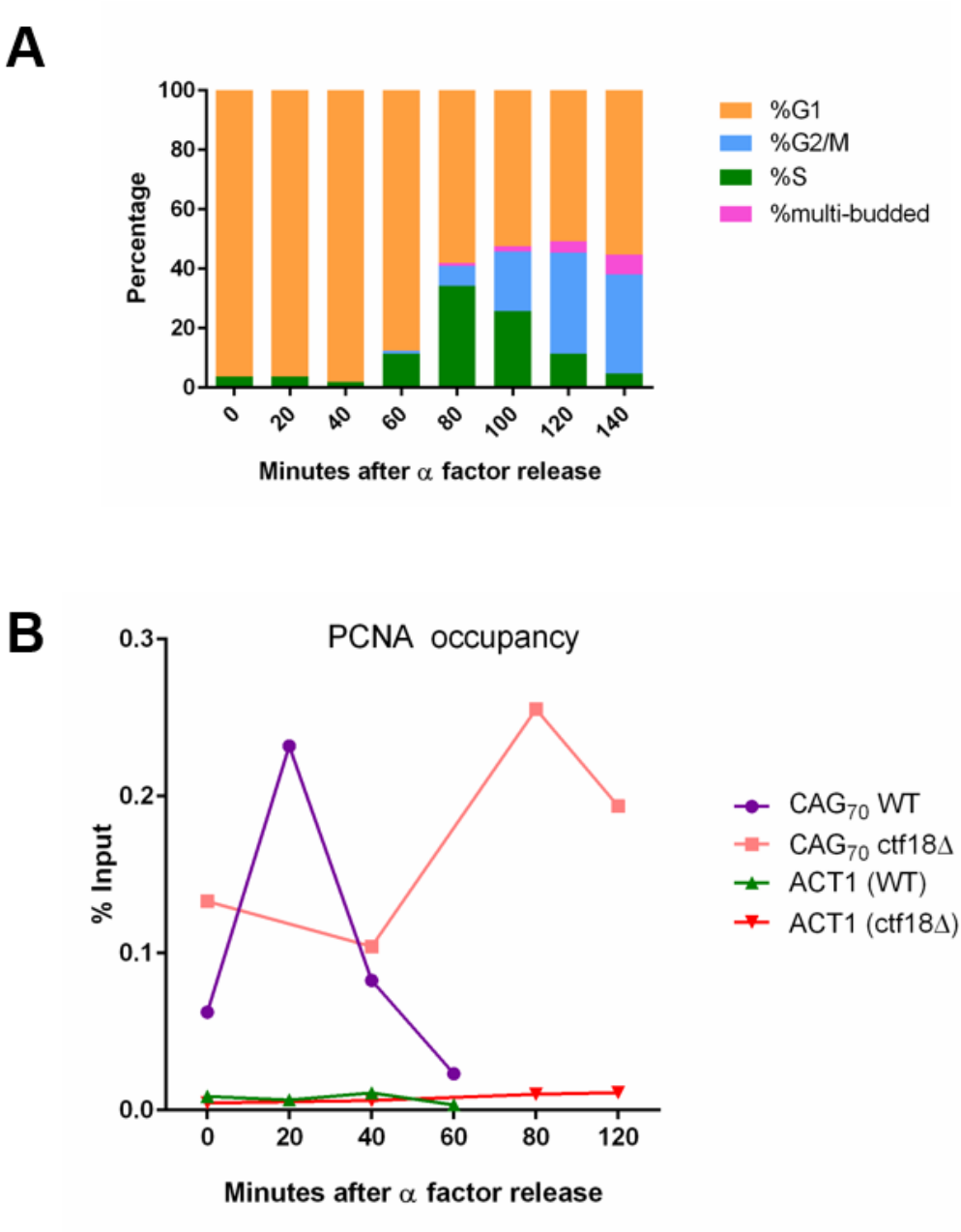

Appendix 4.7. A) *ctf18Δ* cell cycle progression after α factor release. Cell cycle was determined based on morphology of cells as observed under a compound microscope (G1: unbudded, S: small budded, G2/M: large budded-at least 1/3 size of mother cell). Based on cell cycle progression, time points for *ctf18Δ* were adjusted (0, 40, 80, 120) to match wildtype cell cycle progression. B) Representation of %Input ($2^{-\Delta CT}$) for wildtype and *ctf18Δ* using CAG primers and ACT1 primers.

Preliminary conclusion: In wildtype, the increase in PCNA signal coincides with S phase at 20 minutes. In *ctf18Δ*, while this increase doesn't occur until 80 minutes, this is S phase for these strains based on the cell cycle data. It does not seem like there is a persistent PCNA signal in *ctf18Δ* but more time points would need to be gathered to make that final conclusion

Appendix 4.9

Raw data for ChIP Rfa1-Myc to CAG_{130} on Chromosome VI

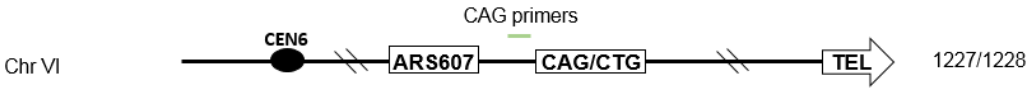

(Primers located 0.1kb from repeat and will result in a 168bp amplicon)

		Sample	Mean CT	ΔCT	%Input	ΔΔCT	Fold Enrichment
Wildtype CAG_{130}	CAG primers	IP 0 min	26.11	6.12	0.0144	0.46	0.73
		IP 20 min	26.88	6.87	0.0086	1.01	0.50
		IP 40 min	25.01	5.84	0.0174	0.40	0.76
		IP 60 min	25.32	4.28	0.0514	0.86	0.55
		IP 80 min	23.87	4.48	0.0447	0.99	0.51
		Input 0 min	24.31				
		Input 20 min	24.33				
		Input 40 min	23.49				
		Input 60 min	25.36				
		Input 80 min	23.70				
	ACT1 primers	IP 0 min	24.87	5.67	0.0197		
		IP 20 min	25.04	5.85	0.0173		
		IP 40 min	23.94	5.44	0.0230		
		IP 60 min	23.97	3.42	0.0936		
		IP 80 min	22.22	3.50	0.0885		
		Input 0 min	23.53				
		Input 20 min	23.51				
		Input 40 min	22.82				
		Input 60 min	24.88				
		Input 80 min	23.04				

		Sample	Mean CT	ΔCT	%Input	ΔΔCT	Fold Enrichment
ctf18Δ CAG_{130}	CAG primers	IP 0 min	20.66	-6.09	67.91	-0.82	1.77
		IP 20 min	21.38	-5.47	44.19	-0.55	1.47
		IP 40 min	20.69	-4.10	17.09	-0.32	1.25
		IP 60 min	24.51	-1.32	2.49	-0.84	1.79
		IP 80 min	20.03	-5.12	34.73	-0.58	1.49
		IP 100 min	20.50	-4.73	26.49	-0.88	1.85
		Input 0 min	31.07				
		Input 20 min	31.17				
		Input 40 min	29.11				
		Input 60 min	30.15				
		Input 80 min	29.47				
		Input 100 min	29.55				
	ACT1 primers	IP 0 min	20.11	-5.26	38.41		
		IP 20 min	20.74	-4.91	30.10		
		IP 40 min	20.29	-3.78	13.70		
		IP 60 min	23.87	-0.48	1.39		
		IP 80 min	19.28	-4.54	23.31		
		IP 100 min	20.07	-3.84	14.35		
		Input 0 min	29.69				
		Input 20 min	29.98				
		Input 40 min	28.39				
		Input 60 min	28.67				
		Input 80 min	28.14				
		Input 100 min	28.23				

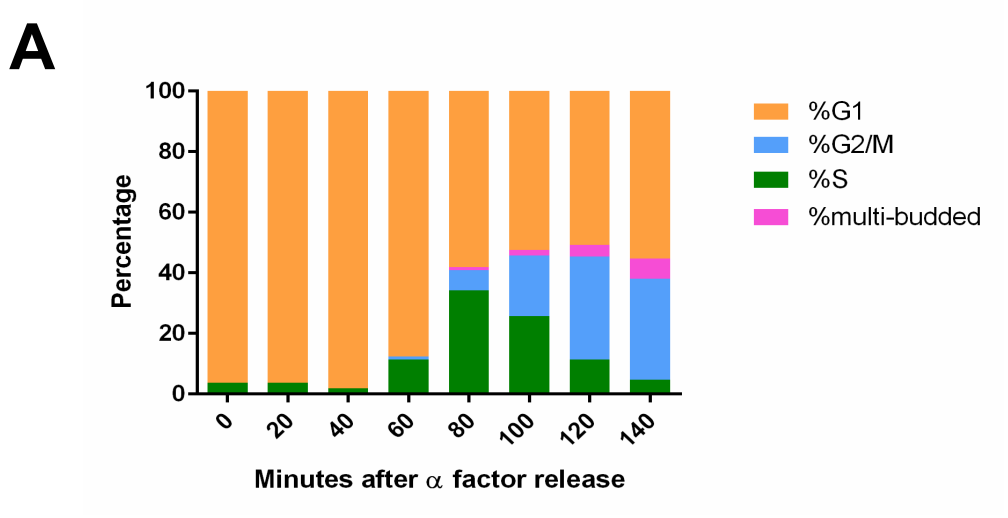

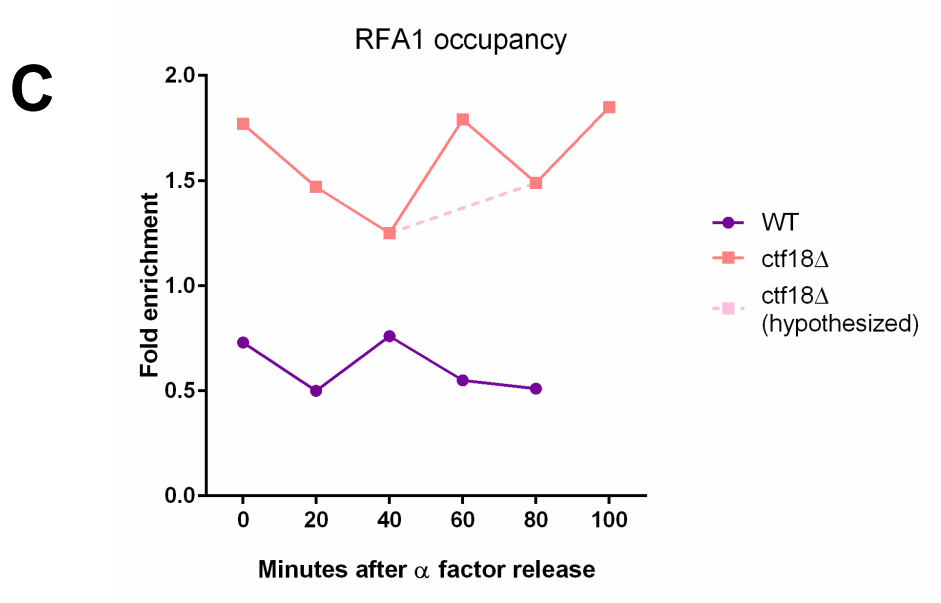

Appendix 4.8. Representation of fold enrichment ($2^{-\Delta\Delta CT}$) of Rfa1 at CAG_{130} on Chr VI over the cell cycle using primers 0.1kb from the repeat tract and normalized to the ACT1 locus. For *ctf18Δ*, light pink dotted line represents data without 60 minute time point, which might not be reliable due to low DNA recovery

Preliminary conclusion: This data suggests in wildtype cells, there is no accumulation of RPA at repeats as cells progress through S phase. In *ctf18Δ* cells, there is an overall enrichment of RPA compared to wildtype.

The persistent RPA signal suggests there could be continuous fork stalling occurring at the repeats (or perhaps there is ssDNA present for another reason). Based on the cell cycle phases in (A), it could be possible that the experiment wasn't run long enough to catch a decrease in RPA signal occurring after the peak at the 100 minute time point. This experiment will need to be repeated

Appendix 4.10

Strain Table

Strain	Background	Genotype	Reference
CFY766	BY4705	*MATα, ade2Δ::hisG, his3Δ200, leu2Δ0, lys2Δ0, met15Δ0, trp1Δ63, ura3Δ0, can^R* YAC: *LEU2* CAG-70 *URA3*	Kerrest et al. 2009
CFY1628	BY4705	*MATa, ade2Δ::hisG, his3Δ200, leu2Δ0, lys2Δ0, met15Δ0, trp1Δ63, ura3Δ0, can^R* YAC: *LEU2* CAG-70 *URA3*	Nguyen et al. in prep
CFY2285 **CFY2286**	BY4705	*MATα, ade2Δ::hisG, his3Δ200, leu2Δ0, lys2Δ0, met15Δ0, trp1Δ63, ura3Δ0, can^R ctf18::HIS3MX6* YAC: *LEU2* CAG-70 *URA3*	Gellon et al. 2011
CFY2638 **CFY2639**	BL0035	*MATα*, ade2*Δ*, ade8*Δ*, ura3-52, hom3-10, trp1*Δ*, his3-KpnI, met4, met13 leu2*Δ*, pol30K164R* YAC:LEU+, URA+	This study
CFY3662 **CFY3663**	BL0035	*MATα*, ade2*Δ*, ade8*Δ*, ura3-52, hom3-10, trp1*Δ*, his3-KpnI, met4, met13 leu2*Δ*, pol30K164R ctf18::HIS3MX6* YAC:LEU+, URA+	This study
CFY3922	BY4705	*MATa, ade2Δ, ade8Δ, ura3-52, hom3-10, trp1Δ, his3-KpnI, met4, met13 leu2 Δ, pol30K164R* YAC*: LEU2* CAG-70 URA3	This study
CFY3944	BY4705	*MATa, ade2Δ, ade8Δ, ura3-52, hom3-10, trp1Δ, his3-KpnI, met4, met13 leu2 Δ, pol30K164R ctf18::HIS* YAC*: LEU2* CAG-70 URA3	This study
CFY1666	BY4705	*MATα, ade2Δ::hisG, his3Δ200, leu2Δ0, lys2Δ0, met15Δ0, trp1Δ63, ura3Δ0, can^R, rad5::KANMX6* YAC: *LEU2* CAG-70 *URA3*	Nguyen et al. in prep
CFY2399 **CFY2400**	BY4705	*MATα, ade2Δ::hisG, his3Δ200, leu2Δ0, lys2Δ0, met15Δ0, trp1Δ63, ura3Δ0, can^R rad5::KANMX6 ctf18::HIS3MX6* YAC: *LEU2* CAG-70 *URA3*	This study
CFY2867	W303	*LSY1519-1Δ; MATa, ade2-nde1-::TRP1::ade2-I-Sce1+/aatII-; RAD5+, ade2-1 trp1-1 his3-11,15 can1-100 ura3-1 leu2-3,112*	Mozlin, et al. 2008
CFY3848 **CFY3849**	W303	*LSY1519-1Δ; MATa, ade2-nde1-::TRP1::ade2-I-Sce1+/aatII-;*	This study

		RAD5+, ade2-1 trp1-1 his3-11,15 can1-100 ura3-1 leu2-3,112 ctf18::HIS3MX6	
CFY3379		*MATa, ade2Δ::hisG, his3Δ200, leu2Δ0, lys2Δ0, met15Δ0, trp1Δ63, ura3Δ0, can^R rad18::KANMX6*	
CFY3626	BY4705	YAC: *LEU2* CAG-70 *URA3*	This study
CFY3627		*MATa, ade2Δ::hisG, his3Δ200, leu2Δ0, lys2Δ0, met15Δ0, trp1Δ63, ura3Δ0, can^R rad18::KANMX6 ctf18::HIS3MX6*	
CFY3628	BY4705	YAC: *LEU2* CAG-70 *URA3*	This study
CFY3393		*MATa, ade2Δ::hisG, his3Δ200, leu2Δ0, lys2Δ0, met15Δ0, trp1Δ63, ura3Δ0, can^R rev1::TRP*	
CFY3394	BY4705	YAC: *LEU2* CAG-70 *URA3*	This study
CFY3481		*MATa, ade2Δ::hisG, his3Δ200, leu2Δ0, lys2Δ0, met15Δ0, trp1Δ63, ura3Δ0, can^R rev3::KANMX6*	
CFY3482	BY4705	YAC: *LEU2* CAG-70 *URA3*	This study
CFY3485		*MATa, ade2Δ::hisG, his3Δ200, leu2Δ0, lys2Δ0, met15Δ0, trp1Δ63, ura3Δ0, can^R rad30::HYG*	
CFY3486	BY4705	YAC: *LEU2* CAG-70 *URA3*	This study
CFY3487		*MATa, ade2Δ::hisG, his3Δ200, leu2Δ0, lys2Δ0, met15Δ0, trp1Δ63, ura3Δ0, can^R rev1::TRP rad30::HYG*	
CFY3488	BY4705	YAC: *LEU2* CAG-70 *URA3*	This study
CFY3508		*MATa, ade2Δ::hisG, his3Δ200, leu2Δ0, lys2Δ0, met15Δ0, trp1Δ63, ura3Δ0, can^R rev3::KANMX6 rad30::HYG*	
CFY3509	BY4705	YAC: *LEU2* CAG-70 *URA3*	This study
CFY3725		*MATa, ade2Δ::hisG, his3Δ200, leu2Δ0, lys2Δ0, met15Δ0, trp1Δ63, ura3Δ0, can^R rev1::TRP rev3::KANMX6 rad30::HYG*	
CFY3725	BY4705	YAC: *LEU2* CAG-70 *URA3*	This study
CFY3492		*MATa, ade2Δ::hisG, his3Δ200, leu2Δ0, lys2Δ0, met15Δ0, trp1Δ63, ura3Δ0, can^R rev1::TRP ctf18::HIS3MX6*	
CFY3493	BY4705	YAC: *LEU2* CAG-70 *URA3*	This study
CFY3494		*MATa, ade2Δ::hisG, his3Δ200, leu2Δ0, lys2Δ0, met15Δ0, trp1Δ63, ura3Δ0, can^R rev3::KANMX6 ctf18::HIS3MX6*	
CFY3495	BY4705	YAC: *LEU2* CAG-70 *URA3*	This study

CFY3575 **CFY3576** **CFY3613**	BY4705	*MATa, ade2Δ::hisG, his3Δ200, leu2Δ0, lys2Δ0, met15Δ0, trp1Δ63, ura3Δ0, can^R rev3::KANMX6 rad30::HYG ctf18::HIS3MX6* YAC: *LEU2* CAG-70 *URA3*	This study
CFY3749 **CFY3750**	BY4705	*MATa, ade2Δ::hisG, his3Δ200, leu2Δ0, lys2Δ0, met15Δ0, trp1Δ63, ura3Δ0, can^R rev1::TRP rev3::KANMX6 rad30::HYG ctf18::HIS3MX6* YAC: *LEU2* CAG-70 *URA3*	This study
CFY927 **CFY928**	BY4742	*MATα, his3Δ1, leu2Δ0, lys2Δ0, ura3Δ0, can^R, srs2::KANMX6* YAC: *LEU2* CAG-70 *URA3*	Kerrest et al. 2009
CFY2623	BY4705	*MATα, ade2Δ::hisG, his3Δ200, leu2Δ0, lys2Δ0, met15Δ0, trp1Δ63, ura3Δ0, can^R, srs2::TRP* YAC: LEU2 CAG-70 URA3	Nguyen et al. in prep
CFY2299 **CFY2300**	BY4705	*MATα, ade2Δ::hisG, his3Δ200, leu2Δ0, lys2Δ0, met15Δ0, trp1Δ63, ura3Δ0, can^R, srs2::srs2 (1-998)-HIS3MX6* YAC: *LEU2* CAG-70 *URA3*	Nguyen et al. in prep
CFY3883	BY4705	*MATa his3Δ1, leu2Δ0, lys2Δ0, ura3Δ0, can^R, srs2::KANMX6 ctf18::HIS3MX6* YAC: *LEU2* CAG-70 *URA3*	This study
CFY3776 **CFY3777**	BY4705	*MATα, ade2Δ::hisG, his3Δ200, leu2Δ0, lys2Δ0, met15Δ0, trp1Δ63, ura3Δ0, can^R, srs2::srs2 (1-998)-HIS3MX6 ctf18::TRP* YAC: LEU2 CAG-70 URA3	This study
CFY3888 **CFY3889**	BY4705	*MATα his3Δ1, leu2Δ0, lys2Δ0, ura3Δ0, can^R, srs2::TRP rad5::KANMX6 ctf18::HIS3MX6* YAC: *LEU2* CAG-70 *URA3*	This study
CFY3890	BY4705	*MATα his3Δ1, leu2Δ0, lys2Δ0, ura3Δ0, can^R, srs2::TRP rad18::KANMX6 ctf18::HIS3MX6* YAC: *LEU2* CAG-70 *URA3*	This study
CFY3891	BY4705	*MATa his3Δ1, leu2Δ0, lys2Δ0, ura3Δ0, can^R, srs2::TRP rad18::KANMX6 ctf18::HIS3MX6* YAC: *LEU2* CAG-70 *URA3*	This study
CFY3084 **CFY3085**	BY4705	*MATa, ade2Δ::hisG, his3Δ200, leu2Δ0, lys2Δ0, met15Δ0, trp1Δ63, ura3Δ0, can^R siz1::TRP* YAC: *LEU2* CAG-70 *URA3*	This study
CFY3160 **CFY3225**	BY4705	*MATa, ade2Δ::hisG, his3Δ200, leu2Δ0, lys2Δ0, met15Δ0, trp1Δ63,*	This study

		ura3Δ0, can^R siz1::TRP ctf18::HIS YAC: *LEU2* CAG-70 *URA3*	
CFY3860 **CFY3861**	BY4705	*MATa, ade2Δ::hisG, his3Δ200, leu2Δ0, lys2Δ0, met15Δ0, trp1Δ63, ura3Δ0, can^R pYes-URA3 -(CAG)$_{130}$*	This study
CFY3862	BY4705	*MATa, ade2Δ::hisG, his3Δ200, leu2Δ0, lys2Δ0, met15Δ0, trp1Δ63, ura3Δ0, can^R pYes-URA3-(CTG)$_{130}$*	This study
CFY3903 **CFY3904**	BY4705	*MATa, ade2Δ::hisG, his3Δ200, leu2Δ0, lys2Δ0, met15Δ0, trp1Δ63, ura3Δ0, can^R* yEP24-CGG40-URA3	This study
CFY3905 **CFY3906**	BY4705	*MATa, ade2Δ::hisG, his3Δ200, leu2Δ0, lys2Δ0, met15Δ0, trp1Δ63, ura3Δ0, can^R* yEP24-CCG40-URA3	This study
CFY3924 **CFY3925**	BY4705	*MATa, ade2Δ::hisG, his3Δ200, leu2Δ0, lys2Δ0, met15Δ0, trp1Δ63, ura3Δ0, can^R ctf18::HIS3MX6* yEP24-CGG40-URA3	This study
CFY3926 **CFY3927**	BY4705	*MATa, ade2Δ::hisG, his3Δ200, leu2Δ0, lys2Δ0, met15Δ0, trp1Δ63, ura3Δ0, can^R ctf18::HIS3MX6* yEP24-CCG40-URA3	This study
CFY3919	W303	*MATα RAD5+ ade2-1 can1-100 his3-11,15 leu2-3,112 trp1-1 ura3-1 Chr6int2::CAG130-HPH (Chr6int2 is 7645 bp from Chr6int and 560 bp upstream of tA(AGC)F) RFA1-TRP-myc*	This study
CFY3928 **CFY3929**	W303	*MATα RAD5+ ade2-1 can1-100 his3-11,15 leu2-3,112 trp1-1 ura3-1 Chr6int2::CAG130-HPH (Chr6int2 is 7645 bp from Chr6int and 560 bp upstream of tA(AGC)F) ctf18:HIS3MX6 RFA1-TRP-myc*	This study

Appendix 4.11

Primer Table

#	Primer Name	Purpose	Sequence
Tract length Primers			
2076	newCAGfor	Anneals 42bp from CAG repeat, on centromeric side	CCTCAGCCTGGCCG AAAGAAAGAAA
2077	newCAGrev	Anneals 117bp from CAG repeat, on the telomeric side	CAGTCACGACGTTGT AAAACGACGG
1533	CAGfor60bp	Anneals 60bp from CAG repeat, on centromeric side	TTGCCCATCCACGTC AGGG
1534	CAGrev35bp	Anneals 35bp from CAG repeat, on telomeric side	GAACGGGGCTCGAA GGGTC
Mutant creation primers			
1442	Ctf18_upstrea m	Amplify across Ctf18 locus	gaggacagttttgagggtag
1443	Ctf18_downstr eam	Amplify across Ctf18 locus	gcttcttaagagagactgcg
1445	5'ctf18verif	5' junction check at Ctf18 locus	cgctggtcaagcgatatacc
1671	Ctf18int_1218-1238for	Internal primer to check absence of Ctf18 ORF	ggagatcagacgacacgtac
1672	Ctf18int_2789-2810rev	Internal primer to check absence of Ctf18 ORF	gccacccttacatcaaatcc
2047	pFaF1+40bpu pstream	Amplifies pFa marker with 40bp extra upstream (used to co transform with gene to tag it)	AACGCGGCCGCCAG CTGAAGCTTCGTACG CTGCAGGTCGACGG ATCCCCGGGTTAATT AA
2048	3'Pol30+pFaF 140upstream	Amplifies 3' end of Pol30 with homology to primer 2047 for co transformation	TCG ACC TGC AGC GTA CGA AGC TTC AGC TGG CGG CCG CGT TAC TAT ATA GAT AAT TTA CAT
2049	pFaR1+3'dow nstreamPol30	Amplifies 3' end of pFa marker to integrate at POL30 locus	ACT TTA CTG TTT TTT TTT TGT TTA TTA TTT TTA GTA TAC AGA ATT CGA GCT CGT TTA AAC
1818	Pol30_150bpu pstream	Amplify across Pol30 locus	CGTACTTTGCTTCCT CTGGTAC

1819	Pol30_200bpdownstream	Amplify across Pol30 locus	GGA AGG GTT CAT AGC AAA AG
1820	Pol30_234-255for	To sequence point mutation	CCT ACG TTG TGG TAA CAA CAC C
1917	Siz1_577-598F	Internal primer to check absence of Siz1 ORF	GTG ATG AAC GTG GAA GTC ACA G
1918	Siz1_2023-2043R	Internal primer to check absence of Siz1 ORF	CGT TGG GGA TGA TAC GCT AAC
1298	Siz1pfaKO_for	Amplify KO marker off pFa plasmids for Siz1	caactcaaacagttgagtgttccatatacattctgtttcacggatccccgggttaattaa
1299	Siz1pfaKO_rev	Amplify KO marker off pFa plasmids for Siz1	tgaaagagctggacggaaccgtccaattttagcctcgtttgaattcgagctcgtttaaac
722	siz1 241bp upstream for	5' junction check at Siz1 locus	gagcgagcagaaggttcctct
495	Rad5upstream for	Amplify across Rad5 locus	cttactgctaagcgcattgctc
496	Rad5dwnstreamrev	Amplify across Rad5 locus	gaagttgcatgaagtagctg
1115	Rad5-ForChk	5' junction check at Rad5 locus	CATTCTGGACCTTTCTGCAC
1935	rad5internalfor_161bpfromstart	Internal primer to check absence of Rad5 ORF	CAACAGAAGGAGAGGGAGAC
1936	rad5internalrev_2732bpfromstart	Internal primer to check absence of Rad5 ORF	GCAGATGGAGCACTCTAAGG
1198	Rad18 KO For	Amplify KO marker off pFa plasmids for Rad18	gagcatcacagctactaagaaaaggccattttactactccggatccccgggttaattaa
1199	Rad18 KO Rev	Amplify KO marker off pFa plasmids for Rad18	tgcacaagctaacaaacaggcctgattacatatacacaccgaattcgagctcgtttaaaac
1521	Rad18_400upstream	5' junction check at Rad18 locus	ggatgagtcctaaactgggc
1535	Rad18_int_for	Internal primer to check absence of Rad18 ORF	ggaccaccaaataaccactgc
2016	Rad18_1357-1366R	Internal primer to check absence of Rad18 ORF	CAC CAG CAA CTC TAT CTT CG
1372	Rev1_forKOpFa	Amplify KO marker off pFA plasmids for Rev1	tcaaaataaatcgatactgcatttctaggcatatccagcgcggatccccgggttaattaa

1373	Rev1_revKOpFa	Amplify KO marker off pFA plasmids for Rev1	gtaatgttcgcaaactgcgtgttactgtatgctgaaatggaattcgagctcgtttaaac
1374	Rev1_check	5' junction check at Rev1 locus	gactacgaacttgctgatgtcc
1669	Rev1chk3'_189bpdownstreamORF	3' junction check at Rev1 locus	GTCGGCCATTCCAATACC
1667	Rev1_internal5'_395bpfromstart	Internal primer to check absence of Rev1 ORF	GGGAGGCTTATTTCCACGAG
1668	Rev1_internal3'_2353bpfromstart	Internal primer to check absence of Rev1 ORF	GAGTTTGAAGTCAACCCGGA
1833	Rev1KOfor_200bpupstreamORF	5' upstream of Rev1	CGCATCAACTTAAACATTGGC
1834	Rev1revchk_255bpdownstreamORF	3' downstream of Rev1	GGTGGACAACGGTGATACTG
1389	Rev3 ForKOpFa	Amplify KO marker off pFA plasmid for Rev3	atacaaaactacaagttgtggcgaaataaaatgtttggaacggatccccgggttaattaa
1390	Rev3 RevKOpFa	Amplify KO marker off pFA plasmid for Rev3	ataactactcatcattttgcgagacatatctgtgtctagagaattcgagctcgtttaaac
1391	Rev3 Check	5' junction check at Rev3 locus	GAA TCC CTG TGG TCT CCT AC
1666	Rev3chk3'_137bpdownstreamORF	3' junction check at Rev3 locus	CACTCTCAGCATTGCTGGCC
1664	Rev3_internal5'_381bpfromstart	Internal primer to check absence of Rev3 ORF	CGGCGACAAACTTGGAAATC
1665	Rev3_internal3'_2204bpfromstart	Internal primer to check absence of Rev3 ORF	GAACATCACGGGAATTTCGT
1835	Rev3KOfor_129bpupstreamORF	5' upstream of Rev3	GACGAGTGCAGTGCGTCTAG
1836	Rev3KOrevchk_196bpdownstreamORF	3' downstream of Rev3	GAGGATACGAAGATTCCTC
1526	rad30_200upstream	Amplify across Rad30 locus	cgctacctaatcctgccgatc

1527	rad30_100downstream	Amplify across Rad30 locus	cttatcaacaaaacctggcgcc
1528	rad30_400upstream	5' junction check at Rad30 locus	caatggcatgataggatgttgc
1537	Rad30_Hyg_KO_for	Amplifies Hyg off pAG32 to KO Rad30	CTGCTCATTTTTGAACGGCTTTGATAAAACAAGACAAAGCcagctgaagcttcgtacgc
1538	Rad30_Hyg_KO_rev	Amplifies Hyg off pAG32 to KO Rad30	TTT AGT TGC TGA AGC CAT ATA ATT GTC TAT TTG GAA TAG G ataggccactagtggatctg
1658	Rad30_internal5'_34bpfromstart	Internal primer to check absence of Rad30 ORF	CTTGGTTCCCCCAGTAAAGC
1659	Rad30_internal3'_1392bpfromstart	Internal primer to check absence of Rad30 ORF	GACTCTGGAAATTGATGCCC
1660	Rad30chk3'_80bpdownstreamORF	3' junction check at Rad30 locus	CAACAAAACCTGGCGCCCGT
ChIP Primers			
1227	Chr6-CAG-0.1k ChIP for	amplifies 100bp from CAG130 on ChrVI for ChIP	cctaatccattaccaatccttgc
1228	Chr6-CAG-0.1k ChIP rev	amplifies 100bp from CAG130 on ChrVI for ChIP	gcgaatacgataatacgaatgcg
2D probe primers			
617	yep24probe for	to make probe for 2Ds with Yep24 plasmids, inserts in AseI site	attgttgccgggaagctagagtaa
618	yep24probe rev	to make probe for 2Ds with Yep24 plasmids, inserts in AseI site	attgaaaaaggaagagtatgagta
YAC status check primers			
4	ura3rev	To check loss of right arm of YAC	TCCCAGCCTGCTTTTCTGTA
1347	DrosophW5'rev	To check loss of right arm of YAC	gcacaattggtgacgttacg

Chapter 5

PERSPECTIVE

Over half our genome is composed of repetitive sequences. Structure-forming repeat sequences within our genome can be a source of endogenous damage and in some cases, this damage can manifest into the onset and progression of neurodegenerative diseases. It is important to study how cells traverse these repetitive regions with minimal damage in order to gain an understanding of the dynamics of replication and repair in a cell. My work has provided insight on two distinct but equally important mechanisms needed to protect repeat integrity and overall genome stability.

SUMMARY AND FUTURE DIRECTIONS

The Srs2 helicase plays an important role in protecting genome integrity but also has a specialized role triplet repeat protection (Anand et al., 2012; Bhattacharyya and Lahue, 2004, 2005; Daee et al., 2007; Dhar and Lahue, 2008; Kerrest et al., 2009). The multi-functionality of Srs2 raised the question of whether its functions were all equally needed to maintain repeat integrity. Srs2 is most prominently reported in the literature as an anti-recombinase, and while we found Rad51 displacement was needed to prevent repeat instability, we also identified the helicase activity and PCNA interaction were indispensable for preventing repeat fragility. Our data also provides support for Srs2 facilitating fork restart by unwinding hairpins to prevent the accumulation of joint molecules (reversed forks or recombination intermediates).We hypothesize Srs2 is recruited to

SUMOylated PCNA during replication to allow timely unwinding of hairpin structures to prevent fork stalling and breakage. This is different from what has been previously described, where Srs2 is recruited by PCNA to prevent hyperrecombination (Papouli et al., 2005; Pfander et al., 2005). These ideas are not mutually exclusive, but rather provide insight on how dynamic the Srs2 helicase is in overall genome protection. The separation of function of Srs2 lends support to higher eukaryotes most likely having a combination of helicases performing Srs2 functions. We also characterized the role two other helicases, Mph1 and Rad5, might have in repeat maintenance and fork regression. We found Rad5 had no significant impact on fragility, instability, or formation of joint molecules, in fact there was an increase in joint molecules in *rad5Δ*. This latter result is interesting since there are several reports that show Rad5 can unwind four-way structures mimicking regressed replication forks *in vitro* (Blastyák et al., 2007). Either the joint molecules we see in our experiments don't fully represent reversed forks or perhaps Rad5 doesn't necessarily regress forks *in vivo*. Mph1 had a minor role in preventing repeat fragility and instability, but not joint molecule formation. Together, these data shows the Srs2 helicase has a prominent role in role in repeat protection, differently from other tested helicases.

Despite having a large role in genome protection, an Srs2 human homolog has not been identified, although there have been anti-recombinase helicases that have been hypothesized to be potential orthologs. Since Srs2 has such a highly specialized role for triplet repeat maintenance, we were interested in using that as a method to characterize potential human orthologs. Several helicases had been described to either have similar mutant phenotypes as *srs2Δ* or be able to rescue mutant phenotypes when expressed in cells lacking Srs2. We

characterized the hRTEL1 and hFbh1 helicases by introducing those genes into our yeast strains replacing the SRS2 ORF. We found that RTEL1 could fully complement Srs2's function in preventing repeat fragility and significantly reduce repeat expansions, while hFbh1 had no effect on repeat fragility and only had a modest decrease in repeat expansions. Srs2 is hypothesized to be working on the nascent strand to prevent expansions (Usdin et al., 2015) and RTEL1 could be functioning there as well. Since RTEL1 and Srs2 have opposite polarities (RTEL1 5' to 3', Srs2 3' to 5'), perhaps they are preventing repeat fragility in the same manner but on different ends of the DNA strand. RTEL1 has a PIP box on its C terminal end (Uringa et al., 2011), which could aid in PCNA interaction for recruitment to the replication fork similar to Srs2 recruitment.

We believe the cone seen coming off our 2Ds are a mixture of regressed forks and recombination intermediates. Based on our data, we hypothesize Srs2 is needed to unwind hairpin structures to prevent prolonged fork stalling that would result in increased reversed forks or recombination associated events. Therefore, we believe Srs2 is promoting fork restart by unwinding hairpin structures and is not facilitating fork regression. Since RTEL1 could complement the *srs2Δ* CAG_{70} fragility phenotype, and our data shows Srs2 prevention of fragility is dependent on helicase activity and PCNA interaction, and the catalytic dead mutant of Srs2 (*srs2-K41R*) led to an increase in joint molecule formation, it would be interesting to see if RTEL1 could complement that function of Srs2 and reduce joint molecules that form at CAG repeats to wild-type levels. Additionally Srs2 helicase and PCNA interaction is needed to prevent fork stalling at CGG_{40}/CCG_{40} repeats (Anand et al., 2012); could RTEL substitute for Srs2 to prevent fork stalling at repeats? Further study could determine if RTEL1 can complement

other known Srs2 functions that aren't repeat related. Recent work has shown that Srs2 has yet another role in genome protection by preventing mutagenesis from misincorporated rNMPs during replication. Srs2 unwinds DNA and stimulates Exo1 nuclease activity through direct interaction to remove rNMPs at sites of insertion (Potenski et al., 2015). Srs2 has also been shown to stimulate Mus81-Mms4 nuclease activity at recombination sites and arrested forks (Chavdarova et al., 2015). This is independent of helicase activity and PCNA interaction but anti-recombinase activity is needed to displace Rad51 from substrates to promote Mus81-Mms4 cleavage and resolution. These works show the dynamic nature of Srs2 in genome protection and it would be exciting to determine if RTEL1 also has those roles. It would also be worthwhile to test other potential Srs2 orthologs in these contexts since Srs2 functions could be distributed among various helicases in higher eukaryotes.

The Ctf18-RFC clamp loader is another important factor maintaining genome integrity that was identified to have a specialized role for repeat protection compared to other alternative clamp loaders (Gellon et al., 2011). Loss of Ctf18 leads to various mutant phenotypes such as slowed replication progression, increased asymmetric fork formation in HU, de-repression of late origins, and DNA damage checkpoint defect (Crabbé et al., 2010), highlighting its role in general genome protection. Many previous investigations on Ctf18 used cells treated with HU however this work is using the CAG/CTG repeats as a natural replication barrier to investigate Ctf18's role during replication. We found that Ctf18 is needed to prevent fragility and in its absence, PCNA modification becomes key to prevent a further increase in fragility. In cells without Ctf18, PCNA SUMOylation is needed to recruit Srs2. Both Ctf18 and Srs2 are needed

to prevent repeat fragility and the absence of both genes leads to a synergistic increase in fragility. We also found the DNA damage tolerance (DDT) pathway had minimal effect on repeat fragility, even in the absence of Ctf18, indicating that while DDT is needed to bypass damaged bases, it is not the major pathway for bypassing structure-forming sequences. We hypothesize that Ctf18 and Srs2 work in distinct but parallel pathways to prevent replication fork stalling and breakage when encountering the repeats: Ctf18 mediates hairpin bypass by unloading/loading PCNA while Srs2 can unwind the hairpin structure.

Further work would need to be performed to determine if Ctf18 is unloading/loading PCNA to mediate hairpin bypass to prevent repeat fragility. Importantly, we would be interested in seeing a direct effect on replication progression at a CAG tract in *ctf18Δ* cells. We can do this with 2D gel electrophoresis in strains with repeat sequences that can stall replication (either CGG_{40}/CCG_{40} or CAG_{130}/CTG_{130}) to determine if the absence of Ctf18 will lead to a further increase in replication stalling. We could indirectly test how *ctf18Δ* affects replication by using ChIP with either RPA as an indicator of a stalled replication fork since it's known to coat single stranded DNA at stalled forks (Cimprich and Cortez, 2008) or pol ε to track the replication fork as it progresses through the repeats. It is still unclear what role Ctf18 might have as a clamp loader *in vivo* since studies have shown a decrease in PCNA signal at HU stalled forks in the absence of Ctf18 (supporting a loading function) (Lengronne et al., 2006) but in non-perturbed cells, chromatin-bound PCNA levels are unchanged (Kubota et al., 2011, 2013a). We could use the CAG/CTG repeats as a natural barrier and ChIP PCNA at our repeats in wild-type vs *ctf18Δ* cells to determine if Ctf18 might have a specialized loading/unloading role at structure-forming

sequences. This ChIP can also potentially distinguish whether it's Ctf18's unloading or loading function that is needed to prevent repeat fragility; we would expect to see an increase in PCNA at the repeats if Ctf18 is needed to unload and vise versa. It has been proposed that Ctf18 is needed to facilitate replication through cohesin rings (Lengronne et al., 2006; Terret et al., 2009) so perhaps Ctf18 is needed in the same manner to bypass structures. Ctf18-RFC's role in fork stabilization and cohesion establishment poises it more readily to bypass any structures encountered by replication compared to the other alternative clamp loaders.

Aside from PCNA unloading/loading, Ctf18 could also be acting as a fork stabilizer since it interacts with pol ε (García-Rodríguez et al., 2015; Okimoto et al., 2016) and localizes to HU stalled forks (Lengronne et al., 2006). The increase in fragility that we are seeing could be due to perturbed fork stability. Currently, our data doesn't rule out fork stabilization in the prevention of repeat fragility. Loss of Dcc1 or Ctf8 does not affect PCNA unloading/loading activity *in vitro* (Bermudez et al., 2003b; Bylund and Burgers, 2005; Shiomi et al., 2004), suggesting both do no play a role in PCNA loading. Increased FOA^R in *dcc1* mutants (Gellon et al., 2011) could indicate fork destabilization but not PCNA unloading/loading is needed to prevent repeat fragility. We can distinguish between the two roles by examining fragility rates of an ATPase dead version of Ctf18 since its PCNA unloading/loading activities are ATP dependent (Bermudez et al., 2003b; Bylund and Burgers, 2005). If the increase in fragility in *ctf18Δ* is due to a defect in PCNA unloading/loading, we expect to see the same result for an ATPase dead mutant. We currently have a plasmid with an ATPase dead Ctf18 gene. Previous attempts to amplify and clone this for yeast transformation

were unsuccessful but we can further optimize future attempts. We could also observe fragility rates in Ctf18 truncation mutants that can no longer interact with pol ε (García-Rodríguez et al., 2015). If the increase in *ctf18Δ* is due to fork destabilization, we should see an increase in fragility in these mutants.

Further characterization of how Ctf18 is preventing repeat instability could also be investigated. We've previously shown an increase in repeat instability in the absence of Ctf18 (Gellon et al., 2011) but our current data do not show a clear story as to what the mechanism resulting in that might be. The high contraction frequency could indicate Ctf18 is working on the template strand to prevent loss of repeats and this would be complementary to Srs2 working on the nascent strand, providing more support for the need for both of these proteins in repeat maintenance.

The divergent growth profiles of *srs2Δctf18Δ* and *srs2 (1-998) ctf18Δ* strains highlights Srs2's role in checkpoint recovery. Srs2 Rad51 displacement activity was needed for efficient checkpoint recovery (Yeung and Durocher, 2011), which is still retained in the *srs2 (1-998)* allele. *srs2Δ* does not have a slow growth phenotype on its own and *ctf18Δ* slow growth was not as severe as the double. Perhaps in the *srs2Δctf18Δ*, after checkpoint activation occurs in response to damage, cells remain arrested and can no longer proliferate or adapt due to lack of Srs2 Rad51 displacement activity. To test this, we could look at the growth profile for *srs2Δ875-902ctf18Δ* to confirm the need for Rad51 displacement activity in checkpoint recovery. We could also look at the status of Rad53 phosphorylation in *srs2Δctf18Δ*, which should be elevated in response to damage.

The dual need for Srs2 and Ctf18 to prevent repeat fragility in yeast could be extended to the human genes since Ctf18 is conserved and we have characterized a potential Srs2 human ortholog through this work. In mice, loss of RTEL1 leads to slowed replication and an increase in asymmetrical forks, suggesting a role for RTEL at preventing fork stalling and breakage (Vannier et al., 2013), similar to Ctf18-deficient cells. RTEL1 is needed to unwind T loops at telomeres to prevent telomere fragility and Ctf18 has been shown to facilitate replication through telomeres to maintain telomere length (Hanna et al., 2001) positioning these proteins in a manner that could promote complementary roles in genome maintenance.

We have provided insight on two proteins that play an important role in general genome maintenance and highlighted their specialized functions in repeat protection. This work can guide future studies in understanding the onset and progression of neurodegenerative diseases that are repeat associated. This research has also garnered a better understanding of how replication and repair occurs naturally when encountering repetitive sequences, which constitute the majority of our genome.

References

Aboussekhra, A., Chanet, R., Zgaga, Z., Cassier-Chauvat, C., Heude, M., and Fabre, F. (1989). RADH, a gene of Saccharomyces cerevisiae encoding a putative DNA helicase involved in DNA repair. Characteristics of radH mutants and sequence of the gene. Nucleic Acids Res. *17*, 7211–7219.

Aboussekhra, A., Chanet, R., Adjiri, A., and Fabre, F. (1992). Semidominant suppressors of Srs2 helicase mutations of Saccharomyces cerevisiae map in the RAD51 gene, whose sequence predicts a protein with similarities to procaryotic RecA proteins. Mol. Cell. Biol. *12*, 3224–3234.

Aguilera, A., and García-Muse, T. (2013). Causes of genome instability. Annu. Rev. Genet. *47*, 1–32.

Aguilera, A., and Klein, H.L. (1988). Genetic control of intrachromosomal recombination in Saccharomyces cerevisiae. I. Isolation and genetic characterization of hyper-recombination mutations. Genetics *119*, 779–790.

Anand, R.P., Shah, K.A., Niu, H., Sung, P., Mirkin, S.M., and Freudenreich, C.H. (2012). Overcoming natural replication barriers: differential helicase requirements. Nucleic Acids Res. *40*, 1091–1105.

Andersen, P.L., Xu, F., and Xiao, W. (2008). Eukaryotic DNA damage tolerance and translesion synthesis through covalent modifications of PCNA. Cell Res. *18*, 162–173.

Antony, E., Tomko, E.J., Xiao, Q., Krejci, L., Lohman, T.M., and Ellenberger, T. (2009). Srs2 Disassembles Rad51 Filaments by a Protein-Protein Interaction Triggering ATP Turnover and Dissociation of Rad51 from DNA. Mol. Cell *35*, 105–115.

Aparicio, O., Geisberg, J. V., Sekinger, E., Yang, A., Moqtaderi, Z., and Struhl, K. (2005). Chromatin Immunoprecipitation for Determining the Association of Proteins with Specific Genomic Sequences In Vivo. 1–33.

Aparicio, O.M., Weinstein, D.M., and Bell, S.P. (1997). Components and dynamics of DNA replication complexes in S. cerevisiae: Redistribution of MCM proteins and Cdc45p during S phase. Cell *91*, 59–69.

Atkinson, J., and McGlynn, P. (2009). Replication fork reversal and the maintenance of genome stability. Nucleic Acids Res. *37*, 3475–3492.

Bagni, C., Tassone, F., Neri, G., and Hagerman, R. (2012). Science in medicine Fragile X syndrome : causes , diagnosis , mechanisms , and therapeutics. *122*.

Bai, Y., and Symington, L.S. (1996). A Rad52 homolog is required for RAD51-independent mitouc recombination in Saccharom yces cerevisiae. Genes Dev. 2025–2037.

Bailly, V., Lamb, J., Sung, P., Prakash, S., and Prakash, L. (1994). Specific complex formation between yeast RAD6 and RAD18 proteins: A potential mechanism for targeting RAD6 ubiquitin-conjugating activity to DNA damage sites. Genes Dev. *8*, 811–820.

Bailly, V., Prakash, S., and Prakash, L. (1997). Domains required for dimerization

of yeast Rad6 ubiquitin-conjugating enzyme and Rad18 DNA binding protein. Mol. Cell. Biol. *17*, 4536–4543.

Balakumaran, B.S., Freudenreich, C.H., and Zakian, V.A. (2000). CGG / CCG repeats exhibit orientation-dependent instability and orientation-independent fragility in Saccharomyces cerevisiae. *9*, 93–100.

Ballew, B.J., Joseph, V., De, S., Sarek, G., Vannier, J.B., Stracker, T., Schrader, K.A., Small, T.N., O'Reilly, R., Manschreck, C., et al. (2013). A Recessive Founder Mutation in Regulator of Telomere Elongation Helicase 1, RTEL1, Underlies Severe Immunodeficiency and Features of Hoyeraal Hreidarsson Syndrome. PLoS Genet. *9*.

Barber, L.J., Youds, J.L., Ward, J.D., McIlwraith, M.J., O'Neil, N.J., Petalcorin, M.I.R., Martin, J.S., Collis, S.J., Cantor, S.B., Auclair, M., et al. (2008). RTEL1 maintains genomic stability by suppressing homologous recombination. Cell *135*, 261–271.

Bellaoui, M., Chang, M., Ou, J., Xu, H., Boone, C., and Brown, G.W. (2003). Elg1 forms an alternative RFC complex important for DNA replication and genome integrity. EMBO J. *22*, 4304–4313.

Bermudez, V.P., Lindsey-Boltz, L. a, Cesare, A.J., Maniwa, Y., Griffith, J.D., Hurwitz, J., and Sancar, A. (2003a). Loading of the human 9-1-1 checkpoint complex onto DNA by the checkpoint clamp loader hRad17-replication factor C complex in vitro. Proc. Natl. Acad. Sci. U. S. A. *100*, 1633–1638.

Bermudez, V.P., Maniwa, Y., Tappin, I., Ozato, K., Yokomori, K., and Hurwitz, J. (2003b). The alternative Ctf18-Dcc1-Ctf8-replication factor C complex required for sister chromatid cohesion loads proliferating cell nuclear antigen onto DNA. Proc. Natl. Acad. Sci. U. S. A. *100*, 10237–10242.

Berti, M., and Vindigni, A. (2016). Replication stress: getting back on track. Nat. Struct. Mol. Biol. *23*, 103–109.

Bhattacharyya, S., and Lahue, R.S. (2004). Saccharomyces cerevisiae Srs2 DNA helicase selectively blocks expansions of trinucleotide repeats. Mol. Cell. Biol. *24*, 7324–7330.

Bhattacharyya, S., and Lahue, R.S. (2005). Srs2 helicase of Saccharomyces cerevisiae selectively unwinds triplet repeat DNA. J. Biol. Chem. *280*, 33311–33317.

Bienko, M. (2005). Ubiquitin-binding domains in Y-family polymerases regulate translesion synthesis. Science (80-.). *310*, 1821–1824.

Bikard, D., Loot, C., Baharoglu, Z., and Mazel, D. (2010). Folded DNA in action: hairpin formation and biological functions in prokaryotes. Microbiol. Mol. Biol. Rev. *74*, 570–588.

Blastyák, A., Pintér, L., Unk, I., Prakash, L., Prakash, S., and Haracska, L. (2007). Yeast Rad5 Protein Required for Postreplication Repair Has a DNA Helicase Activity Specific for Replication Fork Regression. Mol. Cell *28*, 167–175.

Blastyák, A., Hajdú, I., Unk, I., and Haracska, L. (2010). Role of double-stranded DNA translocase activity of human HLTF in replication of damaged DNA. Mol.

Cell. Biol. *30*, 684–693.

Bochman, M.L., Paeschke, K., and Zakian, V. a. (2012). DNA secondary structures: stability and function of G-quadruplex structures. Nat. Rev. Genet. *13*, 770–780.

Branzei, D. (2011). Ubiquitin family modifications and template switching. FEBS Lett. *585*, 2810–2817.

Branzei, D., and Szakal, B. (2016). Priming for tolerance and cohesion at replication forks. Nucleus *1034*, 00–00.

Bravo, R., Frank, R., Blundell, P.A., and Macdonald-Bravo, H. (1987). Cyclin/PCNA is the auxiliary protein of DNA polymerase-delta. Nature *326*, 515–517.

Le Breton, C., Dupaigne, P., Robert, T., Le Cam, E., Gangloff, S., Fabre, F., and Veaute, X. (2008). Srs2 removes deadly recombination intermediates independently of its interaction with SUMO-modified PCNA. Nucleic Acids Res. *36*, 4964–4974.

Broomfield, S., Chow, B.L., and Xiao, W. (1998). MMS2, encoding a ubiquitin-conjugating-enzyme-like protein, is a member of the yeast error-free postreplication repair pathway. Proc. Natl. Acad. Sci. *95*, 5678–5683.

Budworth, H., and Mcmurray, C.T. (2014). A brief history of triplet repeat diseases. 3–17.

Burgers, P.M. (1991). Saccharomyces cerevisiae replication factor C. II. Formation and activity of complexes with the proliferating cell nuclear antigen and with DNA polymerases delta and epsilon. J. Biol. Chem. *266*, 22698–22706.

Burgess, R.C., Lisby, M., Altmannova, V., Krejci, L., Sung, P., and Rothstein, R. (2009). Localization of recombination proteins and Srs2 reveals anti-recombinase function in vivo. J. Cell Biol. *185*, 969–981.

Burkovics, P., Sebesta, M., Sisakova, A., Plault, N., Szukacsov, V., Robert, T., Pinter, L., Marini, V., Kolesar, P., Haracska, L., et al. (2013). Srs2 mediates PCNA-SUMO-dependent inhibition of DNA repair synthesis. EMBO J. *32*, 742–755.

Burkovics, P., Dome, L., Juhasz, S., Altmannova, V., Sebesta, M., Pacesa, M., Fugger, K., Sorensen, C.S., Lee, M.Y.W.T., Haracska, L., et al. (2016). The PCNA-associated protein PARI negatively regulates homologous recombination via the inhibition of DNA repair synthesis. Nucleic Acids Res. gkw024 – .

Bylund, G.O., and Burgers, P.M.J. (2005). Replication protein A-directed unloading of PCNA by the Ctf18 cohesion establishment complex. Mol. Cell. Biol. *25*, 5445–5455.

Byun, T.S., Pacek, M., Yee, M.C., Walter, J.C., and Cimprich, K. a. (2005). Functional uncoupling of MCM helicase and DNA polymerase activities activates the ATR-dependent checkpoint. Genes Dev. *19*, 1040–1052.

Callahan, J.L., Andrews, K.J., Zakian, V.A., and Freudenreich, C.H. (2003). Mutations in yeast replication proteins that increase CAG/CTG expansions also

increase repeat fragility. Mol. Cell. Biol. *23*, 7849–7860.

Chavdarova, M., Marini, V., Sisakova, A., Sedlackova, H., Vigasova, D., Brill, S.J., Lisby, M., and Krejci, L. (2015). Srs2 promotes Mus81-Mms4-mediated resolution of recombination intermediates. Nucleic Acids Res. *43*, 3626–3642.

Cherng, N., Shishkin, A.A., Schlager, L.I., Tuck, R.H., Sloan, L., Matera, R., Sarkar, P.S., Ashizawa, T., Freudenreich, C.H., and Mirkin, S.M. (2011). Expansions, contractions, and fragility of the spinocerebellar ataxia type 10 pentanucleotide repeat in yeast. Proc. Natl. Acad. Sci. U. S. A. *108*, 2843–2848.

Cheung-ong, K., Giaever, G., and Nislow, C. (2013). Perspective DNA-Damaging Agents in Cancer Chemotherapy : Serendipity and Chemical Biology. Chem. Biol. *20*, 648–659.

Chiolo, I., Carotenuto, W., Maffioletti, G., Petrini, J.H.J., Foiani, M., and Liberi, G. (2005). Srs2 and Sgs1 DNA helicases associate with Mre11 in different subcomplexes following checkpoint activation and CDK1-mediated Srs2 phosphorylation. Mol. Cell. Biol. *25*, 5738–5751.

Chiolo, I., Saponaro, M., Baryshnikova, A., Kim, J.-H., Seo, Y.-S., and Liberi, G. (2007). The human F-Box DNA helicase FBH1 faces Saccharomyces cerevisiae Srs2 and postreplication repair pathway roles. Mol. Cell. Biol. *27*, 7439–7450.

Chu, W.K., Payne, M.J., Beli, P., Hanada, K., Choudhary, C., and Hickson, I.D. (2015). FBH1 influences DNA replication fork stability and homologous recombination through ubiquitylation of RAD51. Nat. Commun. *6*, 1–9.

Cimprich, K.A., and Cortez, D. (2008). ATR: an essential regulator of genome integrity. Nat. Rev. Mol. Cell Biol. *9*, 616–627.

Colavito, S., Macris-Kiss, M., Seong, C., Gleeson, O., Greene, E.C., Klein, H.L., Krejci, L., and Sung, P. (2009). Functional significance of the Rad51-Srs2 complex in Rad51 presynaptic filament disruption. Nucleic Acids Res. *37*, 6754–6764.

Consortium, I.H.G.S. (2001). Initial sequencing and analysis of the human genome. Nature *409*.

Cotta-Ramusino, C., Fachinetti, D., Lucca, C., Doksani, Y., Lopes, M., Sogo, J., and Foiani, M. (2005). Exo1 processes stalled replication forks and counteracts fork reversal in checkpoint-defective cells. Mol. Cell *17*, 153–159.

Courcelle, J., Donaldson, J.R., Chow, K.-H., and Courcelle, C.T. (2003). DNA damage-induced replication fork regression and processing in Escherichia coli. Science *299*, 1064–1067.

Crabbé, L., Thomas, A., Pantesco, V., De Vos, J., Pasero, P., and Lengronne, A. (2010). Analysis of replication profiles reveals key role of RFC-Ctf18 in yeast replication stress response. Nat. Struct. Mol. Biol. *17*, 1391–1397.

Cullmann, G., Fien, K., Kobayashi, R., and Stillman, B. (1995). Characterization of the five replication factor C genes of Saccharomyces cerevisiae. Mol. Cell. Biol. *15*, 4661–4671.

Daee, D.L., Mertz, T., and Lahue, R.S. (2007). Postreplication repair inhibits

CAG.CTG repeat expansions in Saccharomyces cerevisiae. Mol. Cell. Biol. *27*, 102–110.

Dai, X., and Greizerstein, M.B. (1997). Supercoil-induced extrusion of a regulatory DNA hairpin. PNAS *94*, 2174–2179.

Daigaku, Y., Davies, A. a, and Ulrich, H.D. (2010). Ubiquitin-dependent DNA damage bypass is separable from genome replication. Nature *465*, 951–955.

Darlow, J.M., and Leach, D.R.F. (1998). Secondary Structures in d (CGG) and d (CCG) Repeat Tracts. J. Mol. Biol. *3*, 3–16.

Davies, A.A., Huttner, D., Daigaku, Y., Chen, S., and Ulrich, H.D. (2008). Activation of ubiquitin-dependent DNA damage bypass is mediated by replication protein a. Mol. Cell *29*, 625–636.

Debauve, G., Capouillez, A., Belayew, A., and Saussez, S. (2008). The Helicase-Like Transcription Factor and its implication in cancer progression. Cell. Mol. Life Sci. *65*, 591–604.

DeJesus-Hernandez, M., Mackenzie, I.R., Boeve, B.F., Boxer, A.L., Baker, M., Rutherford, N.J., Nicholson, A.M., Finch, N. a., Flynn, H., Adamson, J., et al. (2011). Expanded GGGGCC Hexanucleotide Repeat in Noncoding Region of C9ORF72 Causes Chromosome 9p-Linked FTD and ALS. Neuron *72*, 245–256.

Dhar, A., and Lahue, R.S. (2008). Rapid unwinding of triplet repeat hairpins by Srs2 helicase of Saccharomyces cerevisiae. Nucleic Acids Res. *36*, 3366–3373.

Ding, H., Schertzer, M., Wu, X., Gertsenstein, M., Selig, S., Kammori, M., Pourvali, R., Poon, S., Vulto, I., Chavez, E., et al. (2004). Regulation of murine telomere length by Rtel: An essential gene encoding a helicase-like protein. Cell *117*, 873–886.

Dupaigne, P., Le Breton, C., Fabre, F., Gangloff, S., Le Cam, E., and Veaute, X. (2008). The Srs2 Helicase Activity Is Stimulated by Rad51 Filaments on dsDNA: Implications for Crossover Incidence during Mitotic Recombination. Mol. Cell *29*, 243–254.

Fouché, N., Özgür, S., Roy, D., and Griffith, J.D. (2006). Replication fork regression in repetitive DNAs. Nucleic Acids Res. *34*, 6044–6050.

Freidburg, E.C., Mcdaniel, L.D., and Schultz, R.A. (2004). The role of endogenous and exogenous DNA damage and mutagenesis. Curr. Opin. Genet. Dev.

Freudenreich, C.H. (2007). Chromosome fragility: molecular mechanisms and cellular consequences. Program 4911–4924.

Freudenreich, C.H., Stavenhagen, J.B., and Zakian, V.A. (1997). Stability of a CTG/CAG trinucleotide repeat in yeast is dependent on its orientation in the genome. Mol. Cell. Biol. *17*, 2090–2098.

Freudenreich, C.H., Kantrow, S.M., and Zakian, V. a (1998). Expansion and length-dependent fragility of CTG repeats in yeast. Science *279*, 853–856.

Frizzell, A., Nguyen, J.H.G., Petalcorin, M.I.R., Turner, K.D., Boulton, S.J.,

Freudenreich, C.H., and Lahue, R.S. (2014). RTEL1 inhibits trinucleotide repeat expansions and fragility. Cell Rep. *6*, 827–835.

Froget, B., Blaisonneau, J., Lambert, S., and Baldacci, G. (2008). Cleavage of stalled forks by fission yeast Mus81/Eme1 in absence of DNA replication checkpoint. Mol. Biol. Cell *19*, 445–456.

Fry, M., and Loeb, L.A. (1994). The fragile X syndrome d (CGG). nucleotide repeats form a stable tetrahelical structure. PNAS *91*, 4950–4954.

Fugger, K., Mistrik, M., Neelsen, K.J., Yao, Q., Zellweger, R., Kousholt, A.N., Haahr, P., Chu, W.K., Bartek, J., Lopes, M., et al. (2015). FBH1 Catalyzes Regression of Stalled Replication Forks. Cell Rep. *10*, 1749–1757.

Gacy, A.M., and McMurray, C.T. (1998). Influence of Hairpins on Template Reannealing at Trinucleotide Repeat Duplexes : A Model for Slipped DNA †. Biochemistry *2960*, 9426–9434.

Gacy, A.M., Goellner, G., Juranic, N., Macura, S., and Mcmurray, C.T. (1995). Trinucleotide Repeats That Expand in Human Disease Form Hairpin Structures In Vitro. *91*, 533–540.

Gacy, A.M., Goellner, G.M., Spiro, C., Chen, X., Gupta, G., Bradbury, E.M., Dyer, R.B., Mikesell, M.J., Yao, J.Z., Johnson, A.J., et al. (1998). GAA Instability in Friedreich's Ataxia Shares a Common, DNA-Directed and Intraallelic Mechanism with Other Trinucleotide Diseases. Mol. Cell *1*, 583–593.

Gangloff, S., Soustelle, C., and Fabre, F. (2000). Homologous recombination is responsible for cell death in the absence of the Sgs1 and Srs2 helicases. Nat. Genet. *25*, 192–194.

García-Rodríguez, L.J., De Piccoli, G., Marchesi, V., Jones, R.C., Edmondson, R.D., and Labib, K. (2015). A conserved Polε binding module in Ctf18-RFC is required for S-phase checkpoint activation downstream of Mec1. Nucleic Acids Res. *43*, 8830–8838.

Gari, K., Décaillet, C., Stasiak, A.Z., Stasiak, A., and Constantinou, A. (2008). The Fanconi Anemia Protein FANCM Can Promote Branch Migration of Holliday Junctions and Replication Forks. Mol. Cell *29*, 141–148.

Gavin, A.-C., Aloy, P., Grandi, P., Krause, R., Boesche, M., Marzioch, M., Rau, C., Jensen, L.J., Bastuck, S., Dümpelfeld, B., et al. (2006). Proteome survey reveals modularity of the yeast cell machinery. Nature *440*, 631–636.

Gellon, L., Razidlo, D.F., Gleeson, O., Verra, L., Schulz, D., Lahue, R.S., and Freudenreich, C.H. (2011). New functions of Ctf18-RFC in preserving genome stability outside its role in sister chromatid cohesion. PLoS Genet. *7*.

Geng, L., Huntoon, C.J., and Karnitz, L.M. (2010). RAD18-mediated ubiquitination of PCNA activates the Fanconi anemia DNA repair network. J. Cell Biol. *191*, 249–257.

Gomes, X. V., and Burgers, P.M.J. (2001). ATP utilization by yeast replication factor C: I. ATP-mediated interaction with DNA and with proliferating cell nuclear antigen. J. Biol. Chem. *276*, 34768–34775.

Guo, C., Tang, T.-S., Bienko, M., Parker, J.L., Bielen, A.B., Sonoda, E., Takeda, S., Ulrich, H.D., Dikic, I., and Friedberg, E.C. (2006). Ubiquitin-Binding Motifs in REV1 Protein Are Required for Its Role in the Tolerance of DNA Damage. Mol. Cell. Biol. *26*, 8892–8900.

Gupta, S., Yeeles, J.T.P., and Marians, K.J. (2014). Regression of replication forks stalled by leading-strand template damage: I. Both RecG and RuvAB catalyze regression, but RuvC cleaves the holliday junctions formed by RecG preferentially. J. Biol. Chem. *289*, 28376–28387.

Hall, M.C., and Matson, S.W. (1999). Helicase motifs: the engine that powers DNA unwinding. Mol. Microbiol. *34*, 867–877.

Hanna, J.S., Kroll, E.S., Lundblad, V., and Spencer, F.A. (2001). Saccharomyces cerevisiae CTF18 and CTF4 are required for sister chromatid cohesion. Mol. Cell. Biol. *21*, 3144–3158.

Hedglin, M., Kumar, R., and Benkovic, S.J. (2013). Replication clamps and clamp loaders. Cold Spring Harb. Perspect. Biol. *5*, 1–19.

Helleday, T., Eshtad, S., and Nik-zainal, S. (2014). Mechanisms underlying mutational signatures in human cancers. Nat. Publ. Gr. *15*, 585–598.

Hickson, I.D. (2014). The dissolution of double Holliday junctions. Cold Spring Harb. Perspect. Biol. *6*, a016477.

Hoege, C., Pfander, B., Moldovan, G.-L., Pyrowolakis, G., and Jentsch, S. (2002). RAD6-dependent DNA repair is linked to modification of PCNA by ubiquitin and SUMO. Nature *419*, 135–141.

Hofmann, R.M., and Pickart, C.M. (1999). Noncanonical MMS2-encoded ubiquitin-conjugating enzyme functions in assembly of novel polyubiquitin chains for DNA repair. Cell *96*, 645–653.

House, N.C.M., Yang, J.H., Walsh, S.C., Moy, J.M., and Freudenreich, C.H. (2014). NuA4 Initiates Dynamic Histone H4 Acetylation to Promote High-Fidelity Sister Chromatid Recombination at Postreplication Gaps. Mol. Cell *55*, 818–828.

Huang, J., Huen, M.S.Y., Kim, H., Chung, C., Leung, Y., Mark, J.N., Yu, X., and Chen, J. (2009). RAD18 transmits DNA damage signaling to elicit homologous recombination repair. *11*, 592–603.

Ira, G., Malkova, A., Liberi, G., Foiani, M., and Haber, J.E. (2003). Srs2 and Sgs1-Top3 Suppress Crossovers during Double-Strand Break Repair in Yeast. Cell *115*, 401–411.

Ivessa, A.S., Lenzmeier, B. a., Bessler, J.B., Goudsouzian, L.K., Schnakenberg, S.L., and Zakian, V. a. (2003). The Saccharomyces cerevisiae Helicase Rrm3p Facilitates Replication Past Nonhistone Protein-DNA Complexes. Mol. Cell *12*, 1525–1536.

Jackson, S.P., and Bartek, J. (2009). The DNA-damage response in human biology and disease. Nature *461*, 1071–1078.

Jeong, Y.T., Rossi, M., Cermak, L., Saraf, A., Florens, L., Washburn, M.P., Sung, P., Schildkraut, C., and Pagano, M. (2013). FBH1 promotes DNA double-strand

breakage and apoptosis in response to DNA replication stress. J. Cell Biol. *200*, 141–149.

Johnson, A., and O'Donnell, M. (2005). Cellular DNA Replicases: Components and Dynamics at the Replication Fork. Annu. Rev. Biochem. *74*, 283–315.

Johnson, R.E., Henderson, S.T., Petes, T.D., Prakash, S., Bankmann, M., and Prakash, L. (1992). Saccharomyces cerevisiae RAD5-encoded DNA repair protein contains DNA helicase and zinc-binding sequence motifs and affects the stability of simple repetitive sequences in the genome. Mol. Cell. Biol. *12*, 3807–3818.

Johnson, R.E., Prakash, S., and Prakash, L. (1994). Yeast DNA repair protein RAD5 that promotes instability of simple repetitive sequences is a DNA-dependent ATPase. J. Biol. Chem. *269*, 28259–28262.

Kai, M., Boddy, M.N., Russell, P., and Wang, T.S.F. (2005). Replication checkpoint kinase Cds1 regulates Mus81 to preserve genome integrity during replication stress. Genes Dev. *19*, 919–932.

Kang, S., Ohshima, K., Shimizu, M., Amirhaeri, S., and Wells, R.D. (1995). Pausing of DNA Synthesis in Vitro at Specific Loci in CTG and CGG Triplet Repeats from Human Hereditary Disease Genes *. Jounal Biol. Chem. *270*, 27014–27021.

Kang, Y.H., Munashingha, P.R., Lee, C.H., Nguyen, T.A., and Seo, Y.S. (2012). Biochemical studies of the Saccharomyces cerevisiae Mph1 helicase on junction-containing DNA structures. Nucleic Acids Res. *40*, 2089–2106.

Karpenshif, Y., and Bernstein, K.A. (2012). From yeast to mammals: Recent advances in genetic control of homologous recombination. DNA Repair (Amst). *11*, 781–788.

Karras, G.I., and Jentsch, S. (2010). The RAD6 DNA damage tolerance pathway operates uncoupled from the replication fork and is functional beyond S phase. Cell *141*, 255–267.

Kelman, Z., and O'Donnell, M. (1995). DNA polymerase III holoenzyme: structure and function of a chromosomal replicating machine. Annu. Rev. Biochem. *64*, 171–200.

Kerrest, A., Anand, R.P., Sundararajan, R., Bermejo, R., Liberi, G., Dujon, B., Freudenreich, C.H., and Richard, G.-F. (2009). SRS2 and SGS1 prevent chromosomal breaks and stabilize triplet repeats by restraining recombination. Nat. Struct. Mol. Biol. *16*, 159–167.

Kim, H., and Brill, S.J. (2001). Rfc4 Interacts with Rpa1 and Is Required for Both DNA Replication and DNA Damage Checkpoints in Saccharomyces cerevisiae Rfc4 Interacts with Rpa1 and Is Required for Both DNA Replication and DNA Damage Checkpoints in Saccharomyces cerevisiae. *21*, 3725–3737.

Kim, J.C., and Mirkin, S.M. (2013). The balancing act of DNA repeat expansions. Curr. Opin. Genet. Dev. *23*, 280–288.

Kim, J., Kim, J.-H., Lee, S.-H., Kim, D.-H., Kang, H.-Y., Bae, S.-H., Pan, Z.-Q., and Seo, Y.-S. (2002). The novel human DNA helicase hFBH1 is an F-box

protein. J. Biol. Chem. *277*, 24530–24537.

Kim, J., Robertson, K., Mylonas, K.J.L., Gray, F.C., Charapitsa, I., and Macneill, S.A. (2005). Contrasting effects of Elg1 – RFC and Ctf18 – RFC inactivation in the absence of fully functional RFC in fission yeast. *33*, 4078–4089.

Kohzaki, M., Hatanaka, A., Sonoda, E., Yamazoe, M., Kikuchi, K., Vu Trung, N., Szüts, D., Sale, J.E., Shinagawa, H., Watanabe, M., et al. (2007). Cooperative roles of vertebrate Fbh1 and Blm DNA helicases in avoidance of crossovers during recombination initiated by replication fork collapse. Mol. Cell. Biol. *27*, 2812–2820.

Kolesar, P., Altmannova, V., Silva, S., Lisby, M., and Krejci, L. (2016). Pro-recombination role of Srs2 requires SUMO but is independent of PCNA interaction Peter. J. Biol. Chem. *291*, 9–16.

Van Komen, S., Reddy, M.S., Krejci, L., Klein, H., and Sung, P. (2003). ATPase and DNA Helicase Activities of the Saccharomyces cerevisiae Anti-recombinase Srs2. J. Biol. Chem. *278*, 44331–44337.

Krejci, L., Van Komen, S., Li, Y., Villemain, J., Reddy, M.S., Klein, H., Ellenberger, T., and Sung, P. (2003). DNA helicase Srs2 disrupts the Rad51 presynaptic filament. Nature *423*, 305–309.

Krejci, L., Macris, M., Li, Y., Van Komen, S., Villemain, J., Ellenberger, T., Klein, H., and Sung, P. (2004). Role of ATP hydrolysis in the antirecombinase function of Saccharomyces cerevisiae Srs2 protein. J. Biol. Chem. *279*, 23193–23199.

Krejci, L., Altmannova, V., Spirek, M., and Zhao, X. (2012). Homologous recombination and its regulation. Nucleic Acids Res. *40*, 5795–5818.

Krishna, T.S.R., Fenyö, D., Kong, X.-P., Gary, S., Chait, B.T., Burgers, P., and Kuriyan, J. (1994). Crystallization of Proliferating Cell Nuclear Antigen (PCNA) from Saccharomyces cerevisiae. J. Mol. Biol. *241*, 265–268.

Kubota, T., Hiraga, S., Yamada, K., Lamond, A.I., and Donaldson, A.D. (2011). Quantitative proteomic analysis of chromatin reveals that Ctf18 acts in the DNA replication checkpoint. Mol. Cell. Proteomics *10*, M110.005561.

Kubota, T., Nishimura, K., Kanemaki, M.T., and Donaldson, A.D. (2013a). The Elg1 Replication Factor C-like Complex Functions in PCNA Unloading during DNA Replication. Mol. Cell *50*, 273–280.

Kubota, T., Myung, K., and Donaldson, A.D. (2013b). Is PCNA unloading the central function of the Elg1/ATAD5 replication factor C-like complex? Cell Cycle *12*, 2570–2579.

Kubota, T., Katou, Y., Nakato, R., Shirahige, K., and Donaldson, A.D. (2015). Replication-Coupled PCNA Unloading by the Elg1 Complex Occurs Genome-wide and Requires Okazaki Fragment Ligation. Cell Rep. *12*, 774–787.

Lambert, S., Mizuno, K., Blaisonneau, J., Martineau, S., Chanet, R., Fréon, K., Murray, J.M., Carr, A.M., and Baldacci, G. (2010). Homologous recombination restarts blocked replication forks at the expense of genome rearrangements by template exchange. Mol. Cell *39*, 346–359.

Langston, L.D., and O'Donnell, M. (2008). DNA polymerase δ is highly processive with proliferating cell nuclear antigen and undergoes collision release upon completing DNA. J. Biol. Chem. *283*, 29522–29531.

Lee, S.K., Johnson, R.E., Yu, S.L., Prakash, L., and Prakash, S. (1999). Requirement of yeast SGS1 and SRS2 genes for replication and transcription. Science (80-.). *286*, 2339–2342.

LeGuen, T., Jullien, L., Touzot, F., Schertzer, M., Gaillard, L., Perderiset, M., Carpentier, W., Nitschke, P., Picard, C., Couillault, G., et al. (2013). Human RTEL1 deficiency causes hoyeraal-hreidarsson syndrome with short telomeres and genome instability. Hum. Mol. Genet. *22*, 3239–3249.

Lehmann, A.R., Niimi, A., Ogi, T., Brown, S., Sabbioneda, S., Wing, J.F., Kannouche, P.L., and Green, C.M. (2007). Translesion synthesis: Y-family polymerases and the polymerase switch. DNA Repair (Amst). *6*, 891–899.

Leman, A.R., and Noguchi, E. (2013). The Replication Fork: Understanding the Eukaryotic Replication Machinery and the Challenges to Genome Duplication.

Lengronne, A., McIntyre, J., Katou, Y., Kanoh, Y., Hopfner, K.P., Shirahige, K., and Uhlmann, F. (2006). Establishment of Sister Chromatid Cohesion at the S. cerevisiae Replication Fork. Mol. Cell *23*, 787–799.

Liberi, G., Chiolo, I., Pellicioli, A., Lopes, M., Plevani, P., Muzi-Falconi, M., and Foiani, M. (2000a). Srs2 DNA helicase is involved in checkpoint response and its regulation requires a functional Mec1-dependent pathway and Cdk1 activity. Embo J *19*, 5027–5038.

Liberi, G., Chiolo, I., Pellicioli, A., Lopes, M., Plevani, P., Muzi-falconi, M., and Foiani, M. (2000b). Srs2 DNA helicase is involved in checkpoint response and its regulation requires a functional Mec1-dependent pathway and Cdk1 activity. *19*, 5027–5038.

Liberi, G., Cotta-Ramusino, C., Lopes, M., Sogo, J., Conti, C., Bensimon, A., and Foiani, M. (2006). Methods to Study Replication Fork Collapse in Budding Yeast. Methods Enzymol. *409*, 442–462.

Lindahl, T. (2000). Suppression of spontaneous mutagenesis in human cells by DNA base excision-repair. Mutat. Res. - Rev. Mutat. Res. *462*, 129–135.

Lisby, M., Rothstein, R., and Mortensen, U.H. (2001). Rad52 forms DNA repair and recombination centers during S phase. Proc. Natl. Acad. Sci. U. S. A. *98*, 8276–8282.

Liu, G., Chen, X., Bissler, J.J., Sinden, R.R., and Leffak, M. (2010). Replication-dependent instability at (CTG) x (CAG) repeat hairpins in human cells. Nat. Chem. Biol. *6*, 652–659.

Long, D.T., and Kreuzer, K.N. (2008). Regression supports two mechanisms of fork processing in phage T4. Proc. Natl. Acad. Sci. U. S. A. *105*, 6852–6857.

Long, D.T., and Kreuzer, K.N. (2009). Fork regression is an active helicase-driven pathway in bacteriophage T4. EMBO Rep. *10*, 394–399.

Longtine, M.S., McKenzie, A., Demarini, D.J., Shah, N.G., Wach, A., Brachat, A.,

Philippsen, P., and Pringle, J.R. (1998). Additional modules for versatile and economical PCR-based gene deletion and modification in Saccharomyces cerevisiae. Yeast *14*, 953–961.

Lopes, M., Cotta-Ramusino, C., Pellicioli, A., Liberi, G., Plevani, P., Muzi-Falconi, M., Newlon, C.S., and Foiani, M. (2001). The DNA replication checkpoint response stabilizes stalled replication forks. Nature *412*, 557–561.

López Castel, A., Cleary, J.D., and Pearson, C.E. (2010). Repeat instability as the basis for human diseases and as a potential target for therapy. Nat. Rev. Mol. Cell Biol. *11*, 165–170.

Lorenz, A., Osman, F., Folkyte, V., Sofueva, S., and Whitby, M.C. (2009). Fbh1 limits Rad51-dependent recombination at blocked replication forks. Mol. Cell. Biol. *29*, 4742–4756.

MacDonald, M.E., Ambrose, C.M., Duyao, M.P., Myers, R.H., Lin, C., Srinidhi, L., Barnes, G., Taylor, S. a., James, M., Groot, N., et al. (1993). A novel gene containing a trinucleotide repeat that is expanded and unstable on Huntington's disease chromosomes. Cell *72*, 971–983.

Mace, D.C., and Alberts, B.M. (1984). T4 DNA polymerase. Rates and processivity on single-stranded DNA templates. J Mol Biol *177*, 295–311.

Majka, J., and Burgers, P.M.J. (2003). Yeast Rad17/Mec3/Ddc1: a sliding clamp for the DNA damage checkpoint. Proc. Natl. Acad. Sci. U. S. A. *100*, 2249–2254.

Majka, J., and Burgers, P.M.J. (2004). The PCNA-RFC Families of DNA Clamps and Clamp Loaders. Prog. Nucleic Acid Res. Mol. Biol. *78*, 227–260.

Maki, H., and Kornberg, A. (1985). The polymerase subunit of DNA polymerase III of Escherichia coli. II. Purification of the ?? subunit, devoid of nuclease activities. J. Biol. Chem. *260*, 12987–12992.

Mariappan, S.V.S., Catasti, P., Iii, L.A.S., Bradbury, E.M., and Gupta, G. (1999). The High-resolution Structure of the Triplex Formed by the GAA / TTC Triplet Repeat Associated with Friedreich ' s Ataxia. *285*, 2035–2052.

Marini, V., and Krejci, L. (2010). Srs2: the "Odd-Job Man" in DNA repair. DNA Repair (Amst). *9*, 268–275.

Mayer, M.L., Gygi, S.P., Aebersold, R., and Hieter, P. (2001). Identification of RFC(Ctf18p, Ctf8p, Dcc1p): An alternative RFC complex required for sister chromatid cohesion in S. cerevisiae. Mol. Cell *7*, 959–970.

Mazón, G., and Symington, L.S. (2013). Mph1 and Mus81-Mms4 prevent aberrant processing of mitotic recombination intermediates. Mol. Cell *52*, 63–74.

McInerney, P., Johnson, A., Katz, F., and O'Donnell, M. (2007). Characterization of a Triple DNA Polymerase Replisome. Mol. Cell *27*, 527–538.

McMurray, C.T. (2010). Mechanisms of trinucleotide repeat instability during human development. Nat. Rev. Genet. *11*, 786–799.

Miret, J.J., Pessoa-Brandão, L., and Lahue, R.S. (1998). Orientation-dependent and sequence-specific expansions of CTG/CAG trinucleotide repeats in

Saccharomyces cerevisiae. Proc. Natl. Acad. Sci. U. S. A. *95*, 12438–12443.

Mirkin, S.M. (2006). DNA structures , repeat expansions and human hereditary disorders. 351–358.

Mirkin, S.M. (2007). Expandable DNA repeats and human disease. Nature *447*, 932–940.

Mirkin, E. V, and Mirkin, S.M. (2007). Replication fork stalling at natural impediments. Microbiol. Mol. Biol. Rev. *71*, 13–35.

Mitas, M. (1997). Trinucleotide repeats associated with human disease. *25*, 2245–2253.

Moinova, H.R., Chen, W.-D., Shen, L., Smiraglia, D., Olechnowicz, J., Ravi, L., Kasturi, L., Myeroff, L., Plass, C., Parsons, R., et al. (2002). HLTF gene silencing in human colon cancer. Proc. Natl. Acad. Sci. *99*, 4562–4567.

Moldovan, G.L., Dejsuphong, D., Petalcorin, M.I.R., Hofmann, K., Takeda, S., Boulton, S.J., and D'Andrea, A.D. (2012). Inhibition of homologous recombination by the PCNA-interacting protein PARI. Mol. Cell *45*, 75–86.

Moldovan, G.-L., Pfander, B., and Jentsch, S. (2007). PCNA, the Maestro of the Replication Fork. Cell *129*, 665–679.

Morishita, T., Morishita, T., Furukawa, F., Furukawa, F., Sakaguchi, C., Sakaguchi, C., Toda, T., Toda, T., Carr, A.M., Carr, A.M., et al. (2005). Role of the Schizosaccharomyces pombe F-Box DNA Helicase in Processing Recombination Intermediates. Society *25*, 8074–8083.

Mozlin, A.M., Fung, C.W., and Symington, L.S. (2008). Role of the Saccharomyces cerevisiae Rad51 Paralogs in Sister Chromatid Recombination. *126*, 113–126.

Murakami, T., Takano, R., Takeo, S., Taniguchi, R., Ogawa, K., Ohashi, E., and Tsurimoto, T. (2010). Stable interaction between the human proliferating cell nuclear antigen loader complex Ctf18-replication factor C (RFC) and DNA polymerase {epsilon} is mediated by the cohesion-specific subunits, Ctf18, Dcc1, and Ctf8. J. Biol. Chem. *285*, 34608–34615.

Neelsen, K.J., and Lopes, M. (2015). Replication fork reversal in eukaryotes: from dead end to dynamic response. Nat. Rev. Mol. Cell Biol. *16*, 207–220.

O'Donnell, M.E., and Kornberg, A. (1985). Dynamics of DNA polymerase III holoenzyme of Escherichia coli in replication of a multiprimed template. J. Biol. Chem. *260*, 12875–12883.

Oberlé, I., Rousseau, F., Heitz, D., Kretz, C., Devys, D., Hanauer, a, Boué, J., Bertheas, M.F., and Mandel, J.L. (1991). Instability of a 550-base pair DNA segment and abnormal methylation in fragile X syndrome. Science *252*, 1097–1102.

Ogi, T., Limsirichaikul, S., Overmeer, R.M., Volker, M., Takenaka, K., Cloney, R., Nakazawa, Y., Niimi, A., Miki, Y., Jaspers, N.G., et al. (2010). Three DNA Polymerases, Recruited by Different Mechanisms, Carry Out NER Repair Synthesis in Human Cells. Mol. Cell *37*, 714–727.

Okimoto, H., Tanaka, S., Araki, H., Ohashi, E., and Tsurimoto, T. (2016). Conserved interaction of Ctf18-RFC with DNA polymerase ε is critical for maintenance of genome stability in *saccharomyces cerevisiae*. Genes to Cells n/a – n/a.

Onrust, R., and O'Donnell, M. (1993). DNA polymerase III accessory proteins. II. Characterization of delta and delta'. J. Biol. Chem. *268*, 11766–11772.

Osman, F., Dixon, J., Barr, A.R., and Whitby, M.C. (2005). The F-Box DNA helicase Fbh1 prevents Rhp51-dependent recombination without mediator proteins. Mol. Cell. Biol. *25*, 8084–8096.

Paeschke, K., Capra, J. a., and Zakian, V. a. (2011). DNA Replication through G-Quadruplex Motifs Is Promoted by the Saccharomyces cerevisiae Pif1 DNA Helicase. Cell *145*, 678–691.

Papamichos-Chronakis, M., and Peterson, C.L. (2008). The Ino80 chromatin-remodeling enzyme regulates replisome function and stability. Nat. Struct. Mol. Biol. *15*, 338–345.

Papouli, E., Chen, S., Davies, A.A., Huttner, D., Krejci, L., Sung, P., and Ulrich, H.D. (2005). Crosstalk between SUMO and ubiquitin on PCNA is mediated by recruitment of the helicase Srs2p. Mol. Cell *19*, 123–133.

Parker, J.L., and Ulrich, H.D. (2009). Mechanistic analysis of PCNA poly-ubiquitylation by the ubiquitin protein ligases Rad18 and Rad5. EMBO J. *28*, 3657–3666.

Parker, J.L., Bucceri, A., Davies, A.A., Heidrich, K., Windecker, H., and Ulrich, H.D. (2008). SUMO modification of PCNA is controlled by DNA. EMBO J. *27*, 2422–2431.

Pearson, C.E., and Sinden, R.R. (1996). Alternative DNA structures within the trinucleotide repeats of the myotonic dystrophy and fragile X locus. Biochemistry *35*, 5041–5053.

Pearson, C.E., and Sinden, R.R. (1998). Trinucleotide repeat DNA structures : dynamic mutations from dynamic DNA. Curr Opin Struct Biol *8*, 321–330.

Pearson, C.E., Zorbas, H., Price, G.B., and Zannis-Hadjopoulos, M. (1996). Inverted Repeats , Stem-Loops , and Cruciforms : Significance for Initiation of DNA Replication. *22*, 1–22.

Pearson, C.E., Nichol Edamura, K., and Cleary, J.D. (2005). Repeat instability: mechanisms of dynamic mutations. Nat. Rev. Genet. *6*, 729–742.

Pelletier, R., Krasilnikova, M.M., Samadashwily, G.M., Lahue, R., and Mirkin, S.M. (2003). Replication and expansion of trinucleotide repeats in yeast. Mol. Cell. Biol. *23*, 1349–1357.

Petermann, E., and Helleday, T. (2010). Pathways of mammalian replication fork restart. Nat. Rev. Mol. Cell Biol. *11*, 683–687.

Pfander, B., Moldovan, G.-L., Sacher, M., Hoege, C., and Jentsch, S. (2005). SUMO-modified PCNA recruits Srs2 to prevent recombination during S phase. Nature *436*, 428–433.

Potenski, C.J., Niu, H., Sung, P., and Klein, H.L. (2015). Avoidance of rNMP-induced mutations via RNaseH2 and Srs2-Exo1 dependent mechanisms. *73*, 389–400.

Prakash, R., Krejci, L., Van Komen, S., Schürer, K.A., Kramer, W., and Sung, P. (2005). Saccharomyces cerevisiae MPH1 gene, required for homologous recombination-mediated mutation avoidance, encodes a 3′ to 5′ DNA helicase. J. Biol. Chem. *280*, 7854–7860.

Prakash, R., Satory, D., Dray, E., Papusha, A., Scheller, J., Kramer, W., Krejci, L., Klein, H., Haber, J.E., Sung, P., et al. (2009). Yeast Mphl helicase dissociates Rad51-made D-loops: Implications for crossover control in mitotic recombination. Genes Dev. *23*, 67–79.

Prelich, G., Tan, C.K., Kostura, M., Mathews, M.B., So, a G., Downey, K.M., and Stillman, B. (1987). Functional identity of proliferating cell nuclear antigen and a DNA polymerase-delta auxiliary protein. Nature *326*, 517–520.

Raghuraman, M.K., Winzeler, E.A., Collingwood, D., Hunt, S., Wodicka, L., Conway, A., Lockhart, D.J., Davis, R.W., Brewer, B.J., and Fangman, W.L. (2001). Replication dynamics of the yeast genome. Science *294*, 115–121.

Rajeswari, M.R. (2012). DNA triplex structures in neurodegenerative disorder , Friedreich's ataxia. *37*, 519–532.

Rattray, A.J., and Symington, L.S. (1994). Use of a chromosomal inverted repeat to demonstrate that the RAD51 and RAD52 genes of Saccharomyces cerevisiae have different roles in mitotic recombination. Genetics *138*, 587–595.

Ray Chaudhuri, A., Hashimoto, Y., Herrador, R., Neelsen, K.J., Fachinetti, D., Bermejo, R., Cocito, A., Costanzo, V., and Lopes, M. (2012). Topoisomerase I poisoning results in PARP-mediated replication fork reversal. Nat. Struct. Mol. Biol. *19*, 417–423.

Razidlo, D.F., and Lahue, R.S. (2008). Mrc1, Tof1 and Csm3 inhibit CAG??CTG repeat instability by at least two mechanisms. DNA Repair (Amst). *7*, 633–640.

Renton, A.E., Majounie, E., Waite, A., Simón-Sánchez, J., Rollinson, S., Gibbs, J.R., Schymick, J.C., Laaksovirta, H., van Swieten, J.C., Myllykangas, L., et al. (2011). A hexanucleotide repeat expansion in C9ORF72 is the cause of chromosome 9p21-linked ALS-FTD. Neuron *72*, 257–268.

Rhodes, D., and Lipps, H.J. (2015). G-quadruplexes and their regulatory roles in biology. 1–11.

Ribeyre, C., Lopes, J., Boulé, J.B., Piazza, A., Guédin, A., Zakian, V. a., Mergny, J.L., and Nicolas, A. (2009). The yeast Pif1 helicase prevents genomic instability caused by G-quadruplex-forming CEB1 sequences in vivo. PLoS Genet. *5*.

Richard, G.F., and Pâques, F. (2000). Mini- and microsatellite expansions: the recombination connection. EMBO Rep. *1*, 122–126.

Richard, G.F., Cyncynatus, C., and Dujon, B. (2003). Contractions and expansions of CAG/CTG trinucleotide repeats occur during ectopic gene conversion in yeast, by a MUS81-independent mechanism. J. Mol. Biol. *326*, 769–782.

Richard, G.F., Viterbo, D., Khanna, V., Mosbach, V., Castelain, L., and Dujon, B. (2014). Highly specific contractions of a single CAG/CTG trinucleotide repeat by TALEN in yeast. PLoS One *9*.

Richard, G.-F., Kerrest, A., and Dujon, B. (2008). Comparative genomics and molecular dynamics of DNA repeats in eukaryotes. Microbiol. Mol. Biol. Rev. *72*, 686–727.

Robu, M.E., Inman, R.B., and Cox, M.M. (2001). RecA protein promotes the regression of stalled replication forks in vitro. Proc. Natl. Acad. Sci. U. S. A. *98*, 8211–8218.

Rong, L., and Klein, H.L. (1993). Purification and characterization of the SRS2 DNA helicase of the yeast Saccharomyces cerevisiae. J Biol Chem *268*, 1252–1259.

Ross, C.A., and Tabrizi, S.J. (2011). Huntington ' s disease : from molecular pathogenesis to clinical treatment. Lancet Neurol. *10*, 83–98.

Saini, N., Zhang, Y., Nishida, Y., Sheng, Z., Choudhury, S., Mieczkowski, P., and Lobachev, K.S. (2013). Fragile DNA Motifs Trigger Mutagenesis at Distant Chromosomal Loci in Saccharomyces cerevisiae. *9*, 1–12.

Sakamoto, N., Larson, J.E., Iyer, R.R., Montermini, L., Pandolfo, M., and Wells, R.D. (2001). GGA/TCC-interrupted Triplets in Long GAA/TTC Repeats Inhibit the Formation of Triplex and Sticky DNA Structures , Alleviate Transcription Inhibition , and Reduce Genetic Instabilities *. *276*, 27178–27187.

Samadashwily, G.M., Raca, G., and Mirkin, S.M. (1997). Trinucleotide repeats affect DNA replication in vivo. Nat. Genet. *17*, 298–304.

Schiestl, R.H., Prakash, S., and Prakash, L. (1990). The SRS2 suppressor of rad6 mutations of Saccharomyces cerevisiae acts by channeling DNA lesions into the RAD52 DNA repair pathway. Genetics *124*, 817–831.

Schurtenberger, P., Egelhaaf, S.U., Hindges, R., Maga, G., Jónsson, Z.O., May, R.P., Glatter, O., and Hübscher, U. (1998). The solution structure of functionally active human proliferating cell nuclear antigen determined by small-angle neutron scattering. J. Mol. Biol. *275*, 123–132.

Schvartzman, J.B., Martínez-Robles, M.L., López, V., Hernández, P., and Krimer, D.B. (2012). 2D gels and their third-dimension potential. Methods *57*, 170–178.

Seigneur, M., Bidnenko, V., Ehrlich, S.D., and Michel, B. (1998). RuvAB acts at arrested replication forks. Cell *95*, 419–430.

Shao, J., and Diamond, M.I. (2007). Polyglutamine diseases : emerging concepts in pathogenesis and therapy. *16*, 115–123.

Shete, S., Hosking, F.J., Robertson, L.B., Dobbins, S.E., Sanson, M., Malmer, B., Simon, M., Marie, Y., Boisselier, B., Delattre, J.-Y., et al. (2009). Genome-wide association study identifies five susceptibility loci for glioma. Nat. Genet. *41*, 899–904.

Shiomi, Y., Shinozaki, A., Sugimoto, K., Usukura, J., Obuse, C., and Tsurimoto, T. (2004). The reconstituted human Chl12-RFC complex functions as a second

PCNA loader. Genes to Cells *9*, 279–290.

Shiomi, Y., Masutani, C., Hanaoka, F., Kimura, H., and Tsurimoto, T. (2007). A second proliferating cell nuclear antigen loader complex, Ctf18-replication factor C, stimulates DNA polymerase η activity. J. Biol. Chem. *282*, 20906–20914.

Shishkin, A.A., Voineagu, I., Matera, R., Cherng, N., Chernet, B.T., Krasilnikova, M.M., Narayanan, V., Lobachev, K.S., and Mirkin, S.M. (2009). Large-Scale Expansions of Friedreich's Ataxia GAA Repeats in Yeast. Mol. Cell *35*, 82–92.

Smirnova, M., and Klein, H.L. (2003). Role of the error-free damage bypass postreplication repair pathway in the maintenance of genomic stability. Mutat. Res. - Fundam. Mol. Mech. Mutagen. *532*, 117–135.

Sogo, J.M., Lopes, M., and Foiani, M. (2002). Fork Reversal and ssDNA Accumulation at Stalled Replication Forks Owing to Checkpoint Defects. Sci. *297* , 599–602.

Stelter, P., and Ulrich, H.D. (2003). Control of spontaneous and damage-induced mutagenesis by SUMO and ubiquitin conjugation. Nature *425*, 188–191.

Stukenberg, P.T., Studwell-Vaughan, P.S., O'Donnell, M., and O'Donnell, M. (1991). Mechanism of the sliding beta-clamp of DNA polymerase III holoenzyme. J. Biol. Chem. *266*, 11328–11334.

Su, X.A., Dion, V., Gasser, S.M., and Freudenreich, C.H. (2015). Regulation of recombination at yeast nuclear pores controls repair and triplet repeat stability. Genes Dev. *29*, 1006–1017.

Sun, W., Nandi, S., Osman, F., Ahn, J.S., Jakovleska, J., Lorenz, A., and Whitby, M.C. (2008). The FANCM ortholog Fml1 promotes recombination at stalled replication forks and limits crossing over during DNA double-strand break repair. Mol. Cell *32*, 118–128.

Sundararajan, R., and Freudenreich, C.H. (2011). Expanded CAG/CTG repeat DNA induces a checkpoint response that impacts cell proliferation in Saccharomyces cerevisiae. PLoS Genet. *7*.

Sundararajan, R., Gellon, L., Zunder, R.M., and Freudenreich, C.H. (2010). Double-strand break repair pathways protect against CAG/CTG repeat expansions, contractions and repeat-mediated chromosomal fragility in Saccharomyces cerevisiae. Genetics *184*, 65–77.

Sutcliffe, J.S., Nelson, D.L., Zhang, F., Pieretti, M., Caskey, C.T., Saxe, D., and Warren, S.T. (1992). DNA methylation represses FMR-1 transcription in fragile X syndrome. Hum. Mol. Genet. *1*, 397–400.

Szüts, D., Simpson, L.J., Kabani, S., Yamazoe, M., and Sale, J.E. (2006). Role for RAD18 in homologous recombination in DT40 cells. Mol. Cell. Biol. *26*, 8032–8041.

Terret, M.-E., Sherwood, R., Rahman, S., Qin, J., and Jallepalli, P. V (2009). Cohesin acetylation speeds the replication fork. Nature *462*, 231–234.

Tobin, A.J., and Signer, E.R. (2000). Huntington's disease : the challenge for cell biologists. *8924*, 531–536.

Torres-Ramos, C. a., Prakash, S., and Prakash, L. (2002). Requirement of RAD5 and MMS2 for Postreplication Repair of UV-Damaged DNA in Saccharomyces cerevisiae. Mol. Cell. Biol. *22*, 2419–2426.

Tsang, E., Miyabe, I., Iraqui, I., Zheng, J., Lambert, S. a E., and Carr, A.M. (2014). The extent of error-prone replication restart by homologous recombination is controlled by Exo1 and checkpoint proteins. J. Cell Sci. *127*, 2983–2994.

Tsuji, Y., Watanabe, K., Araki, K., Shinohara, M., Yamagata, Y., Tsurimoto, T., Hanaoka, F., Yamamura, K. ichi, Yamaizumi, M., and Tateishi, S. (2008). Recognition of forked and single-stranded DNA structures by human RAD18 complexed with RAD6B protein triggers its recruitment to stalled replication forks. Genes to Cells *13*, 343–354.

Ulrich, H.D. (2001). The srs2 suppressor of UV sensitivity acts specifically on the RAD5- and MMS2-dependent branch of the RAD6 pathway. Nucleic Acids Res. *29*, 3487–3494.

Ulrich, H.D. (2009). Regulating post-translational modifications of the eukaryotic replication clamp PCNA. DNA Repair (Amst). *8*, 461–469.

Unk, I., Hajdú, I., Blastyák, A., and Haracska, L. (2010). Role of yeast Rad5 and its human orthologs, HLTF and SHPRH in DNA damage tolerance. DNA Repair (Amst). *9*, 257–267.

Uringa, E.-J., Youds, J.L., Lisaingo, K., Lansdorp, P.M., and Boulton, S.J. (2011). RTEL1: an essential helicase for telomere maintenance and the regulation of homologous recombination. Nucleic Acids Res. *39*, 1647–1655.

Usdin, K., and KJ, W. (1995). CGG repetas associated with DNA instability and chromosome fragility form structures that block DNA synthesis in vitro. *23*, 4202–4209.

Usdin, K., House, N.C.M., and Freudenreich, C.H. (2015). Repeat instability during DNA repair: Insights from model systems. Crit. Rev. Biochem. Mol. Biol. *9238*, 1–26.

Vannier, J.B., Pavicic-Kaltenbrunner, V., Petalcorin, M.I.R., Ding, H., and Boulton, S.J. (2012). RTEL1 dismantles T loops and counteracts telomeric G4-DNA to maintain telomere integrity. Cell *149*, 795–806.

Vannier, J.-B., Sandhu, S., Petalcorin, M.I.R., Wu, X., Nabi, Z., Ding, H., and Boulton, S.J. (2013). RTEL1 is a replisome-associated helicase that promotes telomere and genome-wide replication. Science *342*, 239–242.

Vanoli, F., Fumasoni, M., Szakal, B., Maloisel, L., and Branzei, D. (2010). Replication and recombination factors contributing to recombination-dependent bypass of DNA lesions by template switch. PLoS Genet. *6*.

Vaze, M.B., Pellicioli, A., Lee, S.E., Ira, G., Liberi, G., Arbel-eden, A., Foiani, M., Haber, J.E., and Firc, I. (2002). Recovery from Checkpoint-Mediated Arrest after Repair of a Double-Strand Break Requires Srs2 Helicase. *10*, 373–385.

Veaute, X., Jeusset, J., Soustelle, C., Kowalczykowski, S.C., Le Cam, E., and Fabre, F. (2003). The Srs2 helicase prevents recombination by disrupting Rad51

nucleoprotein filaments. Nature *423*, 309–312.

Venclovas, C., and Thelen, M.P. (2000). Structure-based predictions of Rad1, Rad9, Hus1 and Rad17 participation in sliding clamp and clamp-loading complexes. Nucleic Acids Res. *28*, 2481–2493.

Verkerk, A.J.M.H., Pieretti, M., Sutcliffe, J.S., Fu, Y.-H., Kuhl, D.P.A., Pizzuti, A., Reiner, O., Richards, S., Victoria, M.F., Zhang, F., et al. (1991). Identification of a gene (FMR-1) containing a CGG repeat coincident with a breakpoint cluster region exhibiting length variation in fragile X syndrome. Cell *65*, 905–914.

Viterbo, D., Michoud, G., Mosbach, V., Dujon, B., and Richard, G.-F. (2016). Replication stalling and heteroduplex formation within CAG/CTG trinucleotide repeats by mismatch repair. DNA Repair (Amst).

Walker, F.O. (2007). Huntington ' s disease.

Walne, A.J., Vulliamy, T., Kirwan, M., Plagnol, V., and Dokal, I. (2013). Constitutional mutations in RTEL1 cause severe dyskeratosis congenita. Am. J. Hum. Genet. *92*, 448–453.

Wang, G., and Vasquez, K.M. (2014). Impact of alternative DNA structures on DNA damage, DNA repair, and genetic instability. DNA Repair (Amst). *19*, 143–151.

Waters, L.S., Minesinger, B.K., Wiltrout, M.E., D'Souza, S., Woodruff, R. V, and Walker, G.C. (2009). Eukaryotic translesion polymerases and their roles and regulation in DNA damage tolerance. Microbiol. Mol. Biol. Rev. *73*, 134–154.

Watts, F.Z. (2006). Sumoylation of PCNA: Wrestling with recombination at stalled replication forks. DNA Repair (Amst). *5*, 399–403.

Weisman-shomer, P., Naot, Y., and Fry, M. (2000). Tetrahelical Forms of the Fragile X Syndrome Expanded Sequence d (CGG) n Are Destabilized by Two Heterogeneous Nuclear Ribonucleoprotein-related Telomeric DNA-binding Proteins *. *275*, 2231–2238.

Wolner, B., Van Komen, S., Sung, P., and Peterson, C.L. (2003). Recruitment of the recombinational repair machinery to a DNA double-strand break in yeast. Mol. Cell *12*, 221–232.

Wrensch, M., Jenkins, R.B., Chang, J.S., Yeh, R.-F., Xiao, Y., Decker, P.A., Ballman, K. V, Berger, M., Buckner, J.C., Chang, S., et al. (2009). Variants in the CDKN2B and RTEL1 regions are associated with high-grade glioma susceptibility. Nat. Genet. *41*, 905–908.

Wu, Y., Kantake, N., Sugiyama, T., and Kowalczykowski, S.C. (2008). Rad51 protein controls Rad52-mediated DNA annealing. J. Biol. Chem. *283*, 14883–14892.

Xu, X., Blackwell, S., Lin, A., Li, F., Qin, Z., and Xiao, W. (2015). Error-free DNA-damage tolerance in Saccharomyces cerevisiae. Mutat. Res. Rev. Mutat. Res. *764*, 43–50.

Yabuki, N., Terashima, H., and Kitada, K. (2002). Mapping of early firing origins on a replication profile of budding yeast. Genes to Cells *7*, 781–789.

Yang, W., and Woodgate, R. (2007). What a difference a decade makes: insights into translesion DNA synthesis. Proc. Natl. Acad. Sci. U. S. A. *104*, 15591–15598.

Yeung, M., and Durocher, D. (2011). Srs2 enables checkpoint recovery by promoting disassembly of DNA damage foci from chromatin. DNA Repair (Amst). *10*, 1213–1222.

Yi, E., Lam, N., Beraldi, D., Tannahill, D., and Balasubramanian, S. (2013). G-quadruplex structures are stable and detectable in human genomic DNA. Nat. Commun. *4*, 1796–1798.

Youds, J.L., Mets, D.G., McIlwraith, M.J., Martin, J.S., Ward, J.D., ONeil, N.J., Rose, A.M., West, S.C., Mayer, B.J., and Boulton, S.J. (2010). RTEL-1 Enforces Meiotic Crossover Interference and Homeostasis. 1254–1259.

Zellweger, R., Dalcher, D., Mutreja, K., Berti, M., Schmid, J.A., Herrador, R., Vindigni, A., and Lopes, M. (2015). Rad51-mediated replication fork reversal is a global response to genotoxic treatments in human cells. J. Cell Biol. *208*, 563–579.

Zhang, H., and Freudenreich, C.H. (2007). An AT-Rich Sequence in Human Common Fragile Site FRA16D Causes Fork Stalling and Chromosome Breakage in S . cerevisiae. *27*, 367–379.

Zhang, H., and Lawrence, C.W. (2005). The error-free component of the RAD6/RAD18 DNA damage tolerance pathway of budding yeast employs sister-strand recombination. Proc. Natl. Acad. Sci. U. S. A. *102*, 15954–15959.

Zheng, X.F., Prakash, R., Saro, D., Longerich, S., Niu, H., and Sung, P. (2011). Processing of DNA structures via DNA unwinding and branch migration by the S. cerevisiae Mph1 protein. DNA Repair (Amst). *10*, 1034–1043.

Zhuang, Z., Yoder, B.L., Burgers, P.M.J., and Benkovic, S.J. (2006). The structure of a ring-opened proliferating cell nuclear antigen-replication factor C complex revealed by fluorescence energy transfer. Proc. Natl. Acad. Sci. U. S. A. *103*, 2546–2551.